

การเตรียม TiO_2 บนซีโอไลต์ NaY เป็นสารเร่งปฏิกิริยาเชิงแสง
เพื่อการสลายสีย้อม

นางสาวกุลธิดา พิทยาภรณ์

วิทยานิพนธ์นี้เป็นส่วนหนึ่งของการศึกษาตามหลักสูตรปริญญาวิทยาศาสตรมหาบัณฑิต
สาขาวิชาเคมี
มหาวิทยาลัยเทคโนโลยีสุรนารี
ปีการศึกษา 2553

**PREPARATION OF TiO₂ SUPPORTED ON ZEOLITE
NaY AS PHOTOCATALYST FOR
DEGRADATION OF DYES**

Kultida Pittayaporn

**A Thesis Submitted in Partial Fulfillment of the Requirements for the
Degree of Master of Science in Chemistry
Suranaree University of Technology
Academic Year 2010**

PREPARATION OF TiO₂ SUPPORTED ON ZEOLITE NaY AS PHOTOCATALYST FOR DEGRADATION OF DYES

Suranaree University of Technology has approved this thesis submitted in fulfillment of the requirements for a Master's Degree.

Thesis Examining Committee

(Asst. Prof. Dr. Thanaporn Manyum)

Chairperson

(Asst. Prof. Dr. Kunwadee Rangsriwatananon)

Member (Thesis Advisor)

(Assoc. Prof. Dr. Jatuporn Wittayakun)

Member

(Asst. Prof. Dr. Sanchai Prayoonpokarach)

Member

(Prof. Dr. Sukit Limpijumnong)

Vice Rector for Academic Affairs

(Assoc. Prof. Dr. Prapun Manyum)

Dean of Institute of Science

กุลธิดา พิทยาภรณ์ : การเตรียม TiO_2 บนซีโอไลต์ NaY เป็นสารเร่งปฏิกิริยาเชิงแสงเพื่อ
การสลายสีย้อม (PREPARATION OF TiO_2 SUPPORTED ON ZEOLITE NaY AS
PHOTOCATALYST FOR DEGRADATION OF DYES) อาจารย์ที่ปรึกษา :
ผู้ช่วยศาสตราจารย์ ดร.กุลวดี รังษีวัฒนานนท์, 86 หน้า.

งานนี้ศึกษาการสลายด้วยแสงของสีเมทิลีนบลูและฟิโนซาฟรานีนภายใต้การฉายแสงยูวี
ที่มี TiO_2/NaY เป็นตัวเร่งปฏิกิริยาที่ถูกเตรียมด้วยวิธีที่แตกต่างกัน ตัวอย่างของ TiO_2/NaY ถูก
วิเคราะห์หาเอกลักษณ์ด้วยเทคนิค XRD FT-IR BET ICP และ TEM ซึ่งพบว่าการเตรียมจากวิธี
แลกเปลี่ยนไอออน (IE) ทำให้เอ็บซุ่ม (IMP) และโซลเจล (SG) ตัวที่เหมาะสมที่สุดคือ 15.0 mM
ATO/NaY-IE 27.4wt% Ti/NaY-IMP และ 37.33wt% Ti/NaY-SG ตามลำดับ ภายใต้เงื่อนไข
การศึกษการเตรียมตัวอย่าง ผลของ XRD แสดงให้เห็นว่าเฟสอะนาเทซของ TiO_2 จะพบเฉพาะ
ตัวอย่างที่เตรียมจากวิธีทำให้เอ็บซุ่มและโซลเจลเท่านั้น จากผลของ ICP พบว่า ตัวอย่าง 27.4wt%
Ti/NaY-IMP มีปริมาณ Ti สูงที่สุด ในขณะที่ตัวอย่าง 37.33wt% Ti/NaY-SG มีพื้นที่ผิวภายนอกมาก
ที่สุด ตามผล TEM แสดงจุดสีดำของ TiO_2 จำนวนมากมายกระจายอยู่ทั่วอนุภาค ในการศึกษาการ
สลายด้วยแสงมีการศึกษาผลของความเข้มข้นเริ่มต้นของสีและ pH ของสารละลาย สีที่มีความ
เข้มข้นเริ่มต้นสูงกว่าประสิทธิภาพการสลายด้วยแสงจะลดลงมากกว่า ส่วนผลของ pH ของ
สารละลายต่อการสลายด้วยแสง พบว่า ประสิทธิภาพจะเพิ่มขึ้นเมื่อ pH ของสารละลายสูงขึ้น
นอกจากนี้ พบว่าตัวอย่างที่เตรียมจาก 37.33wt% Ti/NaY-SG มีความสามารถในการเร่งปฏิกิริยา
ด้วยแสงต่อการสลายของสีเมทิลีนบลูได้สูงที่สุดและรวมถึงการสลายของสีฟิโนซาฟรานีนด้วย

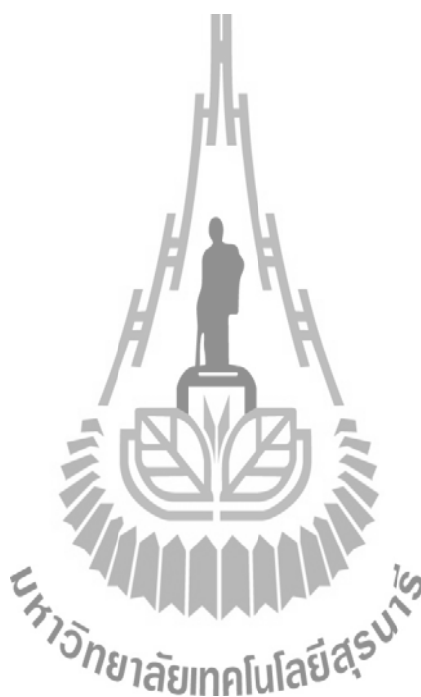
KULTIDA PITTAYAPORN : PREPARATION OF TiO_2 SUPPORTED ON
ZEOLITE NaY AS PHOTOCATALYST FOR DEGRADATION OF DYES.

THESIS ADVISOR : ASST. PROF. KUNWADEE RANGSRIWATANANON,
Ph.D, 86 PP.

PHOTODEGRADATION/PHOTOCATALYST/ZEOLITE Y/ TiO_2 /ANATASE/ION
EXCHANGE/IMPREGNATION/SOL GEL

In this work, the photodegradation of methylene blue and phenosafranin under UV irradiation was investigated in the presence of TiO_2 /NaY catalyst prepared from different methods. The prepared TiO_2 /NaY samples were characterized by XRD, FT-IR, BET, ICP and TEM techniques. It was found that by ion exchange (IE), impregnation (IMP) and sol-gel (SG) method, the optimal TiO_2 /zeolite NaY sample were 15.0 mM ATO/NaY-IE, 27.4wt% Ti/NaY-IMP and 37.33wt% Ti/NaY-SG, respectively. Under the studied preparation condition, XRD showed only the samples prepared by IMP and SG containing anatase phase of TiO_2 . According to ICP, the sample of 27.4wt% Ti/NaY-IMP contained the highest amount of Ti. In contrast, the sample of 37.33wt% Ti/NaY-SG showed the highest external surface area and based on TEM it showed an enormous amount of dark spots of TiO_2 spreading all over the particles. In the study of photodegradation, the effect of initial concentration of dyes and pH of the solution was investigated. At higher initial concentration, the photodegradation efficiency was more decreased. The photodegradation efficiency was increased with an increase in pH of the solution. In addition, the prepared sample

of 37.33wt% Ti/NaY-SG had the highest photocatalytic activity for degradation of methylene blue and also phenosafranin.



School of Chemistry

Academic Year 2010

Student's Signature _____

Advisor's Signature _____

ACKNOWLEDGEMENT

First, I would like to thank my advisor, Assistant Professor Dr. Kunwadee Rangsiwatananon, for her continuous support in the M.Sc. program. She was always there to listen and to give advice. She taught me how to ask questions and express my ideas. She showed me different ways to approach a research problem and the need to be persistent to accomplish any goal. I would not have achieved this far and this thesis would not have been completed without all the support that I have always received from her. I also thank all my thesis committee members Associate Professor Dr. Jatuporn Wittayakun, Assistant Professor Dr. Thanaporn Manyum and Assistant Professor Dr. Sanchai Prayoonpokarach for their valuable and grateful direction, suggestion and criticism. I would like to thank all the staffs at the Center of Scientific and Technological Equipment for their service and helpful suggestions.

I wish to thank Zeolite's group and all my friends for their kindness, help and encouragement. Finally, many thanks for my family, for their love, for educating me with aspects from both arts and sciences, for unconditional support and encouragement to pursue my interests.

Kultida Pittayaporn

CONTENTS

	Page
ABSTRACT IN THAI.....	I
ABSTRACT IN ENGLISH.....	II
ACKNOWLEDGEMENTS.....	IV
CONTENTS.....	V
LIST OF FIGURES.....	IX
ABBREVIATIONS.....	XVII
CHAPTER	
I INTRODUCTION.....	1
1.1 Significance of the Problem.....	1
1.2 Research Objective.....	3
1.3 Scope and Limitation of the Study.....	3
II BACKGROUND AND LITERATURE REVIEW.....	4
2.1 Zeolite Y.....	5
2.2 Principle of Photocatalysis Process.....	8
2.3 Type of Semiconductor.....	11
2.4 Titanium Dioxide (TiO ₂).....	13
2.5 Preparation of TiO ₂ Supported on Zeolite Y.....	15
2.6 Photocatalytic Oxidation Dyes and Organic Compound.....	17

CONTENTS (Continued)

	Page
2.7 Characterization Techniques.....	20
2.7.1 Power X-Ray Diffraction.....	20
2.7.2 Transmission Electron Microscopy.....	21
2.7.3 Brunauer-Emmett-Teller.....	22
2.7.4 Inductively Coupled Plasma Mass Spectrometry.....	23
2.7.5 Ultraviolet Visible Spectroscopy.....	24
III EXPERIMENT.....	26
3.1 Chemicals and Materials.....	26
3.2 Apparatuses.....	27
3.3 Instrumentation.....	28
3.4 Procedures.....	29
3.4.1 Synthesis of Zeolite NaY.....	29
3.4.2 TiO ₂ Supported on Zeolite NaY.....	29
3.4.2.1 Ion Exchange Method.....	30
3.4.2.2 Impregnation Method.....	30
3.4.2.3 Sol Gel Method.....	31
3.5 Characterization of Prepared TiO ₂ Supported on Zeolite NaY.....	31
3.5.1 Study on Crystallization of Zeolite NaY and Crystallization Forms of TiO ₂	31
3.5.2 Determination of Surface Area and Pore Size.....	32

CONTENTS (Continued)

	Page
3.5.3 Determination of Elemental Compositions of TiO_2/NaY	32
3.5.4 Determination of Dye Concentrations.....	33
3.6 The Study of Photodegradation of Methylene Blue using TiO_2 Supported on Zeolite NaY Prepared by Ion Exchange Method.....	33
3.6.1 Effect of TiO_2 Content Loaded on Zeolite NaY.....	33
3.6.2 Effect of Initial Concentration of Methylene Blue.....	34
3.6.3 Effect of pH.....	34
3.7 The Study of Photodegradation of Methylene Blue using TiO_2 Supported on Zeolite NaY Prepared by Impregnation Method.....	35
3.7.1 Effect of TiO_2 Content Loaded on Zeolite NaY.....	35
3.7.2 Effect of Initial Concentration of Methylene Blue.....	35
3.8 The Study of Photodegradation of Methylene Blue Using TiO_2 Supported on Zeolite NaY Prepared by Sol Gel Method.....	35
3.8.1 Effect of TiO_2 Content Loaded on Zeolite NaY.....	35
3.8.2 Effect of Initial Concentration of Methylene Blue.....	36
3.9 The Study of Photodegradation of Phenosafranin using TiO_2 Supported on Zeolite NaY Prepared by different Method.....	36
IV RESULTS AND DISCUSSION	37
4.1 The Characterization of Zeolite NaY and TiO_2 Supported on Zeolite NaY.....	37

CONTENTS (Continued)

	Page
4.1.1 X-Ray Powder Diffraction (XRD).....	37
4.1.1.1 Preparation of TiO ₂ Supported on Zeolite NaY by Ion Exchange Method.....	37
4.1.1.2 Preparation of TiO ₂ Supported on Zeolite NaY by Impregnation Method.....	38
4.1.1.3 Preparation of TiO ₂ Supported on Zeolite NaY by Sol Gel Method.....	38
4.1.2 Surface Area Analysis (BET).....	41
4.1.3 Surface Morphology.....	41
4.1.4 FT-IR Measurement.....	42
4.2 The Photodegradation of Methylene Blue with TiO ₂ Supported on Zeolite NaY.....	47
4.2.1 Control Experiments.....	47
4.2.2 The Photodegradation with TiO ₂ Supported on Zeolite NaY Prepared by Ion Exchange Method.....	48
4.2.2.1 Effect of Amount of TiO ₂ Loaded on Zeolite NaY.....	48
4.2.2.2 Effect of Initial Concentration of Methylene Blue.....	49
4.2.2.3 Effect of pH of the Solution.....	50
4.2.3 The Photodegradation with TiO ₂ Supported on Zeolite NaY Prepared by Impregnation Method.....	55

CONTENTS (Continued)

	Page
4.2.3.1 Effect of Amount of TiO_2 Loaded on Zeolite NaY.....	55
4.2.3.2 Effect of Initial Concentration.....	55
4.2.4 The Photodegradation with TiO_2 Supported on Zeolite NaY Prepared by Sol Gel Method.....	57
4.2.4.1 Effect of TiO_2 Loaded on Zeolite NaY.....	57
4.2.4.2 Effect of Initial Concentration.....	57
4.2.5 Comparison of The Photocatalyst Activity of Catalyst Prepared by Different Methods in Photodegradation of Methylene Blue.....	59
4.3 The Photodegradation of Phenosafranin with TiO_2 Supported on Zeolite NaY.....	61
4.3.1 Effect of Initial Concentration of Phenosafranin.....	62
4.3.2 Effect of pH of the Solution.....	67
4.3.3 Comparison of the Photocatalyst Activity of Catalyst Prepared by 3 Methods.....	66
V CONCLUTIONS.....	69
REFERENCES.....	72
APPENDIX.....	76
CURRICULUM VITAE.....	86

LIST OF FIGURES

Figure	Page
2.1 Structure of zeolite Y.....	7
2.2 Promotion of an electron from the valence band to the conduction band on illumination of semiconductor.....	10
2.3 Crystal structure of Rutile (A), Anatase (B) and Brookite (C).....	14
4.1 X-Ray diffraction pattern of zeolite NaY, TiO ₂ supported on zeolite NaY with different amount of TiO ₂ by ion exchange method and commercial TiO ₂ (Aldrich).....	39
4.2 X-Ray diffraction pattern of zeolite NaY, TiO ₂ supported on zeolite NaY with different amount of TiO ₂ by impregnation method and commercial TiO ₂	40
4.3 X-Ray diffraction pattern of zeolite NaY, TiO ₂ supported on zeolite NaY with different amount of TiO ₂ by sol gel method and commercial TiO ₂	40
4.4 TEM photograph of (a) Zeolite NaY, (b) 15.0 mM ATO/NaY-IE, (c) 4.6wt% Ti/NaY-IMP, (d) 27.4wt% Ti/NaY-IMP, (e) 18.67wt% Ti/NaY-SG and (f) 37.33wt% Ti/NaY-SG.....	43
4.5 FT-IR spectra of zeolite NaY, 15.0mM ATO/NaY-IE, 20.0 ml TiO ₂ sol/NaY-SG, 40.0 ml TiO ₂ sol./NaY-SG, 4.6wt% Ti/NaY-IMP, 27.4wt% Ti/NaY-IMP.....	46

LIST OF FIGURES (Continued)

Figure	Page
4.6 Control experiment of photodegradation with dye solution.....	48
4.7 Photodegradation efficiency of methylene blue with TiO ₂ /zeolite NaY as photocatalyst at different loading of TiO ₂ . Experiment condition: 0.050 g of prepared TiO ₂ /zeolite NaY, 50.0 ml of 0.10 mM of methylene blue at pH 7.....	51
4.8 Photodegradation efficiency of methylene blue with TiO ₂ /zeolite NaY as photocatalyst at different loading of TiO ₂ and also compared with zeolite Y and commercial TiO ₂ (Aldrich). Experiment condition: 0.050 g of prepared TiO ₂ /zeolite NaY, 50.0 ml of 0.10 mM of methylene at pH 7.....	52
4.9 Effect of initial methylene blue concentration on the photodegradation with TiO ₂ /zeolite NaY prepared by ion exchange method. Experiment condition: 0.050 g of prepared TiO ₂ /zeolite NaY, 50.0 ml of various methylene blue concentration at pH 7.....	53
4.10 Effect of the pH of the solution on the photodegradation of methylene blue with TiO ₂ /zeolite NaY prepared by ion exchange method. Experiment condition: 0.050 g of prepared TiO ₂ /zeolite NaY, 50.0 ml of 0.10 mM of methylene blue.....	54

LIST OF FIGURES (Continued)

Figure	Page
4.11 Photodegradation efficiency of methylene blue at various pH of solution during some reaction time. Experiment conditions: 0.050 g of prepared TiO_2 /zeolite NaY, 50 ml of 0.1 mM of methylene blue.....	54
4.12 Effect of TiO_2 loading by impregnation method on photodegradation efficiency of methylene blue. Experiment conditions: 0.050 g of prepared TiO_2 /zeolite NaY, 50 ml of 0.1 mM of methylene blue at pH 8.....	56
4.13 Effect of initial methylene blue concentrations on their degradations with TiO_2 /zeolite Y prepared by impregnation method. Experiment conditions: 0.050 g of prepared TiO_2 /zeolite Y, 50 ml of various methylene blue concentrations at pH 8.....	56
4.14 Effect of TiO_2 loading by sol gel method on the photodegradation efficiency of methylene blue. Experiment conditions: 0.050 g of prepared TiO_2 /zeolite NaY, 50 ml of 0.1 mM of methylene blue at pH 8.....	58
4.15 Effect of initial methylene blue concentrations on their degradations with TiO_2 /zeolite NaY prepared by sol gel method. Experiment conditions: 0.050 g of prepared TiO_2 /zeolite NaY, 50 ml of various methylene blue concentrations at pH 8.....	59

LIST OF FIGURES (Continued)

Figure	Page
4.16 Comparison of the efficiency of photocatalyst prepared by impregnation, ion exchange and sol gel method in photodegradation of methylene blue. Experiment conditions: 0.050 g of prepared TiO ₂ /zeolite Y, 50 ml of 0.10 mM of methylene blue at pH 8.....	60
4.17 The comparison of the efficiency of photocatalyst prepared by impregnation, ion exchange and sol gel method in photodegradation of methylene blue. Experiment conditions: 0.050 g of prepared TiO ₂ /zeolite Y, 50 ml of 0.20 mM of methylene blue at pH 8.....	61
4.18 Effect of initial phenosafranin concentrations on their degradations with TiO ₂ /zeolite Y prepared by ion exchange method. Experiment conditions: 15.0 mM ATO/NaY-IE 0.050 g, 50 ml of 0.10 mM and 0.20 mM PHNS at pH 7.....	62
4.19 Effect of initial phenosafranin concentrations on their degradations with TiO ₂ /zeolite Y prepared by impregnation method. Experiment conditions: 27.4wt% Ti/NaY-IMP 0.050 g, 50 ml of 0.10 mM and 0.20 mM PHNS at pH 7.....	63
4.20 Effect of initial phenosafranin concentrations on their degradations with TiO ₂ /zeolite Y prepared by sol gel method. Experiment conditions: 37.33wt% Ti/NaY-SG 0.050 g, 50 ml of 0.10 mM and 0.20 mM PHNS at pH 7.....	63

LIST OF FIGURES (Continued)

Figure	Page
4.21 Effect of pH of the solution on the photodegradation of phenosafranin with TiO ₂ /zeolite Y prepared by ion exchange method. Experiment conditions: 0.050 g of prepared TiO ₂ /zeolite Y, 50 ml of 0.10 mM of PHNS.....	64
4.22 Effect of pH of the solution on the photodegradation of phenosafranin with TiO ₂ /zeolite Y prepared by impregnation method. Experiment conditions: 0.050 g of prepared TiO ₂ /zeolite Y, 50 ml of 0.10 mM of PHNS.....	65
4.23 Effect of pH of the solution on the photodegradation of phenosafranin with TiO ₂ /zeolite Y prepared by sol gel. Experiment conditions: 0.050 g of prepared TiO ₂ /zeolite Y, 50 ml of 0.10 mM of PHNS.....	66
4.24 The comparison of the photodegradation efficiency of phenosafranin with photocatalysts prepared by impregnation, ion exchange and sol gel method. Experiment conditions: 0.050 g of prepared TiO ₂ /zeolite Y, 50 ml of 0.10 mM of PHNS at pH 8.....	67
4.25 The comparison of the photodegradation efficiency of phenosafranin with photocatalysts prepared by impregnation, ion exchange and sol gel method. Experiment conditions: 0.050 g of prepared TiO ₂ /zeolite Y, 50 ml of 0.20 mM of PHNS at pH 8.....	68

LIST OF ABBREVIATIONS

ATO	=	Ammonium Titanyl Oxalate
BET	=	Brunauer-Emmett-Teller
FT-IR	=	Fourier Transforms Infrared Spectrophotometer
XRD	=	X-ray Diffractometer
ICP-MS	=	Inductively Coupled Plasma Mass Spectrometer
TEM	=	Transmission Electron Microscope
°C	=	Degree Celsius
Å	=	Angstrom
% T	=	Percent Transmittance
cm ⁻¹	=	Per Centimeter
mM	=	Millimolar
g	=	Gram
L	=	Liter
mL	=	Milliliter
MB	=	Methylene Blue
PHEN	=	Phenosafranin
IE	=	Ion Exchange Method
IMP	=	Impregnation Method
SG	=	Sol Gel Method

CHAPTER I

INTRODUCTION

1.1 Significance and Problem of the Study

Wastewater from chemical laboratories and dye manufacturing industries contains various dyestuffs, which are toxic to microorganisms, aquatic life and human beings. It is a serious problem that attracts the attention of many researches during last decades. A substantial amount of dyestuff is lost during the dyeing process in the textile industry, which poses a major problem for the industry as well as a threat to the environment (Faisal *et al.*, 2007 and Saquib *et al.*, 2008). Moreover, some dyes are toxic and mostly non-biodegradable and are also harmful to aquatic life. Therefore, the decolorizing of dye wastewater has become a major environmental control problem and there have been many investigations of physical, chemical and biological methods of removing color from dye wastewater. However, in terms of treating dye wastewater, biological processes are ineffective, and coagulation and adsorption processes merely transfer the dye pollutants from one phase to another, generating a new and different kind of pollution and necessitating further treatment (Wang *et al.*, 2008). During the past two decades, photocatalytic process involving semiconductor particles under UV light illumination has been shown to be potentially advantageous and useful in the treatment of wastewater pollutants. Photocatalytic degradation using the non-toxic, inexpensive and highly reactive nature of TiO_2 under UV irradiation has been adopted to oxidize dyes in wastewater (Saquib *et al.*, 2008 and Wang *et al.*,

2008). The photocatalytic degradation of organic compound is an important branch of the broader subject of photocatalysis. Semiconductor particles are ideal photocatalysis for this reaction. The photocatalysts commonly used are TiO_2 , ZnO , WO_2 , CdS , ZnS , and SrTiO_3 . TiO_2 has been reported as the most active in organic degradation experiment (Lakshmi *et al.*, 1995). The studies of TiO_2 included in zeolite have received much attention in recent years. It has been used as photocatalyst for a wide range of selective reaction in many applications. The efforts to enhance photocatalytic efficiency of TiO_2 /zeolite have been continued to investigate. The photocatalytic efficiency of TiO_2 is greatly influenced by crystal structure, particle size, surface area and porosity (Chen *et al.*, 1999). Increasing the photocatalyst surface area is the most obvious means of improving the efficiency of photocatalytic reaction. Practical application requires these fine TiO_2 particles of high surface area to be fix on inert support so that the recovery from the treated effluent is simplified. Several kinds of supports for TiO_2 loading such as alumina, silica, activated carbon and zeolite have been studied (Xu and Langford, 1995; 1997). Zeolites, due to their large surface areas, internal pore volumes, unique uniform pores and channel sizes, are interesting hosts to disperse semiconductor photocatalyst on their surfaces. Moreover, zeolites show several other specific features that make them suitable for use as hosts for photocatalyst, such as : (I) full photochemical stability and large thermal and chemical inertness; (II) transparency to UV-visible radiation over 240 nm, that means their allowing a certain penetration of the exciting light into the solid opaque powder to reach the substrate molecules located in intraparticle position; (III) zeolite high adsorption for organic compounds from solution concentrating the substrate molecule in the proximity of active site of the photocatalyst; (IV) the polarizing strength inside

the zeolite pores by varying the nature of internal charge balancing cations and the size of the channel; (V) the ability of the framework to participate actively in electron-transfer processes, either as electron acceptor or electron donor (Tayade *et al.*, 2007). In this work, the photocatalysts of TiO₂ supported on zeolite Y were prepared by different methods. As well as the different techniques were employed to characterize the prepared photocatalysts. Finally, they were applied for degradation of dyes under UV irradiation and the reactions were performed under various conditions.

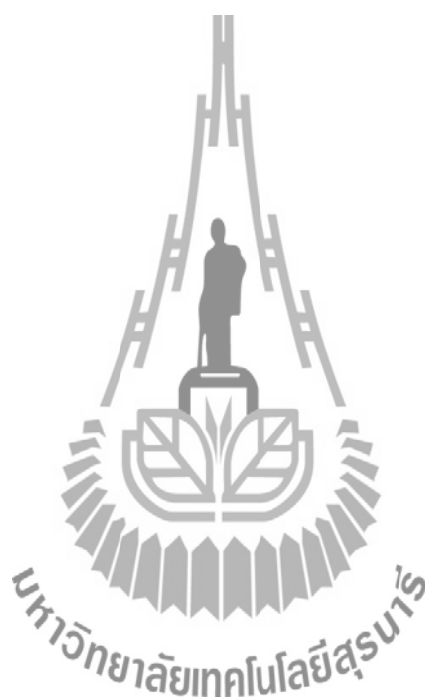
1.2 Research Objectives

1. To prepare TiO₂ supported on zeolite Y samples by ion exchange, impregnation and sol-gel method.
2. To characterize physical and chemical properties of TiO₂ supported on zeolite Y by XRD, FT-IR, TEM, and ICP.
3. To investigate the photodegradation of methylene blue and phenosafranine using the prepared samples as photocatalysts under various affecting factors.

1.3 Scope and Limitation of the Study

This research is focused on the preparation of TiO₂ supported on zeolite Y by ion exchange impregnation and sol-gel method. The prepared samples were characterized by XRD, TEM, and ICP. Surface area and pore volume were also determined by BET method. The prepared photocatalysts were tested for their photocatalytic activity on degradation of textile dyes (methylene blue and phenosafranine) under various conditions namely initial concentration of textile dyes

and amount of TiO_2 loading and pH of solution. The photocatalytic efficiency of these prepared samples were evaluated in terms of discoloration of methylene blue and phenosafranine, and their efficiencies were compared with each other and with TiO_2 powder from Aldrich. The correlations between photoactivity of the prepared samples and their several properties were also studied.



CHAPTER II

BACKGROUND AND LITERATURE REVIEW

2.1 Zeolite Y

Zeolites are microporous crystalline solid with well-defined structures. Generally, they contain silicon, aluminium and oxygen in their framework and cations, water and other molecules within their pores. Many zeolites occur naturally as minerals, and are extensively mined in many parts of the world (Breck, 1974). Zeolites consisting of three dimensional framework structure were composed of TO_4 tetrahedra where T = Si, Al (framework of $[SiO_4]^{4-}$ and $[AlO_4]^{5-}$ tetrahedra). Zeolites have the general chemical formula (Roland and Kleinschmit, 1998):

$$M_{x/n} [(AlO_2)_x (SiO_2)_y] \cdot zH_2O \quad (2.1)$$

$$M_{2/n} O \cdot Al_2 O_3 \cdot y'SiO_2 \cdot z'H_2O \quad (2.2)$$

When formula (2.1) expression enclosed in the square brackets shows the composition of the anionic framework in the crystallographic unit cell; M represents the nonframework metal cation; n is its charge; z is the number of water molecules per unit cell; x and y are the total number of tetrahedra per unit cell and the ratio y/x usually has values of 1-5. Formula (2.2) occurs frequently in the literature and unlike

formula (2.1), where y' is 2 to 10, n is the cation (M) valence, and z' represents the water contained in the voids of the zeolite. The frameworks are open containing channels and cavities where cations and water molecules are located. Zeolites have uniform pore size (0.3 nm to 1.0 nm), which is uniquely determined by the unit structure of the crystal. The various zeolite structures differ not only in the type and dimensionality of their pore systems, but also in the size of the pore apertures. Narrow-pore, medium-pore, and wide-pore zeolites have different pore apertures formed by rings of 8, 10 or 12 T atoms, corresponding to crystallographic diameters of 0.35-0.45, 0.45-0.60, and 0.60-0.80 nm, respectively (Breck, 1974). Zeolite Y was first synthesized in the sodium form in 1964 by Union Carbide. It exhibits the FAU (faujasite) structure shown in the Figure 2.1. Zeolite Y was a 3-dimensional pore structure with pores running perpendicular to each other in the x, y, and z planes similar to LTA, and is made of secondary building units 4, 6, and 6-6. The pore diameter is large at 7.4Å, since the aperture is defined by a 12 member oxygen ring, and leads into a larger cavity of diameter 12Å. The cavity is surrounded by ten sodalite cages (truncated octahedral) connected on their hexagonal faces. The unit cell is cubic ($a = 24.7\text{\AA}$) with Fd-3m symmetry. Zeolite Y has a void volume fraction of 0.48, with a Si/Al ratio of 2.43. It thermally decomposes at 793°C (Herreros, www, 2001; Meier, www, 2001 and Bhatia, 1990). Zeolite Y like zeolite X, is synthesized in a gelling process. Sources of alumina (sodium aluminate) and silica (sodium silicate) are mixed in alkaline (NaOH) aqueous solution to give a gel. The gel is then usually heated to 70-300°C to crystallize the zeolite. The zeolite is present in Na^+ form and can be converted to acid form through NH_4^+ form before being converted to

acidic form (Bhatia, 1990). Because of such interesting properties, zeolites are widely used as catalysts and adsorbents for organic synthesis and decomposition as well as in waste-gas adsorption and waste-water treatment. Since, zeolite Y has relatively large pores than other zeolites. It can be modified through the incorporation of active species in the pores by various methods, such as ion exchange and impregnation (Chen *et al.*, 1999).

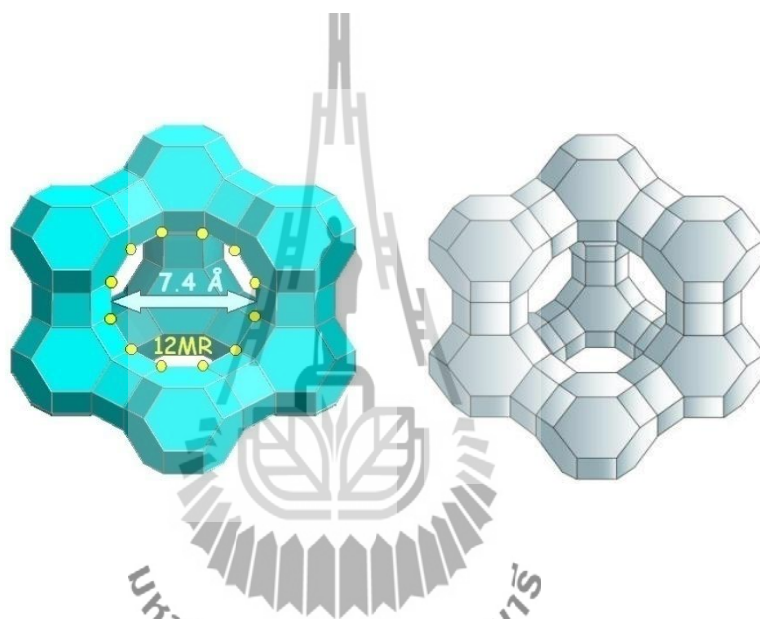


Figure 2.1 The structure of zeolite Y (Grey *et al.*, Adsorption and binding of hydro fluorocarbons (HFC's) in zeolites, www, 2009).

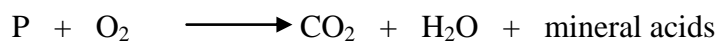
The empty intracrystalline spaces are in the nanometer or sub-nanometer length scale and termed *micropores*. It is possible to accommodate a photoactive guest within the internal voids of these pores created by the rigid framework. The photoactive guests can be an organic photosensitizer, and inorganic semiconductor or a combination of both. Moreover, the presence of heteroatom (Ti, V, and other transition metals) in the zeolite framework can make the structure as a whole act as a photocatalyst (Corma and Garcia, 2004). The combination of a zeolite host and

photoactive sites renders solid photocatalyst in which the high surface area and the absorbent capacity provided an increase in the efficiency of the photocatalytic process. Moreover, the zeolite pores define a compartmentalized space in which multi-component system can be easily assembled by a stepwise procedure. Zeolite based photocatalysts are promising for the abatement of air and water pollution using solar light, as well as for de-NO_x and de-SO_x processes, photoreduction of CO₂ by H₂O, photooxygenation of saturated hydrocarbon, photosplitting of water into hydrogen and oxygen, photogeneration of hydrogen peroxide and other photoprocesses of much current interest, particularly in environmental sciences and for the development of renewable energy resources alternative to fossil fuels (Corma and Garcia, 2004).

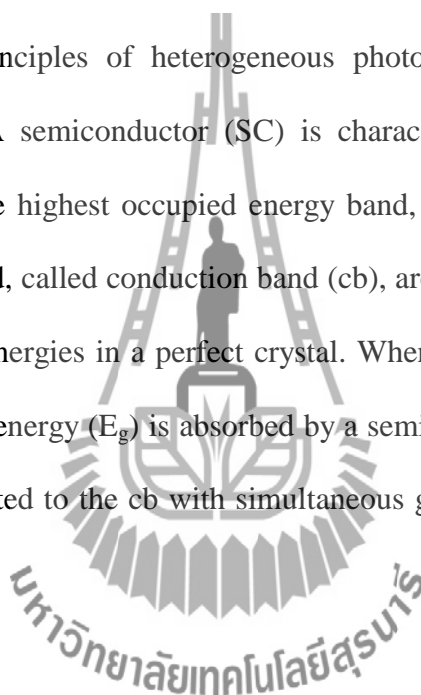
2.2 Principle of Photocatalysis Processes

The term photocatalysis consists of the combination of photochemistry and catalysis and implies that light and a catalyst are necessary to bring about or to accelerate a chemical transformation. In catalysed photolysis, light is absorbed by an adsorbed substrate. In photogenerated catalysis, the photocatalytic activity depends on the ability of the catalyst to create electron-hole pairs, which generate free radicals (hydroxyl radicals: OH[•]) able to undergo secondary reactions. Its comprehension has been made possible ever since the discovery of water electrolysis by means of the titanium dioxide. Commercial application of the process is called advanced oxidation process (AOP). There are several methods of achieving AOP's that can but do not necessarily involve TiO₂ or even the use of UV light. Generally, the defining factor is the production and use of the hydroxyl radical.

The overall process for the photocatalysis reaction of waste material (P), sensitised by semiconductors (SC) is shown



The basic principles of heterogeneous photocatalysis can be summarized shortly as follows. A semiconductor (SC) is characterized by an electronic band structure in which the highest occupied energy band, called valence band (vb), and the lowest empty band, called conduction band (cb), are separated by a bandgap, i.e. a region of forbidden energies in a perfect crystal. When a photon of energy higher or equal to the bandgap energy (E_g) is absorbed by a semiconductor particle, an electron from the vb is promoted to the cb with simultaneous generation of a hole (h^+) in the vb (Litter, 1999).



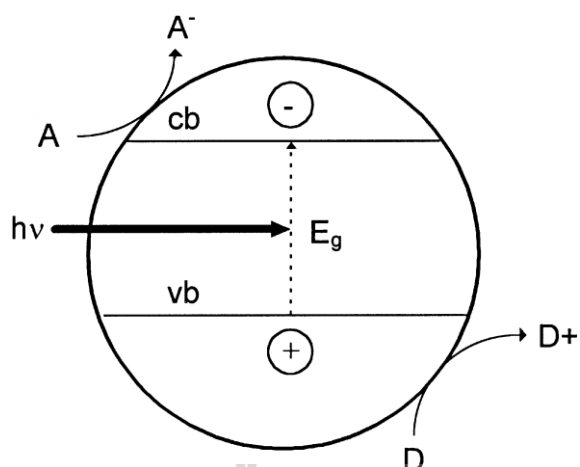


Figure 2.2 Promotion of an electron from the valence band to the conduction band on illumination of a semiconductor (Litter, 1999).

The electron and the hole pair can recombine on the surface or in the bulk of the particle in a few nanoseconds (and the energy dissipated as heat) or can be trapped in surface states where they can react with other species that are adsorbed or close to the surface of the particle. Thereby, subsequent anodic and cathodic redox reactions can be initiated. The energy level at the bottom of the cb is actually the reduction potential of photoelectrons and the energy level at the top of the vb determines the oxidizing ability of photoholes, each value reflecting the ability of the system to promote reductions and oxidations. The flat band potential, V_{fb} , locates the energy of both charge carriers at the SC-electrolyte interface, and depends on the nature of the material and the system equilibria. From a thermodynamic point of view, adsorbed couples can be reduced photocatalytically by cb electrons if they have redox potentials more positive than the V_{fb} of the cb, and can be oxidized by vb holes if they have redox potentials more negative than the V_{fb} of the vb (Litter, 1999).

2.3 Type of Semiconductor

Many semiconductors used as photocatalyst should be an oxide or sulfide of metals such as TiO_2 , ZnO , CdS , ZnS , and WO_3 have been studied for the role of photocatalysts, and TiO_2 was found to be one of the most promising agents for removal of refractory compounds and xenobiotics (Kabir *et al.*, 2006). The energy band gap of the photocatalyst should match the energy gained from a light source. The valence band, conduction band, band gap and band gap wavelength of some semiconductor are shown in Table 2.1. TiO_2 is a popular photocatalyst because the band gap is considerably high, namely 3.0 eV. It can be activated in the near ultraviolet light (~380 nm). Other type of semiconductors that can be used as photocatalysts such as ZnO or CdS , but may not be applicable due to their toxicity. Many investigations have been carried out to observe the effect of the variety of supporting material for degradation of organic compound. In general, it is assumed the good supporting materials for TiO_2 as photocatalyst should have the following attributes (Pozz *et al.*, 1997):

- (1) To be transparent to UV radiation
- (2) To favor strong surface chemical-physical bound with the TiO_2 particles without negative effecting their activity
- (3) To offer a high specific surface area
- (4) To have a good adsorption capability for the organic compound to be degraded
- (5) To be in a physical configuration which favors the liquid-solid separation.

(6) To allow reactor designs that facilitate the mass transfer processes

(7) To be chemically inert

Table 2.1 The band positions of some common semiconductor photocatalysts

(Robertson, 1996).

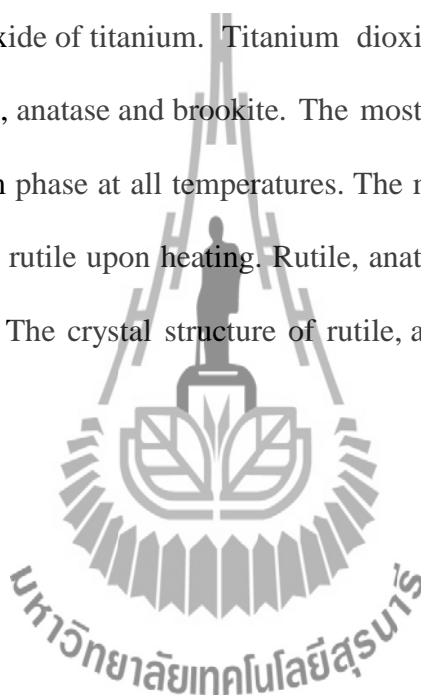
Semiconductor	Valence band (eV)	Conduction band (eV)	Band gap (eV)	Band gap wavelength (nm)
TiO ₂	3.1	0.1	3.0	380
SnO ₂	4.1	0.3	3.9	318
ZnO	3.0	0.2	3.2	390
ZnS	1.4	-2.3	3.7	336
WO ₃	3.0	0.2	2.8	443
CdS	2.1	-0.4	2.5	497
CdSe	1.6	-0.1	1.7	730
GaAs	1.0	-0.4	1.4	887
GaP	1.3	-1	2.3	540

The efficiency of TiO₂ was reported to be influenced by many factors, such as crystalline structure, particle size, and preparation methods. In the past few years, some efforts have been put in increasing the TiO₂ surface area by dispersing nanoparticles of TiO₂ on high surface area materials. The supports have been used

including silica gels, active carbon, zeolites and clays. Some of these studies have also included an effort to increase the adsorption of organic substrates on the catalyst surface for improving the efficiency of catalytic activity (Hsien *et al.*, 2001).

2.4 Titanium Dioxide

Titanium dioxide (TiO_2) also known as titanium (IV) oxide or titania, is the naturally occurring oxide of titanium. Titanium dioxide occurs in nature as well-known minerals rutile, anatase and brookite. The most common form is rutile which is also the equilibrium phase at all temperatures. The metastable anatase and brookite phases both convert to rutile upon heating. Rutile, anatase and brookite all contain six coordinated titanium. The crystal structure of rutile, anatase and brookite are shown in Figure 2.3



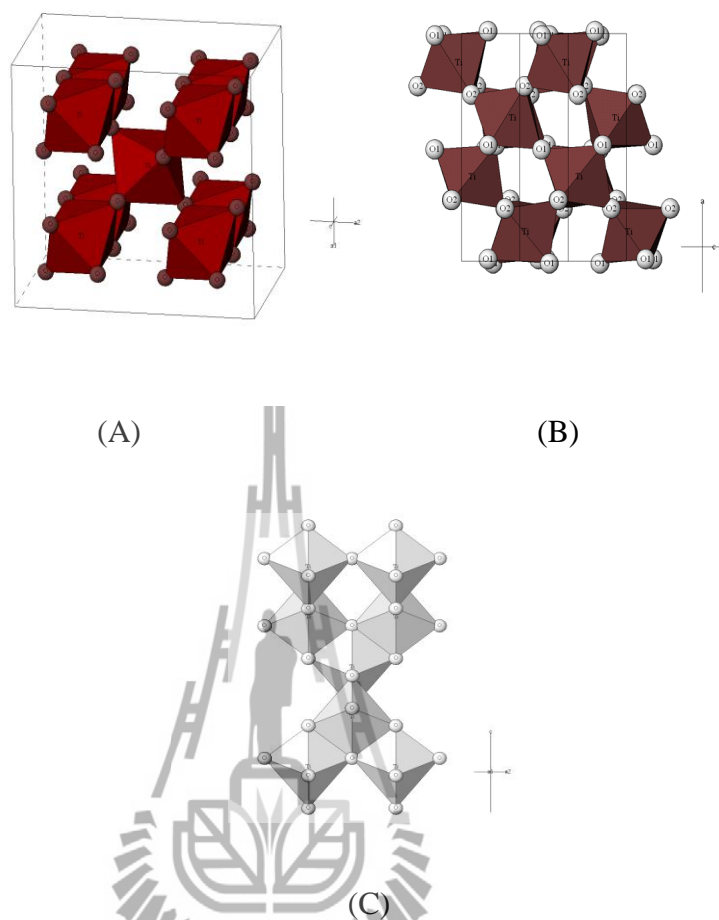


Figure 2.3 Crystal structure of Rutile (A), Brookite (B), and Anatase (C) (Crystal Structure Gallery, [www, 2002](http://www.crystalstructure.com)).

Titanium dioxide, particularly in the anatase form is usually believe to be more photocatalytically active than rutile structure (Liu *et al.*, 2006 and Sen *et al.*, 2005). Recently it has been found that titanium dioxide, when spiked with nitrogen ions or doped with metal oxide like tungsten trioxide, is also a photocatalyst under either visible or UV light. The strong oxidative potential of the positive holes oxidizes water to create hydroxyl radicals. It can also oxidize oxygen or organic materials directly. Titanium dioxide is thus added to paints, cements, windows, tiles, or other products for its sterilizing, deodorizing and anti-fouling properties and is

used as a hydrolysis catalyst. It is also used in dye-sensitized solar cells, which are a type of chemical solar cell (also known as a Graetzel cell).

2.5 Preparation TiO₂ Supported on Zeolite Y

There are many researches on incorporation of TiO₂ on zeolites. The incorporation of TiO₂ in zeolite can be performed by ion exchange, impregnation and sol-gel method and has been used as photocatalyst for study of photocatalytic reaction.

Kruegger *et al.* (1990) and Iu *et al.* (1990) reported the preparation of TiO₂ in zeolite through a sol gel technique and presented diffuse reflectance spectra of the materials obtained. The spectra exhibited a significant blue-shift of the absorption threshold. In 1992, Liu *et al.*, showed reported a new method of incorporating TiO₂ particles into zeolite cavities through ion exchange of zeolites Y with an aqueous solution of ammonium titanyl oxalate monohydrate, (NH₄)₂TiO(C₂O₄)2H₂O. The results showed that Ti species are located inside the zeolite cavities, but not on the external surface of the zeolite. TiO₂/zeolite composites, changes in microporosity of the composites must take place. So, the important to improve the adsorption and catalytic activities is to control of both the dispersed state of TiO₂ and the porosity of the zeolite (Lui *et al.*, 1992; Anandan and Yoon, 2003).

In 1995, Xu and Langford prepared the catalysts by mixing a TiO₂ with the powder of supports such as ZSM-5, Zeolite A, silica and alumina for investigation photocatalytic activity of 4-chlorophenol and acetophenone. The catalysts were prepared by mixing a TiO₂ sol with the powder of supports. It was found that the photocatalytic activity of titanium dioxide on ZSM-5 and zeolite A was higher than

that TiO_2 formed on silica and alumina. $\text{TiO}_2/\text{ZSM-5}$, which showed the highest photoactivity at low Ti content, was observed to have large adsorptivity for the organic substrate. It may be that adsorption and zeolite structure are factors which may be responsible for enhancement of photocatalytic activity of supported TiO_2 . From XRD, BET, FTIR, and Raman indicated that titanium oxide is formed as small particles of anatase on all the supports and that there are also noncrystalline titanium oxide species formed on zeolite supports (Xu and Langford, 1995). In 1997, Xu and Langford studied the photocatalytic degradation of acetophenone in an aqueous medium with the titanium dioxide supported on zeolite X, Y, and MCM-41. The result showed that the highest photoactivity among the supported catalysts is observed for a support that has a lower Si/Al ratio in the framework and relatively large pore size. The photoactivity of the supported catalyst is strongly influenced by method of titania loading, but less effected by the temperature at which the sample was calcined (Xu and Langford, 1997).

In 1999, Chen *et al.* attempted to prepare TiO_2 -dispersed on zeolites with varying TiO_2 amounts by ion-exchange and or impregnation of ammonium titanyl oxalate $(\text{NH}_4)_2\text{TiO}(\text{C}_2\text{O}_4)_2$. The samples were characterized by X-ray diffraction (XRD), IR, EXAFS, and ICP. The results indicated that the framework of zeolite Y was retained through the modification and TiO_2 was incorporated in the form of anatase microcrystals. A part of TiO_2 on the zeolite Y is titanium species bound to the framework through Ti-O-Si bonds. The pore size of TiO_2 modified zeolite Y was proved to be increased with the amount of incorporated TiO_2 (Chen *et al.*, 1999). In 2005, Easvaramoorthi and Natarajan prepared TiO_2 encapsulated in the zeolite cavity with potassium titanooxalate in aqueous solution. They found that TiO_2 nanoparticles

present in the zeolite were too small to be detected by the XRD (Easwaramoorthi and Natarajan, 2005). TiO_2 nanoclusters thus formed are entrapped in the supercages of the zeolite Y and maximum size of the TiO_2 cluster present in the supercage may not be larger than 1.3 nm, the diameter of the supercage.

Impregnation is the other method often used to prepare TiO_2 incorporated in the zeolite by suspending the zeolite with organotitanium in organic solvent. In 2001, Yu-Hsien *et al.* prepared and characterized TiO_2 supported on NaY, Na-mordenite, and MCM-41 by suspending titanium ethoxide $[\text{Ti}(\text{EtOH})_4]$ in hexane/heptane with volumetric ratio of 1/1. The results of XRD showed that the supported TiO_2 was crystallized in anatase form and the intensity of its XRD peaks increase with TiO_2 loading. In contrast, the total area of catalyst decrease with increasing TiO_2 (Hsien *et al.*, 2001). In addition, Wang *et al.* prepared TiO_2 supported on zeolite by using impregnation method. Ti-source, tetraethylorthotitanate, was added to Na-Y zeolite in hexane/heptane with volumetric ratio of 1/1. They studied the operational parameters such as TiO_2 content, calcination temperature and pH. The higher TiO_2 loadings and higher temperatures of calcinations may well produce larger TiO_2 crystallites on the zeolite support (Wang *et al.*, 2008).

2.6 Photocatalytic Oxidation Dyes and Organic Compound

TiO_2 particles have been utilized to promote the photocatalytic degradation of various organic compounds. The photocatalytic efficiency of TiO_2 is greatly influenced by crystal structure, particle size, surface area and porosity as determined by different preparation methods. Increasing the photocatalyst surface area is the most

obvious means of improving the efficiency of photocatalytic oxidation reactions (Xu and Langford, 1997).

In 2001, Corrent *et al.* determined the photophysical properties of TiO_2 included in zeolites Y, β and mordenite by using time-resolved techniques. A blueshift in the groundstate absorption spectra of the zeolite samples compared to bulk anatase was observed and attributed to a direct transition in the semiconductor, rather than a change in the band gap energy due to a size quantization effect. Through time-resolved fluorescence measurements, it was determined that two different Ti sites are present in the nanocluster, depending on sample conditioning: one site consists of Ti in a “closed” environment and the other site has hydroxyl groups bonded to Ti atoms, due to the presence of hydration water, which acts as a ligand. The reduction in intensity that is seen upon heating the samples at 300°C is attributed to the formation of defect sites in the nanocluster, resulting in fewer charge transfer states, and thus a lower emission intensity (Corrent *et al.*, 2001).

Anandan *et al.* prepared and characterized heteropolytungstic ($\text{H}_3\text{PW}_{12}\text{O}_{40}$, HPA) encapsulated into the titanium exchanged-HY (TiHY) zeolite. In the photoreaction study of methyl orange with HPA encapsulated into TiHY zeolite which those are very active as a photocatalyst towards the photoreaction of methyl orange (Anandan and Yoon, 2003). In 2005, Guettä and Amar investigated photocatalytic oxidation of a mono azo dye methyl-orange under various physico-chemical conditions using TiO_2/UV aqueous system and artificial UV-light. It was found that the efficiency of the process strongly depended on the working conditions such as: substrate concentration, catalyst amount and pH of solution. Varieties of commercial TiO_2 catalysts using several crystalline were tested to compare their

photoactivity. As a result, it was found that the efficiency of the process strongly depended on the working conditions (Guettà and Amar, 2005). In 2007, Yahiro and coworkers investigated photocatalytic reaction in the partial oxidation of α -methylstyrene to acetophenone with photocatalysts of TiO_2 supported on zeolite Y, modenite and ZSM-5 zeolite. The catalysts can catalyze the partial oxidation of α -methylstyrene to acetophenone under partial oxidation and light irradiation ($>290\text{nm}$) (Yahiro *et al.*, 2007). Faisal *et al.* investigated the photocatalysed degradation of Acridine Orange and Ethidium Bromide in aqueous suspensions of titanium dioxide under a variety of conditions (types of TiO_2 , reaction pH, catalyst concentration, substrate concentration and in the presence of different electron acceptors). They found that all the above parameters strongly influenced with the degradation rates. In the case of Acridine Orange, the highest efficiency was observed at pH 10 whereas, in the case Ethidium Bromide, a better rate was observed at pH 4.6. The highest efficiency of degradation in alkaline pH could be attributed to more efficient generation of hydroxyl radicals by TiO_2 with increasing concentration of hydroxide ion. In the case of Acridine Orange the most appropriate concentration for the maximum degradation rate was 0.25 mM and a further increase in concentration led to a decrease in the degradation rate. On the other hand for the Ethidium Bromide a decrease in the degradation rate was observed from 0.1 to 0.4 mM (Faisal *et al.*, 2007). Wang *et al.* studied the effects of TiO_2 loading on the performance of the TiO_2 /zeolite catalysts in the photodegradation of C.I. Basic Violet 10. The decolorization rates did not increase linearly with increasing TiO_2 content. Indeed, maximum value was achieved at a medium loading of 20% TiO_2 which might be due to two competitive processes (Wang *et al.*, 2008).

2.7 Characterization Techniques

2.7.1 Power X-ray Diffraction

X-ray diffraction (XRD) is a powerful technique used to uniquely identify the crystalline phases present in materials and to measure the structural properties (strain state, grain size, phase composition, preferred orientation, and defect structure) of these phases. The X-ray region is normally considered to be the part of the electromagnetic spectrum lying between 0.1 and 100 Å bounded by X-ray region to the short wavelength side and the vacuum ultraviolet region to the long wavelength side. In terms of energy, the X-ray region covers the range from about 0.1 to 100 keV. An X-ray diffraction has been used two main areas; the fingerprint characterization of the crystalline materials and the determination of their structure. Each crystalline solid has its unique characteristic X-ray powder pattern, which may be used as a “fingerprint” for its identification. Once the material has been identified, an X-ray crystallography may be used to determine its structure, i.e. how the atoms packed together in the crystalline state and what the inter-atomic distance and angle are. These unique properties make XRD one of the most important characterization tools used in solid state chemistry and the material science. An important equation for XRD is Bragg’s equation, which shows the relationship between X-ray wavelength (λ) with lattice point distance (d) and incident diffraction angle (θ).

$$n\lambda = 2d\sin\theta \quad (2.3)$$

The different crystal plane in the crystal will diffract X-ray at different angles according to the Bragg’s equation. Therefore, by rotating the sample plane with respect to the incident X-ray, the diffracted angles can be recorded by a detector

and the diffraction pattern is obtained. The identification of the sample structure can be done by comparing the spectrum with the pattern stored in the database.

2.7.2 Transmission Electron Microscopy (TEM)

Transmission electron microscopy (TEM) is a microscopy technique whereby a beam of electrons is transmitted through an ultra thin specimen, interacting with the specimen as it passes through. An image is formed from the interaction of the electrons transmitted through the specimen; the image is magnified and focused onto an imaging device, such as a fluorescent screen, on a layer of photographic film, or to be detected by a sensor such as a CCD camera. TEMs are capable of imaging at a significantly higher resolution than light microscopes, owing to the small de Broglie wavelength of electrons. This enables the instrument's user to examine fine detail even as small as a single column of atoms, which is tens of thousands times smaller than the smallest resolvable object in a light microscope. TEM forms a major analysis method in a range of scientific fields, in both physical and biological sciences. TEMs find application in cancer research, virology, materials science as well as pollution and semiconductor research. At smaller magnifications TEM image contrast is due to absorption of electrons in the material, due to the thickness and composition of the material. At higher magnifications complex wave interactions modulate the intensity of the image, requiring expert analysis of observed images. Alternate modes of use allow for the TEM to observe modulations in chemical identity, crystal orientation, electronic structure and sample induced electron phase shift as well as the regular absorption based imaging.

2.7.3 Brunauer-Emmett-Teller (BET)

In 1938, The first developed the BET theory for a flat surface and there is no limit in the number of layers that can be accommodated on the surface. The surface is energetically homogeneous (adsorption energy does not change with the progress of adsorption in the same layer) and there is no interaction among adsorbed molecules.

$$\frac{V}{V_m} = \frac{1}{(1 - P/P_0)} \quad (2.4)$$

Equation 2.4 is the famous BET equation, and it is used extensively for the determination of area because once the monolayer coverage V_m is known and if the area occupied by one molecule is known the surface area of the solid can be calculated. To conveniently determine V_m , the BET equation can be cast into the form, which is amenable for a linear plot as follows:

$$\frac{P}{V(P_0 - P)} = \frac{1}{V_m C} + \left(\frac{C-1}{V_m C} \right) \frac{P}{P_0} \quad (2.5)$$

The pressure range of validity of the BET equation is $P/P_0 = 0.05-0.3$. For relative pressures above 0.3, there exists capillary condensation, which is not amenable to multilayer analysis. A plot of $(P/(V(P_0 - P)))$ versus P/P_0 would yield a straight line with a slope $((C-1)/CV_m)$ and an intercept $(1/CV_m)$. Usually the value of C is very large because the adsorption energy of the first layer is larger than the heat of liquid faction, the slope is then simply the inverse of the monolayer coverage, and the intercept is effectively the origin of such plot. Therefore, very often only one

point is sufficient for the first estimate of the surface area. Once V_m (mole/g) is obtained from the slope, the surface area is calculated from:

$$A = V_m N_A a_m \quad (2.6)$$

Where N_A is the Avogadro number and a_m is the molecular project area (nitrogen = 16 \AA^2 /molecule at 77 K) (Do, 1998).

2.7.4 Inductively Coupled Plasma Mass Spectrometry (ICP-MS)

This is a very powerful tool for *trace* (ppb-ppm) and *ultra-trace* (ppq-ppb) elemental analysis. ICP-MS is rapidly becoming the technique of choice in many analytical laboratories for the accurate and precise measurements needed for today's demanding applications. In ICP-MS, a plasma or gas consisting of ions, electrons and neutral particles is formed from Argon gas. The plasma is used to atomize and ionize the elements in a sample. The resulting ions are then passed through a series of apertures (cones) into the high vacuum mass analyzer. The isotopes of the elements are identified by their mass-to-charge ratio (m/e) and the intensity of a specific peak in the mass spectrum is proportional to the amount of that isotope (element) in the original sample.

2.7.5 Ultraviolet-Visible Spectroscopy

Ultraviolet-visible spectroscopy or ultraviolet-visible spectrophotometry (UV-VIS) refers to absorption spectroscopy or reflectance spectroscopy in the ultraviolet-visible spectral region. This means it uses light in the visible and adjacent (near-UV and near-infrared (NIR)) ranges. The absorption or reflectance in the visible range directly affects the perceived color of the chemicals involved. In this

region of the electromagnetic spectrum molecules undergo electronic transitions. This technique is complementary to fluorescence spectroscopy, in that fluorescence deals with transitions from the excited state to the ground state while absorption measures transitions from the ground state to the excited state.

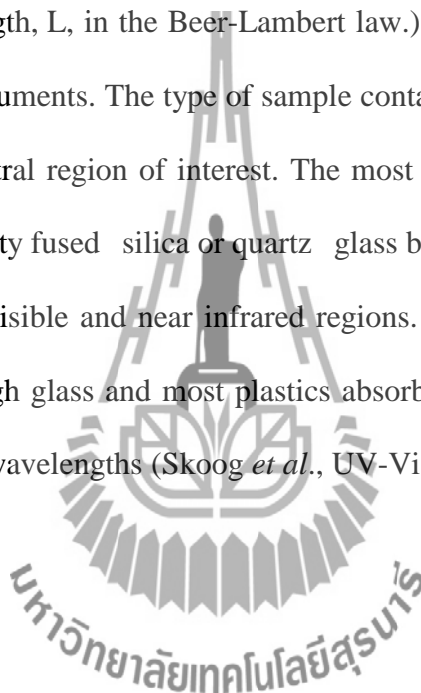
UV/Vis spectroscopy is routinely used in analytical chemistry for the quantitative determination of different analytes, such as transition metal ions, highly conjugated organic compounds and biological macromolecules. Determination is usually carried out in solutions. The method is most often used in a quantitative way to determine concentrations of an absorbing species in solution, using the Beer-Lambert law,

$$A = -\log(I_0/I) = \epsilon \cdot c \cdot L \quad (2.7)$$

Where A is the measured absorbance, I_0 is the intensity of the incident light at a given wavelength, I is the transmitted intensity, L the pathlength through the sample, and c the concentration of the absorbing species. For each species and wavelength, ϵ is a constant known as the molar absorptivity or extinction coefficient. This constant is a fundamental molecular property in a given solvent, at a particular temperature and pressure, and has units of $1/M \cdot \text{cm}$ or often $AU/M \cdot \text{cm}$.

The basic parts of a spectrophotometer are a light source, a holder for the sample, monochromator to separate the different wavelengths of light and a detector. A spectrophotometer can be either single beam or double beam, in a double-beam instrument, the light is split into two beams before it reaches the sample. One beam is used as the reference; the other beam passes through the sample. The reference beam intensity is taken as 100% Transmission (or 0 Absorbance), and the

measurement displayed is the ratio of the two beam intensities. Some double-beam instruments have two detectors (photodiodes), and the sample and reference beam are measured at the same time. Samples for UV/Vis spectrophotometry are most often liquids, although the absorbance of gases and even of solids can also be measured. Samples are typically placed in a transparent cell, known as a cuvette. Cuvettes are typically rectangular in shape, commonly with an internal width of 1 cm. (This width becomes the path length, L , in the Beer-Lambert law.) Test tubes can also be used as cuvettes in some instruments. The type of sample container used must allow radiation to pass over the spectral region of interest. The most widely applicable cuvettes are made of high quality fused silica or quartz glass because these are transparent throughout the UV, visible and near infrared regions. Glass and plastic cuvettes are also common, although glass and most plastics absorb in the UV, which limits their usefulness to visible wavelengths (Skoog *et al.*, UV-Vis spectroscopy, www, 2011).



CHAPTER III

EXPERIMENTAL

3.1 Chemicals and Materials

- Ammonium titanyl oxalate $(\text{NH}_4)_2\text{TiO}(\text{C}_2\text{O}_4)_2$, Analytical reagent, Aldrich, Germany.
- Buffer solution pH 4 (20°C), Analytical reagent, Merck, Germany.
- Buffer solution pH 7 (20°C), Analytical reagent, Merck, Germany.
- Buffer solution pH 10 (20°C), Analytical reagent, Merck, Germany.
- Hexane, C_6H_{14} , Analytical reagent, J.T.baker, Thailand.
- Heptane, C_7H_{16} , Analytical reagent, J.T.baker, Thailand.
- Hydrochloric acid 37% (HCl), Analytical reagent, QRëC, New Zealand.
- Nitric acid 65% (HNO_3), Analytical reagent, QRëC, New Zealand.
- Sodium aluminate ($\text{Na}_2\text{Al}_2\text{O}_4$), Analytical reagent, Riedel-de Haën, Germany.
- Sodium hydroxide (NaOH), Analytical reagent, Merck, Germany.
- Sodium silicate powder (Na_2SiO_3), Analytical reagent, Riedel-de Haën, Germany.
- Titanium (IV) ethoxide $[\text{Ti}(\text{OC}_2\text{H}_5)_4]$, Ti 20%, Analytical reagent, Aldrich, Germany.
- Titanium (IV) oxide (TiO_2), Analytical reagent, Aldrich, Germany.
- Titanium tetraisopropoxide $[\text{Ti}[\text{OCH}(\text{CH}_3)_2]_4]$, Ti $\geq 99\%$, Analytical reagent, Aldrich, Germany.

- Methylene blue ($C_{16}H_{18}ClN_3S$), Analytical reagent, QRëC, New Zealand.
- Phenosafranine ($C_{18}H_{15}ClN_4$), Analytical reagent, Aldrich, Germany.
- Distilled water and deionised water.

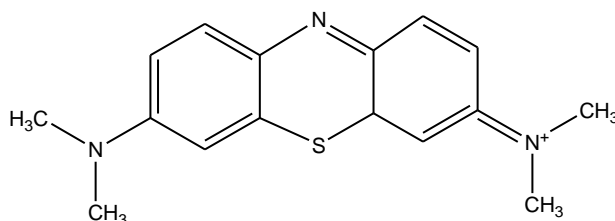


Figure 3.1 The structure of methylene blue.

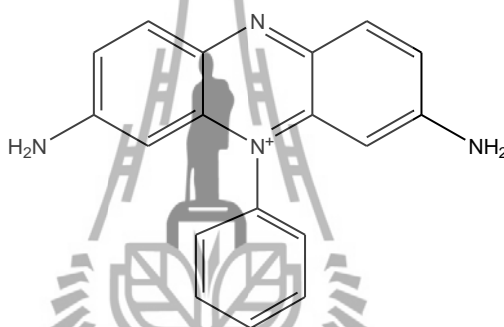


Figure 3.2 The structure of phenosafranine.

3.2 Apparatuses

- Analytical balance (Model 250A, Precisa, Switzerland).
- Black light (40w).
- Centrifuge (Labofuge 200, Heraeus Sepatect).
- Furnace chamber (Carbolite CWF 12/23).
- Glass microfiber filters, (Whatman GF/C diameter 47 mm).
- Hot air oven (Binder).
- Magnetic stirrer (Horst).

- Micropipets.
- pH meter (Mettler Toledo).
- Vacuum filtration apparatus (Gast).

3.3 Instrumentations

- Power X-ray diffractometer, Bruker D5005 powder, was employed to confirmed crystallinity of zeolite Y and TiO_2 .
- The Brunauer-Emmett-Teller (BET) surface area was obtained from BET method with a NOVA 1200E surface area analyzer.
- Fourier transform infrared spectrophotometer (FT-IR), GX-FTIR, was used to detect the functional groups of residual organic species left in TiO_2 /zeolite Y.
- UV-VIS spectrophotometer (Varian model Cary 1E) was used to determined the concentration of dyes solutions.
- Inductively Coupled Plasma Mass Spectrometer (ICP-MS, Agilent 7500 ICP-MS) was employed to determine element compositions of the prepared TiO_2 / zeolite Y.
- Transmission electron microscopy (TEM), JEM-2010 was used to determine a shape and dispersion of TiO_2 loaded on zeolite.

3.4 Procedures

3.4.1 Synthesis of Zeolite Y

Zeolite Y was synthesized by hydrothermal reaction with mole ratio of starting reagent : $4.62\text{Na}_2\text{O} : \text{Al}_2\text{O}_3 : 10\text{SiO}_2 : 180\text{H}_2\text{O}$ (Ginter *et al.*, www, 2005). Firstly, seed gel was prepared by 6.65g of deionized water (DI water) mixed with 1.36 g of NaOH and 0.70 g of $\text{Na}_2\text{Al}_2\text{O}_4$ and stirred in 50 ml plastic bottle until dissolved. Then, 7.57 g of Na_2SiO_3 solution was added in to the mixture, stirred until gel appeared and aged for one day. Feed stock gel was prepared by 43.52 g of DI water mixed with 0.05 g of NaOH and 4.36 g of $\text{Na}_2\text{Al}_2\text{O}_4$. Then, 47.48 g of Na_2SiO_3 solution was added in to the mixture and it was stirred vigorously until the gel was appeared smooth. Finally, 5.50 g of seed gel was added to feedstock gel under stirring vigorously up to 20 minutes. The solution was aged at room temperature for 1 day, then it was crystallized at 100°C for 7 h. The solid phase was separated from the mother liquor by filtration, washed by distilled water until the pH of filtrate became 7, afterwards dried at 110°C for overnight. The synthesized zeolite Y would be used for supporting TiO_2 in the further preparations.

3.4.2 TiO_2 Supported on Zeolite Y

The symbols of Ti/NaY IE, Ti/NaY-IMP and Ti/NaY-SG were denoted as the sample of TiO_2 supported on zeolite NaY prepared by ion exchange, impregnation and sol gel method, respectively.

3.4.2.1 Ion Exchange Method

The TiO_2 supported on zeolite Y sample was prepared by modified method available in the literatures (Liu *et al.*, 1992, and Chen *et al.*, 1999). Zeolite NaY 0.5 g was added in 50 ml of ammonium titanyl oxalate $((\text{NH}_4)_2\text{TiO}(\text{C}_2\text{O}_4)_2, \text{ATO})$ solution, which was used as a precursor for prepared TiO_2 , with concentrations of 5.0, 10.0, 15.0, 20.0, 30.0, and 40.0mM (denoted as 5.0 mM, 10.0 mM, 15.0 mM, 20.0 mM, 30.0 mM and 40.0 mM ATO/NaY-IE, respectively.) and stirred for 24 h. Then, the samples were filtered and washed by deionized water until the pH of filtrate became 7 and dried at 120°C for 3 h. then calcined at 500°C for 2 h.

3.4.2.2 Impregnation Method

The TiO_2 supported on zeolite Y samples were prepared by modified method available in the literature (Hsien *et al.*, 2001). TiO_2 was prepared by using titanium ethoxide $(\text{Ti}(\text{EtOH})_4)$ as a precursor. Titanium ethoxide with different volumes of 0.5, 1.0, 2.0, and 3.0 ml (corresponding to 4.6, 9.2, 18.2, and 27.4wt% Ti/NaY) was added to zeolite NaY 0.50 g suspended in the solvent composed of hexane/heptane with volumetric ratio of 50 ml to 50 ml, and the mixture was stirred for 1 h in air. Then solvent was removed by rotary evaporation. The resultant solid was dried at 120°C and calcined at 550°C for 6 h. In this preparation, the samples with different amounts of Ti such as 0.5, 1.0, 2.0, and 3.0 ml of $(\text{Ti}(\text{EtOH})_4)$ samples were denoted as 4.6, 9.2, 18.2, and 27.4wt% Ti/NaY-IMP.

3.4.2.3 Sol-Gel Method

TiO₂ supported on zeolite Y samples were prepared according to the literature (Xu and Langford, 1995). Firstly, TiO₂ sol-gel was synthesized by method called acid-catalyzed sol-gel formation. The mixture composed of 100 ml of water, 0.50 ml of nitric acid and 14.05 g of titanium tetraisopropoxide (as a precursor for prepared TiO₂) dissolved in 5.0 ml ethanol. The mixture was maintained under stirring for at least 8 h before it was added with water saturated zeolite Y. In a typical preparation of a supported photocatalyst, 2.25 g of zeolite Y saturated with 5.0 ml of water for half an hour was added into TiO₂ sol-gel having different volumes (5.0, 7.0, 10.0, 20.0, and 30.0 ml) and the mixture was still stirred for 1 h. Then it was dried by evaporation at 50°C and followed by heating at 120°C overnight. Finally, the solid was calcined at 450°C for 11 h. The obtained samples with different amounts of Ti were denoted as 9.33, 18.67, 28.0, 37.33, 46.67, and 55.56wt% Ti/NaY-SG.

3.5 Characterization of Prepared TiO₂ Supported on Zeolite Y

The prepared samples from 3.4.2.1-3.4.2.3 including TiO₂ from Aldrich were characterized by XRD, FT-IR, TEM, ICP and BET method.

3.5.1 Study on Crystallization of Zeolite Y and Crystallization Forms of TiO₂

Prior to the measurement, each sample was prepared using a standard method for powder sample preparation. The procedure for powder XRD sample preparation was described as follows: dried the sample in oven at 110°C, ground about 1.00 g of each solid sample to fine powder as homogeneous as possible, and then load into the polymethyl methacrylate (PMMA) sample holder. The X-ray was

generated with a Cu K α target with a current of 35 mA and potential of 35 kV. Each diffraction spectrum was recorded with the condition: 2 θ angle of between 3° and 50° and scan speed of 0.4 degree/0.02 second. Typically, the data was expressed in the plot between intensity of diffraction peaks and 2 θ angle. The position of diffraction peaks were compared with a reference database and the identification of compounds could be obtained. The % crystallite was calculation by equation 3.1 as follows:

$$\% \text{ cry} = \frac{\text{total area of 10 strong peaks of sample}}{\text{total area of 10 strong peaks of standard}} \times 100 \quad (3.1)$$

3.5.2 Determination of Surface Area and Pore Size

The specific surface areas were measured by BET method using adsorption of nitrogen in high vacuum system. An adsorption isotherm was measured using N₂ gas at 76°C. The sample of TiO₂/zeolite Y was degassed to remove impurities from the surface and pore volume of the sample. After degas, an exact weight of each sample (approximately 0.2 g) was recorded before running adsorption step. The volume of adsorbed N₂ was normalized to stand temperature and pressure. The obtained data was displayed as surface area and pore size distribution.

3.5.3 Determination of Element Compositions of TiO₂/Zeolite NaY

Determination of element compositions (Na, Si, Al, O, and Ti) of the samples was carried out using Agilent 7500 ICP-MS. Before measurement, the sample was prepared by digestion in PTFE vessel developed in the laboratory. Concentrated nitric acid (65% w/v), hydrofluoric acid, hydrochloric acid (37% w/v)

and boric acid (4% w/v) were used for digestion and cleaning of the digestion tube. Deionized water (Milli-Q ultrapure water) was used throughout.

3.5.4 Determination of Dye Concentrations

The concentrations of dyes in the reaction were determined by UV-Vis spectroscopy. All of the dye solutions were diluted in order to reach an appropriate absorbance value lying on the calibration curve before analysis with UV-Vis spectroscopy. λ_{max} of methylene blue and phenosafranin were 664 nm and 520 nm, respectively.

3.6 The Study of Photodegradation of Methylene Blue Using TiO₂ Supported on Zeolite NaY Prepared by Ion Exchange Method

3.6.1 Effect of TiO₂ Content Loaded on Zeolite NaY

There were five prepared samples of TiO₂ with different amounts loaded on zeolite NaY (see section 3.4.2.1) used in the photooxidation of methylene blue. The aqueous solution of the studied compound was prepared by dilution of stock solution. The studied solution (50.0 ml) of a known concentration of methylene blue was loaded together with 0.050 g of each sample of TiO₂/zeolite NaY and transferred into a reactor. The reaction was carried out at ambient temperature. For all experiments, the suspension was stirred and allowed to equilibrate in the absence of light for 15 minutes. When the reactor began to be irradiated by lamp, at this time ($t=0$). An aliquot of the irradiated sample mixture (8 ml) was taken out subsequently at desired periods of irradiation. The irradiated samples were centrifuged to separate solid sample before analyzing concentration of methylene blue. The concentration of

methylene blue was measured by UV-VIS spectrophotometry at λ_{\max} 664 nm. The photodegradation efficiency (y) was determined by equation (3.1)

$$y = \frac{C_0 - C}{C_0} \quad (3.2)$$

Where C_0 and C were concentration of methylene blue at initial and at time (t), respectively.

3.6.2 Effect of Initial Concentration of Methylene Blue

The effect of initial concentration of methylene blue was investigated under the following conditions: $\text{TiO}_2/\text{zeolite NaY}$ 0.050 g, pH 7, and the initial concentrations were 0.10, 0.13, 0.16, and 0.2 mM.

3.6.3 Effect of pH

The effect of pH of the solution on the photooxidation rate was studied under following conditions: 0.050 g of $\text{TiO}_2/\text{zeolite NaY}$, initial concentration of methylene blue 0.10 mM, and the pH of the solution was varied from 4.0 to 9.0. The pH of the solution was adjusted by adding a dilute solution of HCl or NaOH.

3.7 The Study of Photodegradation of Methylene Blue Using TiO₂ Supported on Zeolite NaY Prepared by Impregnation Method

3.7.1 Effect of TiO₂ Content Loaded on Zeolite NaY

Various synthesized amounts of TiO₂ loaded on zeolite NaY (see section 3.4.2.2) were used in the photodegradation of methylene blue. The experiments were performed in the same manner as in section 3.6.1 under the condition as follows: 0.050 g of TiO₂/zeolite NaY, 50 ml of 0.1 mM methylene blue, pH 8 and at ambient temperature.

3.7.2 Effect of Initial Concentration of Methylene Blue

The effect of initial concentration of methylene blue was investigated under the following conditions: TiO₂/zeolite NaY 0.050 g, pH 7, and the initial concentrations were 0.10, 0.15, and 0.2 mM.

3.8 The Study of Photodegradation of Methylene Blue Using TiO₂ Supported on Zeolite NaY Prepared by Sol Gel Method

3.8.1 Effect of TiO₂ Content Loaded on Zeolite NaY

There were five synthesized various amounts of TiO₂ loaded on zeolite NaY samples (see section 3.4.2.3) employed in the study of methylene blue degradation. The experiments were performed in the same manner as in section 3.6.1 under the condition as follows: 0.050 g of TiO₂/zeolite NaY, 50 ml of 0.1 mM methylene blue, pH 8 and at ambient temperature.

3.8.2 Effect of Initial Concentration of Methylene Blue

The effect of initial concentration of methylene blue was investigated under the following conditions: $\text{TiO}_2/\text{zeolite NaY}$ 0.050 g, pH 8, and the initial concentrations were 0.10, 0.15, and 0.20 mM.

3.9 The Study of Photodegradation of Phenosafranin Using TiO_2 Supported on Zeolite NaY Prepared by Different Methods

The optimum condition of prepared TiO_2 supported on zeolite NaY used for photodegradation of methylene blue in section 3.6.1, 3.7.1, and 3.8.1 were employed in the study of photodegradation of phenosafranin in this section. All of the experiments were done in the same manner as in section 3.5 under the condition as follows: initial phenosafranin concentrations of 0.10 and 0.20 mM, pH of solution 8.0 and 0.050 g of $\text{TiO}_2/\text{zeolite Y}$ sample prepared by each method in which the prepared sample had the highest efficiency for photodegradation of methylenen blue (i.e. 15.0 mM ATO-Ti/NaY-IE, 24.7wt% Ti/NaY-IMP and 37.33wt% Ti/NaY-SG by ion exchange, impregnation and sol gel method, respectively).

CHAPTER IV

RESULTS AND DISCUSSION

4.1 The Characterization of Zeolite Y and TiO₂ Supported on Zeolite NaY

4.1.1 X-ray Powder Diffraction (XRD)

4.1.1.1 Preparation of TiO₂ Supported on Zeolite NaY by Ion Exchange Method

Pure zeolite NaY was synthesized by hydrothermal reaction and characterized by comparing the observed powder patterns with the calculated ones reported in collection of simulated XRD powder patterns for zeolites (Treacy *et al.*, 2001). Figure 4.1 shows the XRD pattern of synthesized zeolite NaY and TiO₂ supported on zeolite NaY with different TiO₂ loadings. From diffraction patterns, the peak of TiO₂ can not be observed although the maximum volume of ATO was used. It indicated that TiO₂ well dispersed on zeolite NaY and the small amount of well-dispersed TiO₂ on the zeolite inhibited the mutual approach of the finer size. It may be that the TiO₂ species residing in the zeolite cavities does not form a separate phase from the zeolite or is too small to be detected by XRD (Liu *et al.*, 1992; Anandan and Yoon, 2003). The crystallinity of zeolite NaY decreased with increasing concentration of ATO. With low concentration of ATO, the crystallinity of zeolite NaY was not reformed after ion exchange process. This shows that the structural

damage is negligible during the ion exchange. However the crystallinity of samples decreased with increasing TiO₂ content.

4.1.1.2 Preparation of TiO₂ Supported on Zeolite NaY by Impregnation Method

Figure 4.2 shows XRD patterns of the prepared samples with different TiO₂ loadings by impregnation method. It showed that in the experiment with the lowest volume of titanium ethoxide used 4.6wt% Ti/NaY-IME in this method, the samples contained anatase form with the characteristic XRD peaks of anatase phase apparent at $2\theta = 25.4^\circ$, 37.8° , and 48.2° (Hsien *et al.*, 2001; Wang *et al.*, 2008). Many reports suggested that TiO₂ is most photoactive in the anatase form (Xu and Langford, 1995; Liu *et al.*, 2006 and Sen *et al.*, 2005). The crystallinity of zeolite NaY became lower with an increasing in TiO₂ content. It indicates that zeolite framework was destroyed due to more TiO₂ embedded in zeolite and its size became larger with an increase in TiO₂ loading. At low concentration of titanium ethoxide (4.6wt% Ti/NaY-IMP) it is seen that the crystalline zeolite NaY still remained and the peak of anatase was sharper even a decrease in TiO₂ loading. It might be mostly larger particle size of that TiO₂ dispersing on external surface of zeolite NaY. Hence, the high value of micropore surface area was obtained.

4.1.1.3 Preparation of TiO₂ Supported on Zeolite NaY by Sol-Gel Method

Figure 4.3 shows the XRD patterns of TiO₂ supported on zeolite Y at various TiO₂ contents. The peak of intensity at $2\theta = 25.4^\circ$ indicating that the anatase phase slightly increased with increased TiO₂ sol-gel volume until to 40 ml, but the crystallinity of zeolite Y decreased with increasing TiO₂ sol gel volume.

This indicates that the higher the amount of TiO_2 loading, the more crystalline structure of zeolite was destroyed.

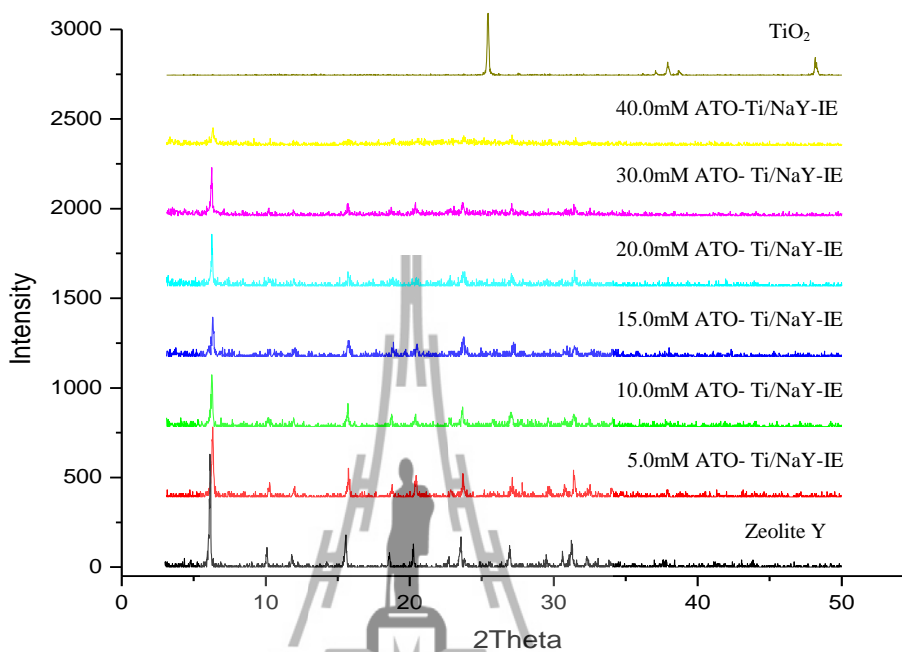


Figure 4.1 X-ray diffraction pattern of zeolite Y, TiO_2 supported on zeolite Y with different amounts of TiO_2 by ion exchange method and commercial TiO_2 (Aldrich).

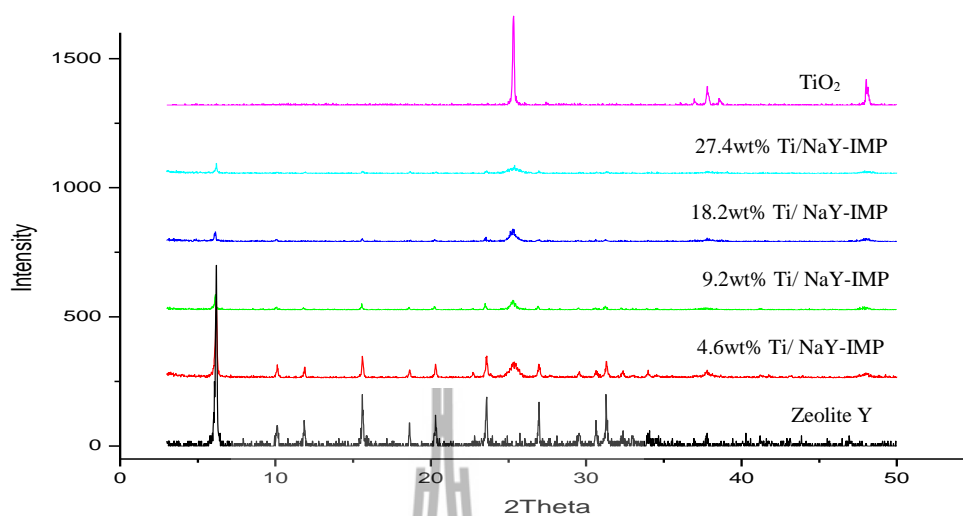


Figure 4.2 X-ray diffraction pattern of zeolite Y, TiO₂ supported on zeolite NaY with different amounts of TiO₂ by impregnation method and commercial TiO₂ (Aldrich).

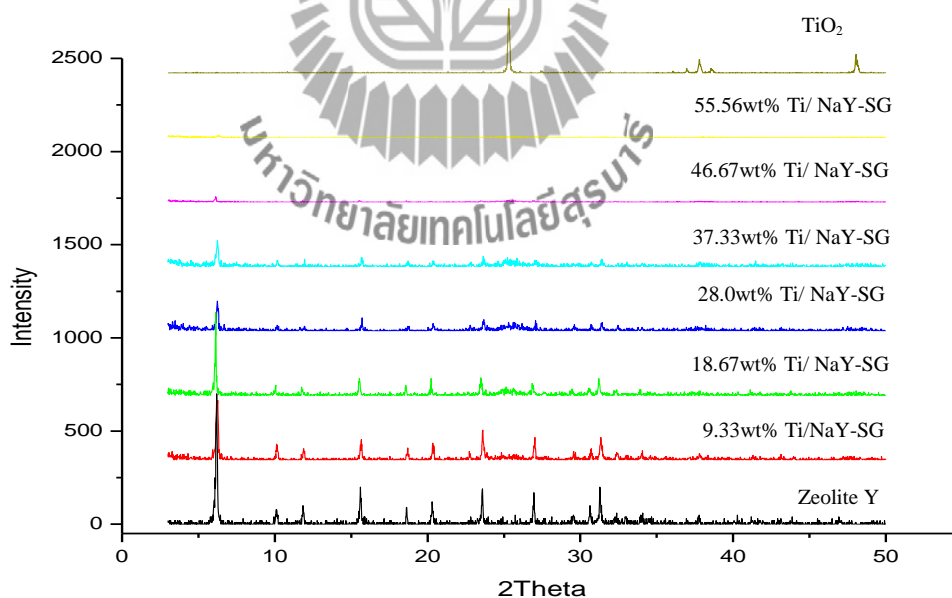


Figure 4.3 X-ray diffraction pattern of zeolite Y, TiO₂ supported on zeolite NaY with different amounts of TiO₂ by sol-gel method and commercial TiO₂ (Aldrich).

4.1.2 Surface Area Analysis (BET)

The surface areas, pore volumes and pore sizes of catalysts are shown in Table 4.1. It is clearly seen that all the samples of TiO_2 supported on zeolite have lower BET surface area than the zeolite. This indicates that TiO_2 particle occupied the zeolite NaY surface. The pore size increased because some fraction of zeolite framework was destroyed. At 27.4wt% of $\text{Ti}(\text{EtOH})_4/\text{NaY-IMP}$, the sample exhibited the lowest surface area because the zeolite structure quit completely destroyed.

Table 4.1 The surface area, pore size and pore volume of zeolite NaY and TiO_2 supported on zeolite Y at different preparations.

Sample	External Surface Area m^2g^{-1}	Micropore Surface Area m^2g^{-1}	BET Surface Area m^2g^{-1}	Pore Size \AA	Pore Volume cm^3g^{-1}	% of Ti ICP %w/w
Zeolite NaY	41.00	738.1	779.1	23.75	0.4626	
15.0 mM ATO/NaY-IE	203.6	449.9	653.5	25.02	0.4088	0.34
4.6wt% Ti/NaY-IMP	57.38	455.3	512.6	29.16	0.3738	0.95
27.4wt% Ti/NaY-IMP	124.3	154.4	287.7	51.97	0.3621	36.8
18.67wt% Ti/NaY-SG	93.09	452.6	545.7	29.1	0.397	13.4
37.33wt% Ti/NaY-SG	466.0	122.8	588.8	43.68	0.643	19.6

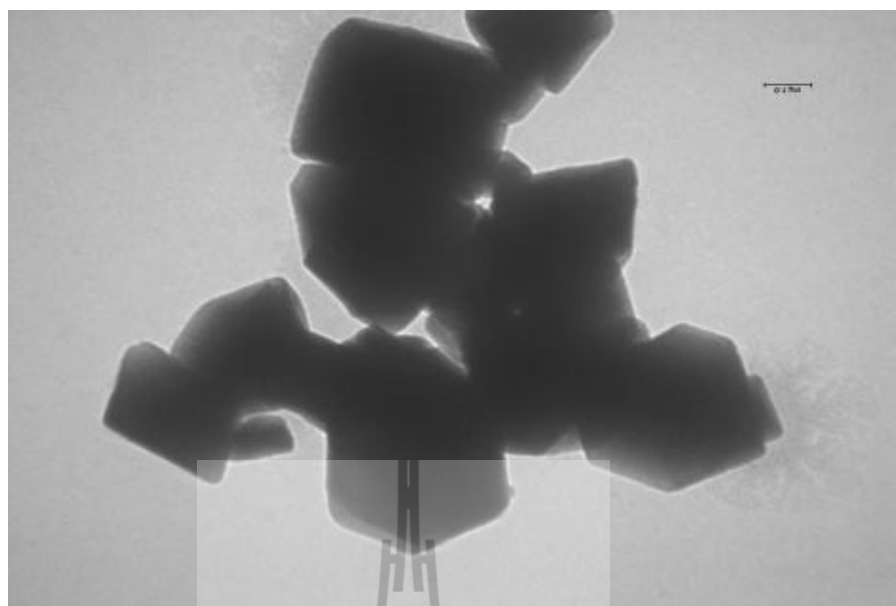
4.1.3 Surface Morphology

The morphology of zeolite NaY and prepared samples TiO_2/NaY were analyzed by transmission electron microscope (TEM). Figure 4.4 shows the TEM morphologies of Zeolite Y, 15.0 mM ATO/NaY-IE, 4.6wt% Ti/NaY-IMP, 27.4wt% Ti/NaY-IMP, 18.67wt% Ti/NaY-SG, and 37.33wt% Ti/NaY-SG. Figure 4.4(a) shows the smooth external surface of zeolite NaY. When the TiO_2 was loaded on the

samples, dark spots seem to spread all over the particles and no aggregation of crystallites on the external surfaces is seen. These results indicate that TiO_2 supported on zeolites probably cannot get into the micro pores and it forms small crystallites aggregated on the external surfaces of the zeolite (Hsien *et al.*, 2001) (see Figure 4.4(d), (e), and (f)). The titanium dioxide particles are also crushed slightly and uniformly spread over the zeolite Y framework (Sharma *et al.*, 2008). The result are consistent with XRD and surface area analysis.

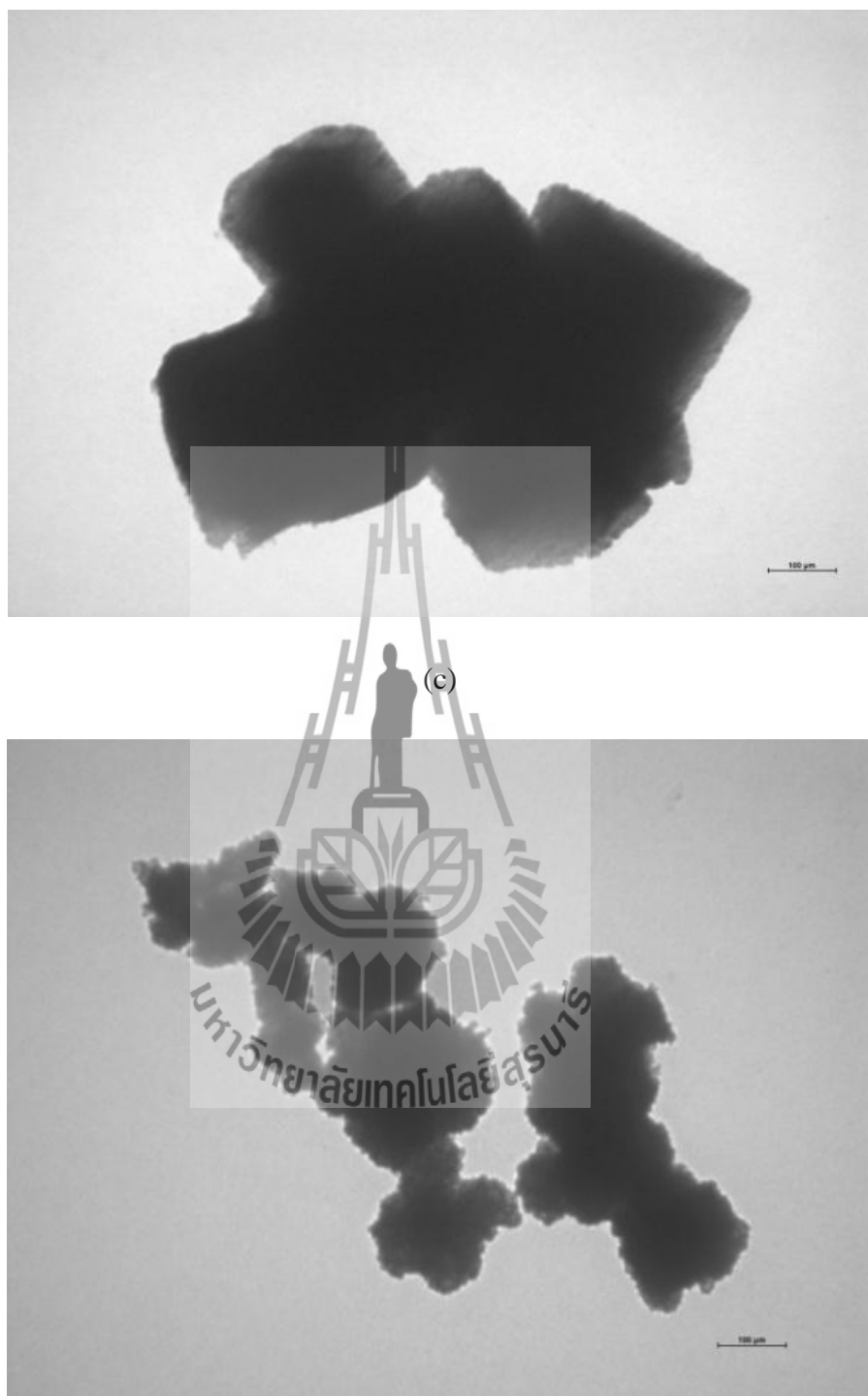
4.1.4 FT-IR Measurement

FT-IR spectra of prepared samples, TiO_2 supported on zeolite NaY, with different methods are shown in Figure 4.5. The band around $3436\text{--}3466\text{ cm}^{-1}$ and $1635\text{--}1640\text{ cm}^{-1}$ were observed in all the sample. They are attributed to O-H stretching and O-H bending vibration of water. The band of zeolite related to asymmetric and symmetric stretching vibration of O-T-O (T = Si or Al) appeared around $1007\text{--}1011\text{ cm}^{-1}$ and 781 cm^{-1} , 700 cm^{-1} , respectively. The characteristic band of zeolite NaY related to vibration of double four membered ring is 572 cm^{-1} (Flanigan *et al.*, 1971). The sample of 15.0 mM ATO/NaY-IE showed new absorption bands at 910 cm^{-1} corresponding to the stretching vibration of Ti-O-Si and Ti-O-Al, similar to the results from Liu *et al.*, 1992 (Li *et al.*, 2005). The small peak centered at about 1385 cm^{-1} appeared in the samples of 18.67wt% Ti/NaY-SG and 37.33wt% Ti/Y corresponding to C-O stretching of residual organic from terminal titanium alkoxide ($-\text{OC}_3\text{H}_7$) (Ding *et al.*, 1998). From the sample of 27.4wt% Ti/NaY-IMP, the characteristic peak of zeolite NaY at 570 cm^{-1} was not observed compared to the other. It indicated that the framework of zeolite Y was rather completely destroyed, consistent with the result from XRD.



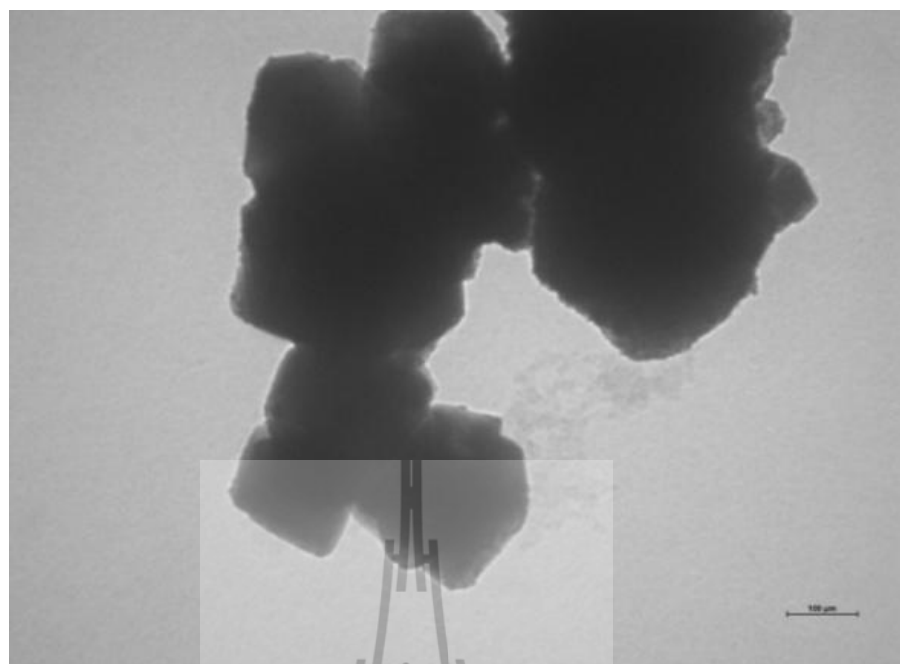
(b)

Figure 4.4 TEM photograph of (a) Zeolite NaY, (b) 15.0mM ATO/NaY-IE, (c) 4.6wt% Ti/NaY-IMP, (d) 27.4wt% Ti/NaY-IMP, (e) 18.67wt% Ti/NaY-SG, and (f) 37.33wt% Ti/NaY-SG.



(d)

Figure 4.4 TEM photograph of (a) Zeolite NaY, (b) 15.0mM ATO/NaY-IE, (c) 4.6wt% Ti/NaY-IMP, (d) 27.4wt% Ti/NaY-IMP, (e) 18.67wt% Ti/NaY-SG, and (f) 37.33wt% Ti/NaY-SG.



(e)



(f)

Figure 4.4 TEM photograph of (a) Zeolite NaY, (b) 15.0mM ATO/NaY-IE, (c) 4.6wt% Ti/NaY-IMP, (d) 27.4wt% Ti/NaY-IMP, (e) 18.67wt% Ti/NaY-SG, and (f) 37.33wt% Ti/NaY-SG.

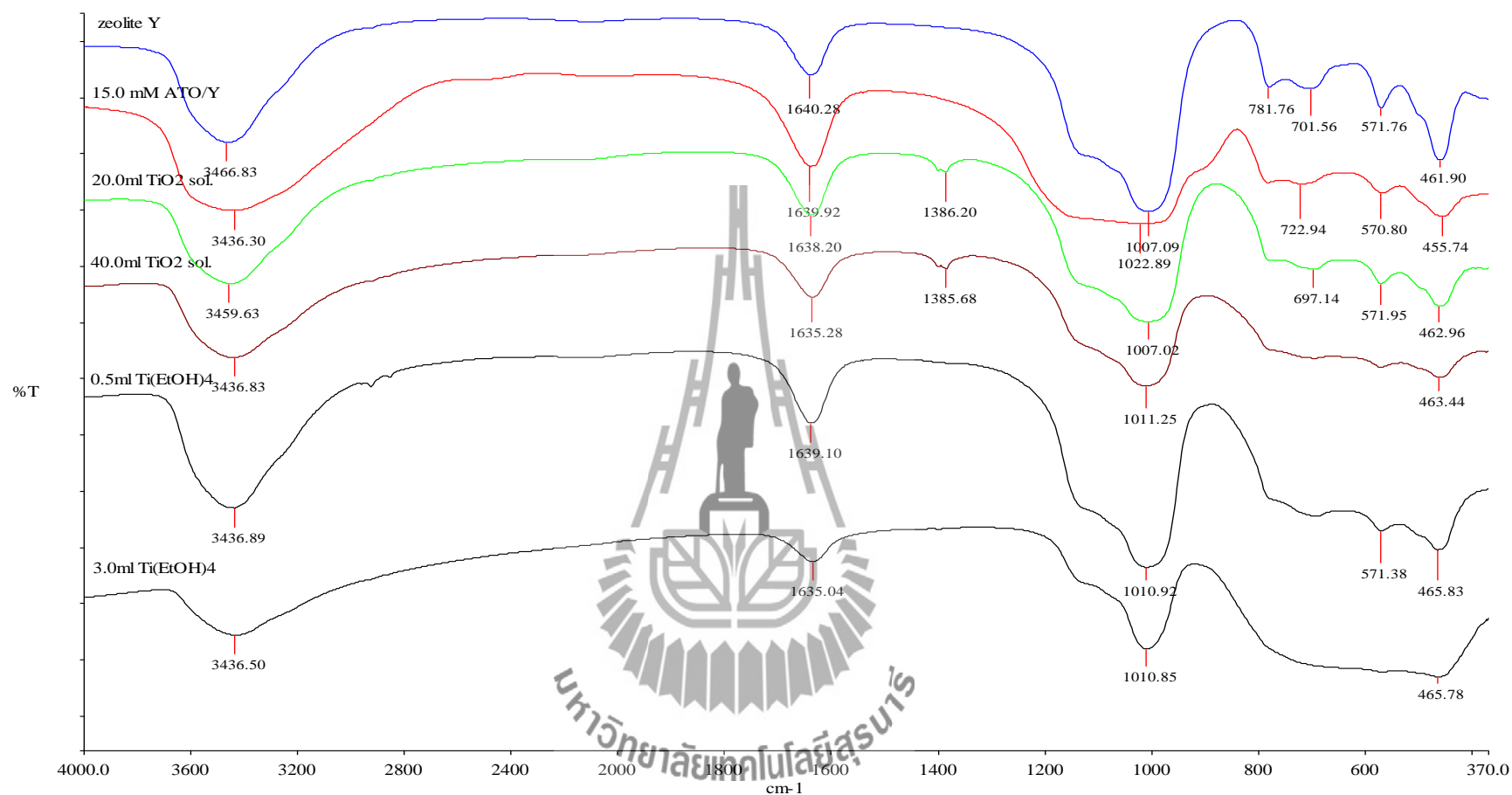


Figure 4.5 FT-IR spectra of zeolite NaY, 15.0mM ATO/NaY-IE, 20.0 ml TiO_2 sol/NaY-SG, 40.0 ml TiO_2 sol./NaY-SG, 4.6wt% Ti/NaY-IMP, 27.4wt% Ti/NaY-IMP

4.2 The Photodegradation of Methylene Blue with TiO₂ Supported on Zeolite NaY

4.2.1 Control Experiments

Two control experiments were done to ensure that there is no reaction rather than TiO₂ loaded on zeolite photosensitization occurred. The first control experiment was only known concentration of dye solution exposed to UV light under continuous stirring without addition of TiO₂ to account for photolysis. The result in Figure 4.6 showed that the degradation of dye by photolysis is very low in comparison with the photosensitization (with TiO₂), as only less than 1% of initial concentration which was in the range of experimental error (3%). The second control experiment was carried out to account for adsorption of dye onto zeolite NaY without exposure. The result showed a decrease in dye concentration due to an adsorption of well crystalline zeolite NaY around 12% of initial dye concentration. However, in the study of TiO₂ loaded on zeolite NaY, the zeolite framework was also destructive in the preparation process, hence the dye adsorption should be much less than 12%.

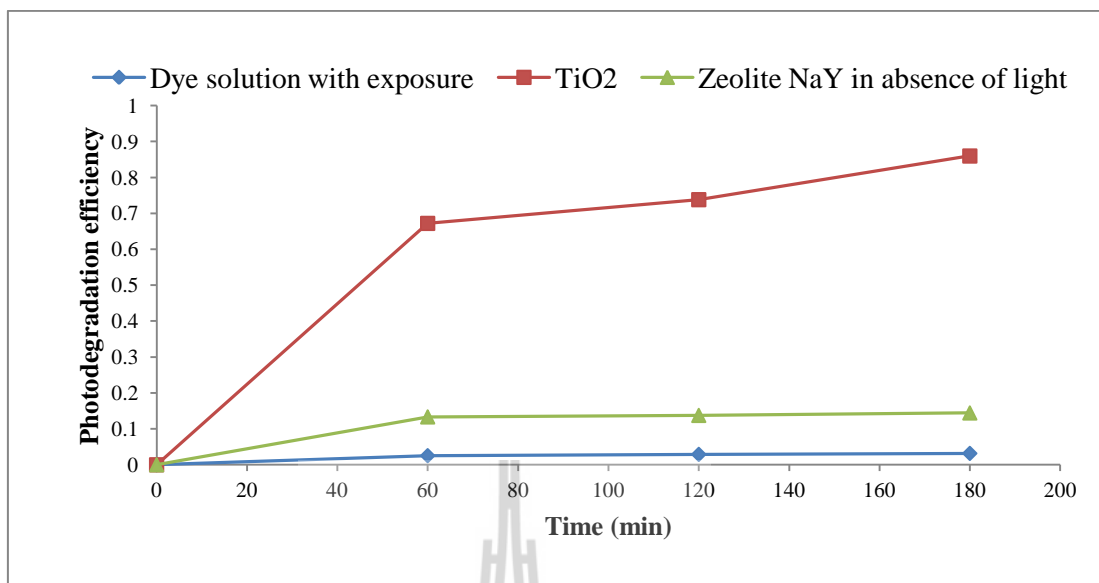


Figure 4.6 Control experiment: Dye solution and dye solution with TiO₂ in the presence of light and zeolite NaY in absence of light.

4.2.2 The Photodegradation with TiO₂ Supported on Zeolite Y Prepared by Ion Exchange Method

4.2.2.1 Effect of amount of TiO₂ loaded on zeolite Y

The TiO₂-sensitized photooxidation of methylene blue was investigated in suspension of TiO₂/zeolite Y prepared by using different concentrations of titanium precursor (ATO's concentration 10.0, 15.0, 20.0, 30.0, and 40.0 mM). Figures 4.7-4.8 show the photodegradation efficiency of methylene blue with different loadings of TiO₂ on zeolite Y and control is zeolite Y in absent of light. It is clearly seen that the optimum concentration of precursor (ATO) used for preparation by ion exchange method to give the highest photocatalytic efficiency, was about 15-20 mM. The result showed that with higher concentration of ATO used (30 and 40 mM), the lower photocatalytic efficiency was observed. It may be caused from the balance of TiO₂ amount loaded on zeolite and its surface area (external and

micropore surface area). With low concentration of ATO (10 mM) the efficiency was lower than 15 mM, it may result from the effect of amount of TiO_2 loading more predominantly than the effect of its surface area. On the other hand with higher concentration the effect of surface area on the efficiency was considerably. Therefore, the optimum of photodegradation efficiency was observed at 15.0 mM ATO loaded on zeolite.

4.2.2.2 Effect of initial concentration of methylene blue

From the result in 4.2.2.1, 15.0 mM ATO/Y was chosen for study the effect of initial dye concentrations. methylene blue had the concentrations of 0.10, 0.13, 0.16 and 0.20 mM. The photodegradation efficiency of methylene blue at various initial concentrations with the prepared samples including commercial TiO_2 and pure zeolite Y was shown in Figure 4.9. The photodegradation efficiency was decreased with an increase in initial dye concentration. It may result from that more dye molecules were absorbed on the surface of the catalyst. When initial concentration was increased, OH radicals were less generated at the catalyst surface due to the active sites occupied by dye cation (Wang *et al.*, 2008). The other reason may be due to the fact that as the initial concentrations of the dye increase, the color of the irradiating mixture becomes more and more intense which prevents the penetration of light to the surface of the catalyst. Hence, the generations of relative amount of OH^\cdot and $\text{O}_2^{\cdot-}$ on the surface of the catalyst do not increase as the intensity of light, illumination time and concentration of the catalyst are constant. Conversely, amount of OH^\cdot and $\text{O}_2^{\cdot-}$ concentrations will decrease with an increase in concentration of the dye as the light photons are largely absorbed and prevented from reaching the

catalyst surface by the dye molecules. Consequently, the degradation efficiency of the dye decreases as the dye concentration increases (Faisal *et al.*, 2007).

4.2.2.3 Effect of pH of the solution

The important parameter in the photocatalytic reactions taking place on the particulate surfaces is the pH of the solution since it dictates the surface charge properties of the photocatalyst and size of aggregates it forms (Faisal *et al.*, 2007). Based on the zero point of the TiO_2 charge, the surface was presumably positively charged in acidic solution and negatively charged in alkaline solution. Thus, it is reasonable to expect that the electrical charge of the dye and the photocatalyst surface will determine the extent of adsorption. In alkaline solution, attractive forces between the cationic dye (Methylene blue and Phenosafranin used in this work) and the photocatalyst surface would favour adsorption and so photodegradation efficiency will be favoured by high pH. In contrast, at low pH the photocatalyst's surface will be positively charged and repulsive forces between the photocatalyst surface and the cationic dye will lead to a decrease in both dye adsorption and photodegradation efficiency (Wang *et al.*, 2008).

From the results previously (see section 4.2.2.1), 15.0 mM ATO/zeolite NaY was chosen for photodegradation of 0.10mM methylene blue. Figures 4.10 and 4.11 show photodegradation efficiency of methylene blue dependent on pH of the solution and reaction time. The efficiency was increased with an increase in pH of the solution until at pH 9 and at this pH the efficiency was significantly decreased at initial duration of reaction compared to pH 8 and then slightly different efficiencies at longer reaction time. It might be that in pH 9 the

formation of OH radicals was reduced due to the repulsion of hydroxide ion by negatively charged catalyst surface (Wang *et al.*, 2008).

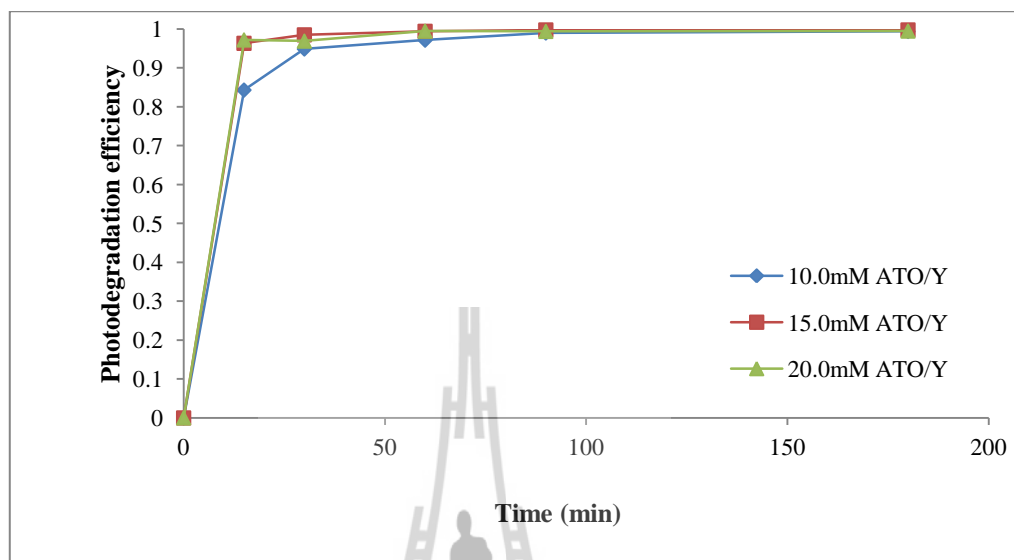


Figure 4.7 Photodegradation efficiency of methylene blue with $\text{TiO}_2/\text{zeolite NaY}$ as photocatalysts at different loadings of TiO_2 . Experiment conditions: 0.050 g of prepared $\text{TiO}_2/\text{zeolite NaY}$, 50 ml of 0.1 mM of methylene blue at pH 7.

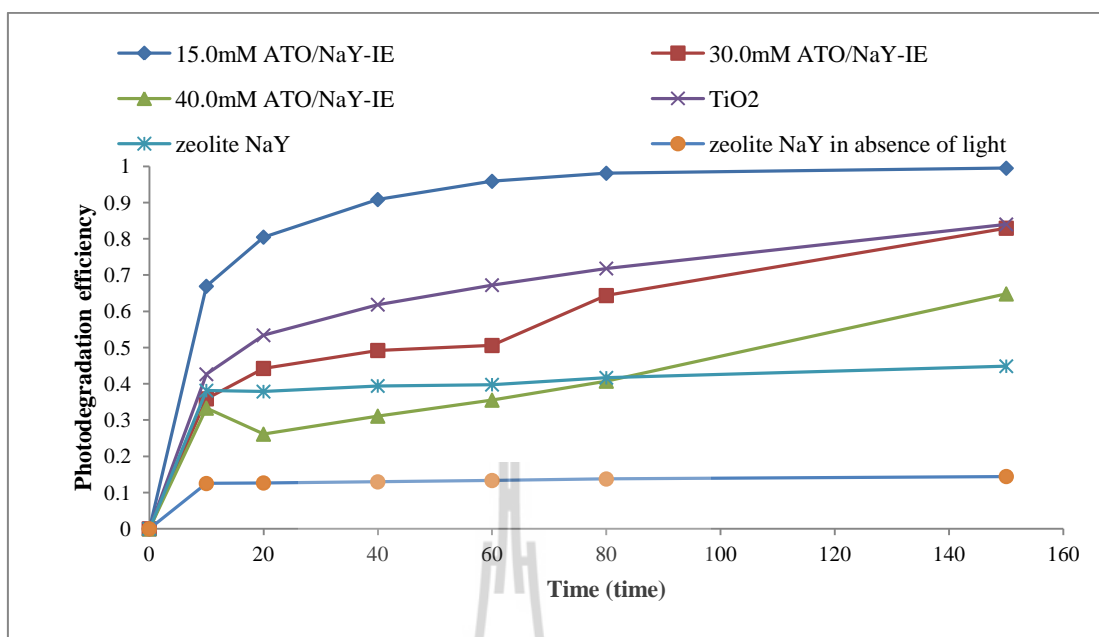


Figure 4.8 Photodegradation efficiency of methylene blue with TiO₂/zeolite NaY as photocatalysts with different loadings of TiO₂ and also compared with zeolite NaY and commercial TiO₂ (Aldrich). Experiment conditions: 0.050 g of prepared TiO₂/zeolite NaY, 50 ml of 0.1 mM of methylene blue at pH 7.

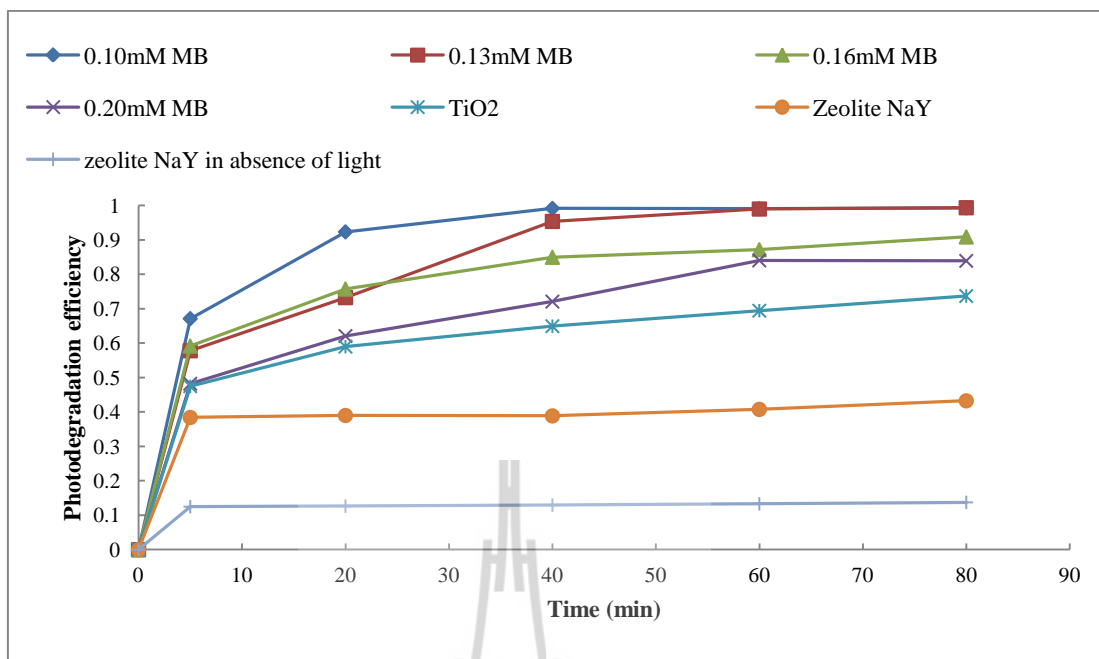


Figure 4.9 Effect of initial methylene blue concentrations on the photodegradation with TiO₂/zeolite NaY prepared by ion exchange method. Experiment conditions: 0.050 g of prepared TiO₂/zeolite NaY, 50 ml of various methylene blue concentration at pH 7.

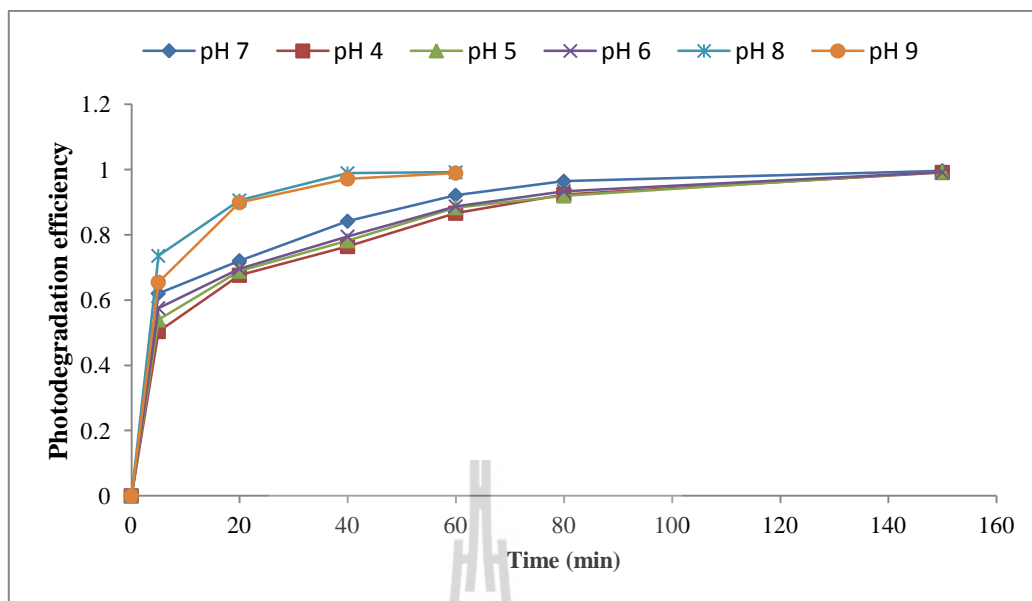


Figure 4.10 Effect of pH of the solution on the photodegradation of methylene blue with TiO_2 /zeolite Y prepared by ion exchange method. Experiment conditions: 0.050 g of prepared TiO_2 /zeolite NaY, 50 ml of 0.1 mM of methylene blue.

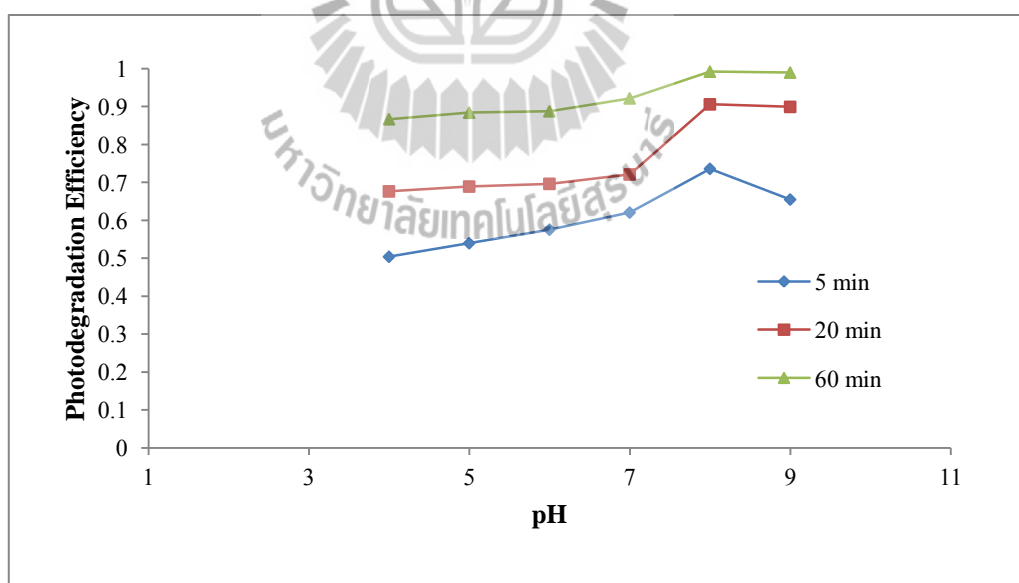


Figure 4.11 Photodegradation efficiency of methylene blue at various pH of solution during some reaction time. Experiment conditions: 0.050 g of prepared TiO_2 /zeolite NaY, 50 ml of 0.1 mM of methylene blue.

4.2.3 The Photodegradation with TiO₂ Supported on Zeolite NaY Prepared by Impregnation Method

4.2.3.1 Effect of amount of TiO₂ loaded on zeolite NaY

The photodegradation efficiency of methylene blue with these prepared samples was shown in Figure 4.12. The efficiency was increased with an increase in amount of TiO₂ loaded on zeolite NaY. It might be that the sample possessed higher external surface area compared to the sample of 4.6wt% Ti/NaY-IMP (see Table 4.1) which matched to TEM in Figure 4.5(c) and (d) exhibiting that dark spots seem to spread all over the particles.

4.2.3.2 Effect of initial concentration

The photocatalyst at 27.4wt% Ti/NaY-IMP was selected for studied the effect of initial concentration of methylene blue. The photodegradation efficiency of methylene blue at various initial concentrations was shown in Figure 4.13. The efficiency was decreased with increasing methylene blue concentration. The result is consistent with the use of prepared sample by ion exchange (see section 4.2.2.2).

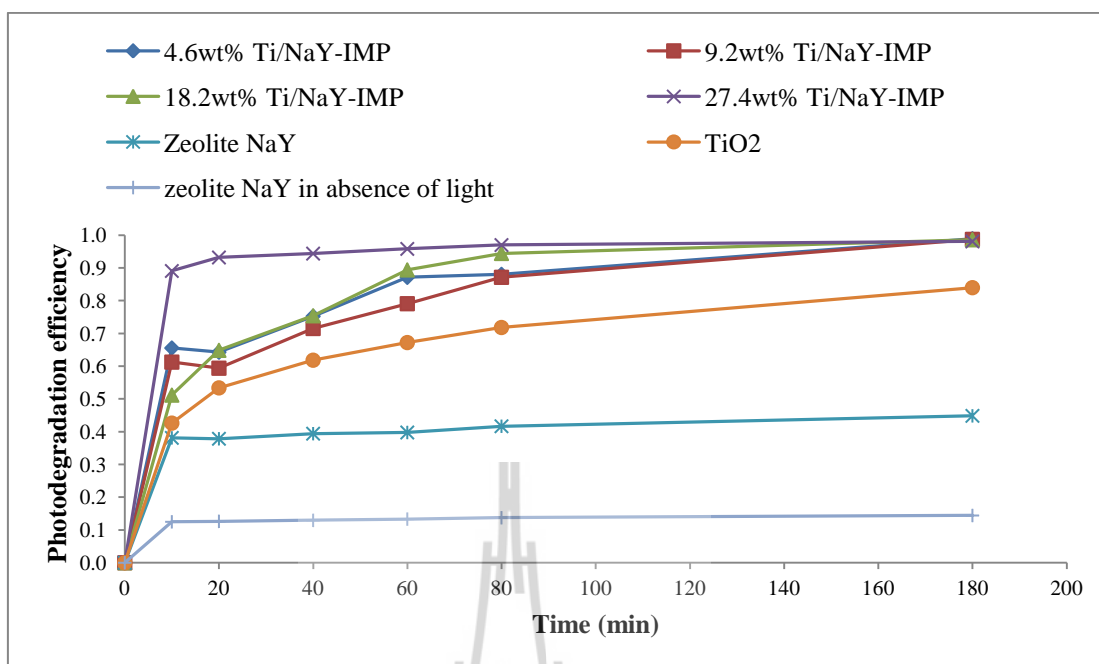


Figure 4.12 Effect of TiO₂ loading by impregnation method on photodegradation efficiency of methylene blue. Experiment conditions: 0.050 g of prepared TiO₂/zeolite NaY, 50 ml of 0.1 mM of methylene blue at pH 8.

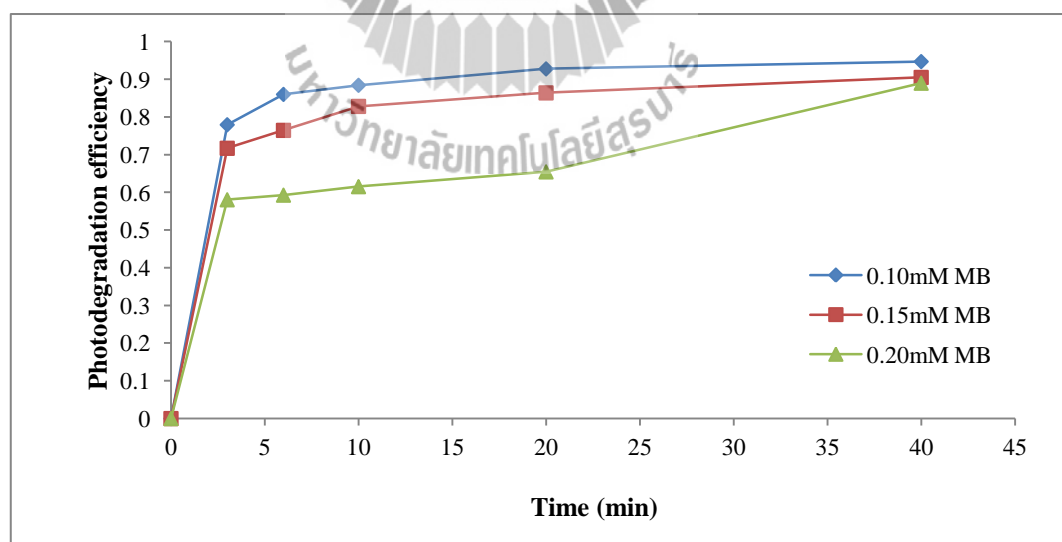


Figure 4.13 Effect of initial methylene blue concentrations on their degradations with TiO₂/zeolite Y prepared by impregnation method. Experiment conditions: 0.050 g of prepared TiO₂/zeolite Y, 50 ml of various methylene blue concentrations at pH 8.

4.2.4 The Photodegradation with TiO₂ Supported on Zeolite NaY by Sol Gel Method

4.2.4.1 Effect of TiO₂ loaded on zeolite NaY

Figure 4.14 shows the photodegradation efficiency of methylene blue with different amounts of TiO₂ loaded on zeolite NaY samples which were prepared by using certain amount of zeolite NaY added to different volumes of TiO₂ sol gel and the control is zeolite Y in absent of light. It shows that the efficiency was increased with an increasing of TiO₂ loaded on zeolite NaY. It might be that the sample had higher external surface area due to an enormous amount of small particles of TiO₂ (see Table 4.1), which matched to TEM in Figure 4.5(e) and (f) showing dark spots spreading all over the particles.

4.2.4.2 Effect of initial concentration

The photocatalyst at 37.33 wt% Ti/NaY-SG was selected for studying the effect of initial concentration of methylene blue. The photodegradation efficiency was decreased with increasing methylene blue concentration as shown in Figure 4.15. The result is in agreement with the use both prepared samples by ion exchange and impregnation (see section 4.2.2.2).

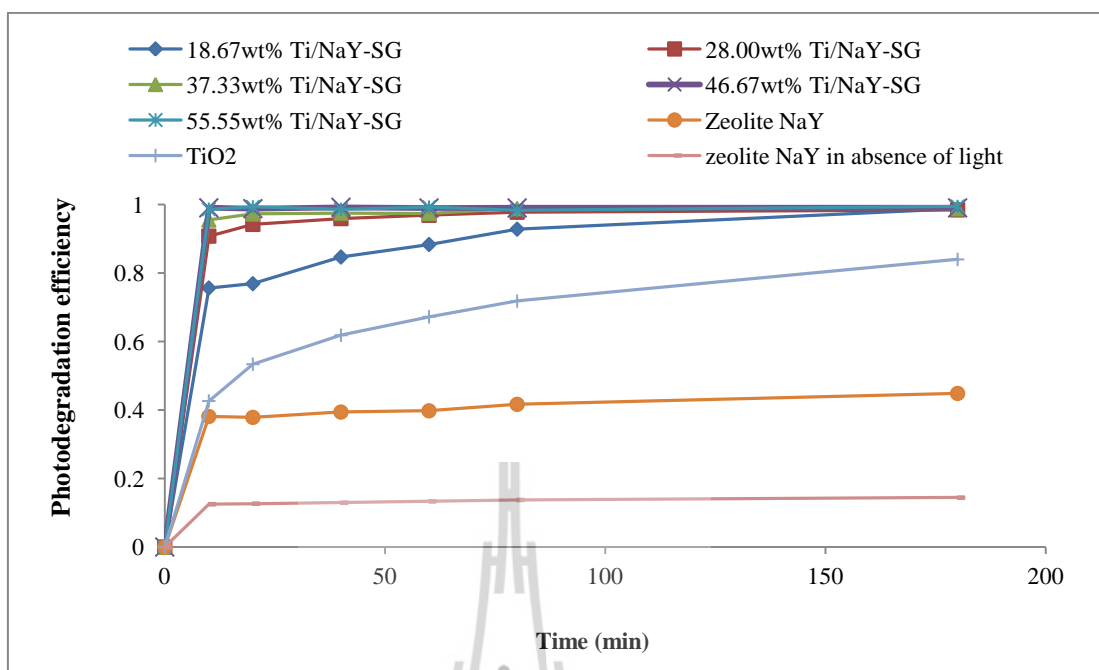


Figure 4.14 Effect of TiO₂ loading by sol gel method on the photodegradation efficiency of methylene blue. Experiment conditions: 0.050 g of prepared TiO₂/zeolite NaY, 50 ml of 0.1 mM of methylene blue at pH 8.

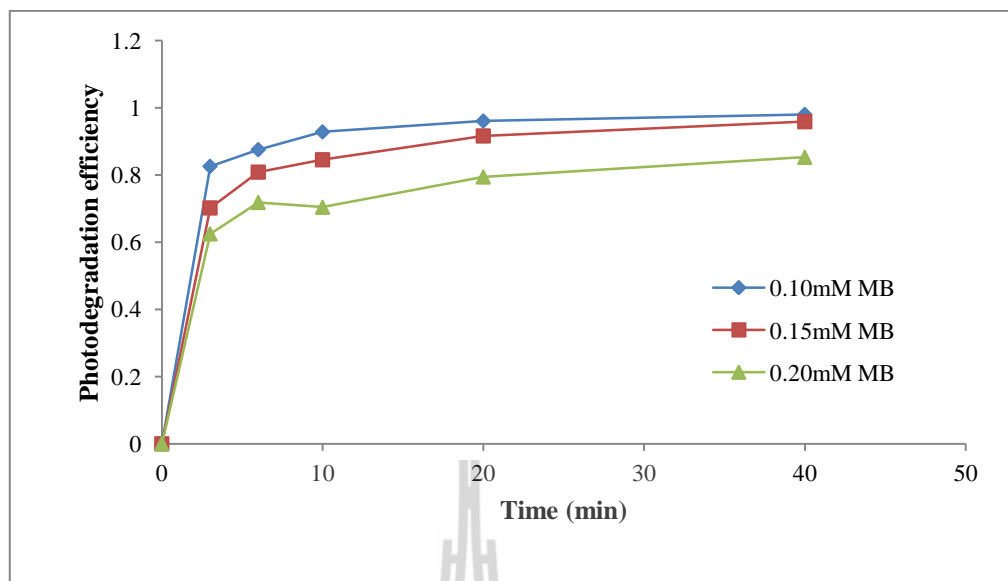


Figure 4.15 Effect of initial methylene blue concentrations on their degradations with TiO_2 /zeolite NaY prepared by sol gel method. Experiment conditions: 0.050 g of prepared TiO_2 /zeolite NaY, 50 ml of various methylene blue concentrations at pH 8.

4.2.5 Comparison of the Photocatalyst Activity of Catalyst Prepared by Different Methods in Photodegradation of Methylene Blue

The optimum catalyst prepared in each method was employed to study photodegradation of methylene blue. It showed that the highest efficiency to degradation methylene blue was observed with catalyst prepared by sol gel method (see Figures 4.16 and 4.17). From ICP result in Table 4.1 show the titanium content in the prepared samples by impregnation higher than that by sol gel method and the minimum Ti content was obtained by ion exchange method. From surface area analysis in Table 4.1, it shows the maximum external surface area of the prepared sample by sol gel method. It indicated that very fine particle size of TiO_2 spread over the zeolite framework (see Figure 4.4) compared to the sample prepared by

impregnation which had more amount of Ti and lower external area indicating that more TiO_2 would be induced greater aggregation of the TiO_2 particles on the surface of zeolite framework, that decreased its photocatalytic activity. Therefore, in this study the sample prepared sol-gel method has the highest efficiency to photodegradation of methylene blue. The control is zeolite Y in absent of light.

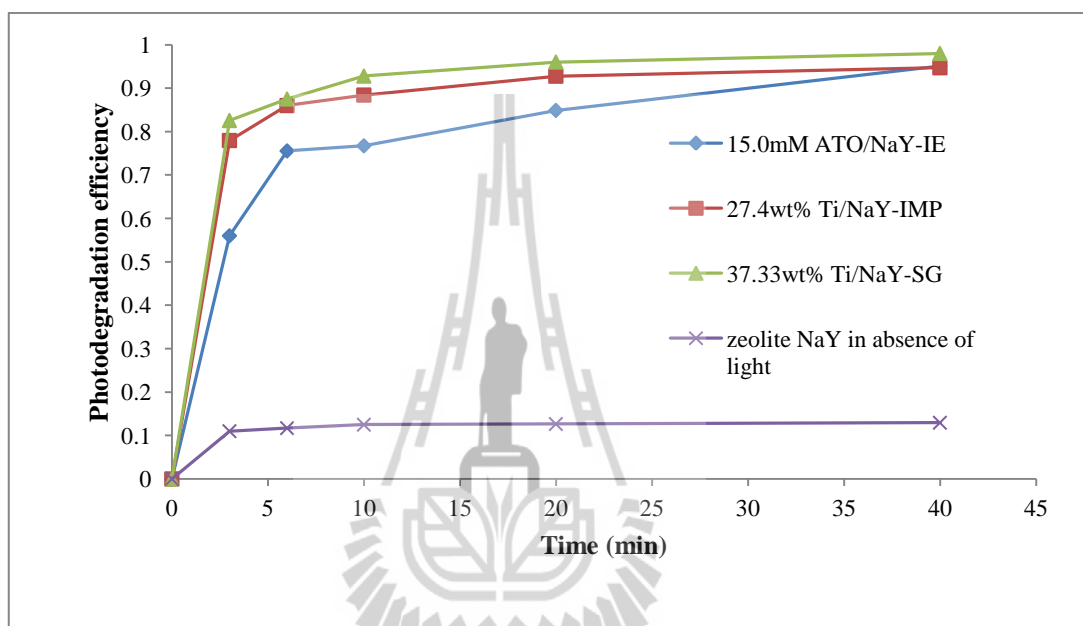


Figure 4.16 Comparison of the efficiency of photocatalyst prepared by impregnation, ion exchange and sol gel method in photodegradation of methylene blue. Experiment conditions: 0.050 g of prepared TiO_2 /zeolite Y, 50 ml of 0.10 mM of methylene blue at pH 8.

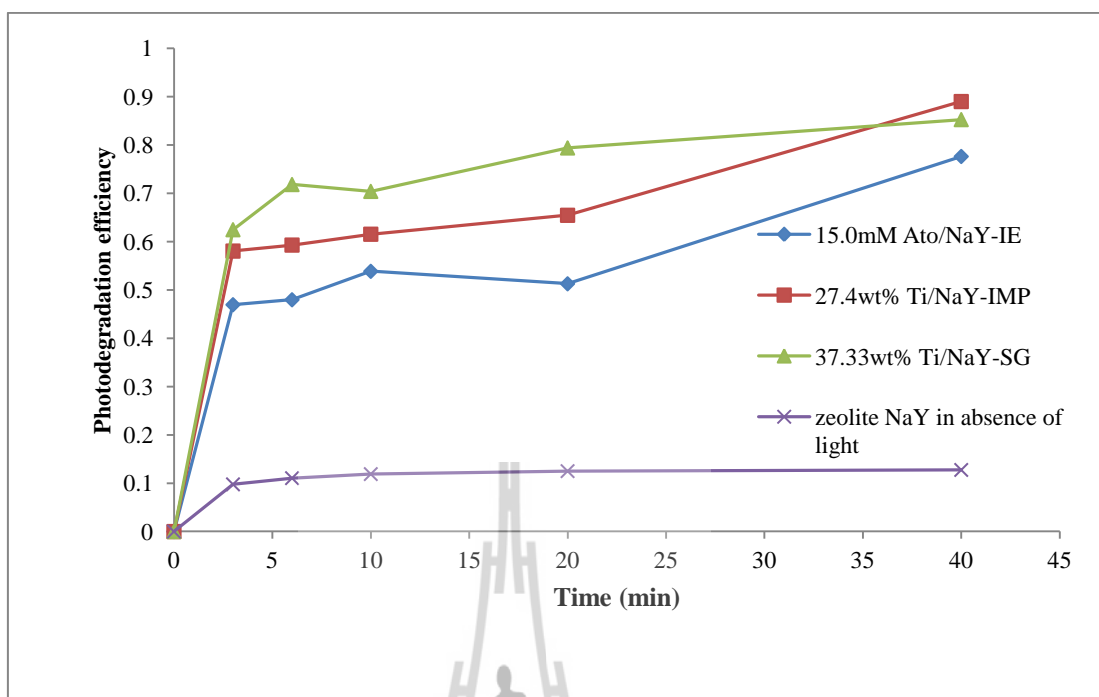


Figure 4.17 The comparison of the efficiency of photocatalyst prepared by impregnation, ion exchange and sol gel method in photodegradation of methylene blue. Experiment conditions: 0.050 g of prepared TiO_2 /zeolite Y, 50 ml of 0.20 mM of methylene blue at pH 8.

4.3 The Photodegradation of Phenosafranin with TiO_2 Supported on Zeolite NaY

This study focused on the optimal photocatalysts prepared from each method in the study of photodegradation of methylene blue to be employed in photodegradation of phenosafranin (PHNS). The optimal photocatalysts were 15.0 mM ATO/NaY-IE, 27.4wt% Ti/NaY-IMP, and 37.33wt% Ti/NaY-SG by ion exchange, impregnation and sol gel method, respectively.

4.3.1 Effect of Initial Concentration of Phenosafranin

The photodegradation efficiency of phenosafranin (PHNS) depending on its initial concentrations with TiO_2 /zeolite NaY prepared by ion exchange, impregnation and sol-gel method were displayed in Figures 4.18, 4.19, and 4.20, respectively. With higher initial concentration of PHNS the photodegradation efficiency was decreased. It corresponds to the result of photodegradation efficiency of methylene blue (see section 4.2.2.2).

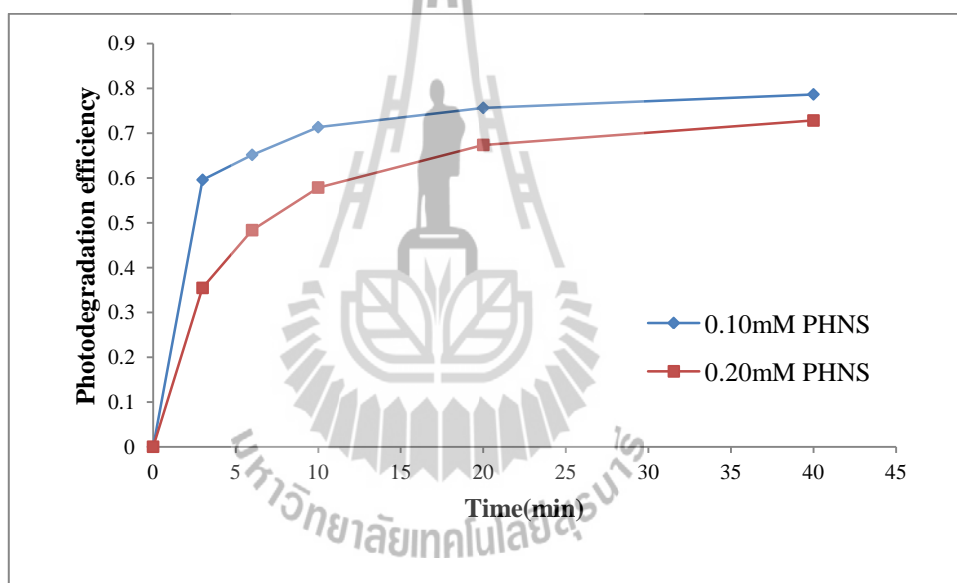


Figure 4.18 Effect of initial phenosafranin concentrations on their degradations with TiO_2 /zeolite Y prepared by ion exchange method. Experiment conditions: 15.0 mM ATO/NaY-IE 0.050 g, 50 ml of 0.10 mM and 0.20 mM PHNS at pH 7.

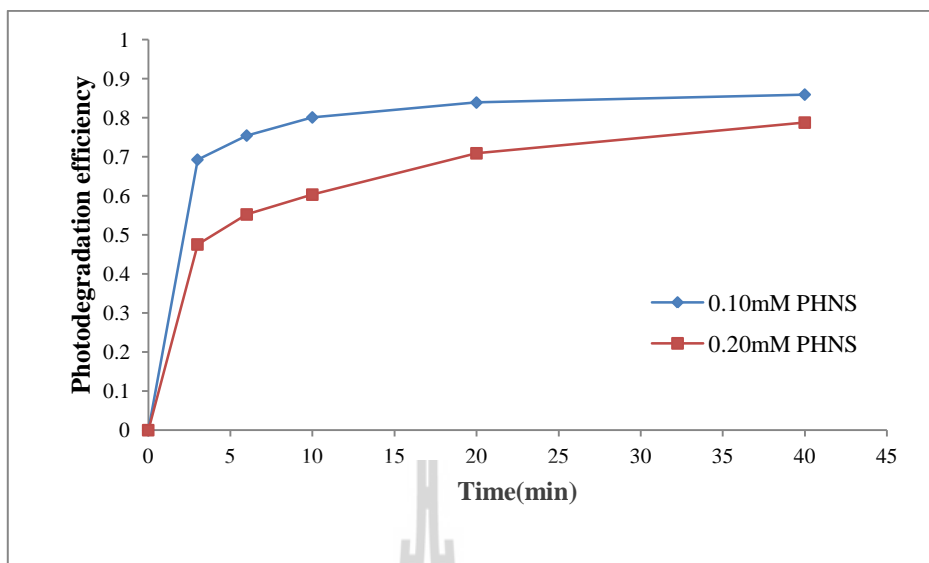


Figure 4.19 Effect of initial phenosafranin concentrations on their degradations with TiO_2 /zeolite Y prepared by impregnation method. Experiment conditions: 27.4wt% Ti/NaY-IMP 0.050 g, 50 ml of 0.10 mM and 0.20 mM PHNS at pH 7.

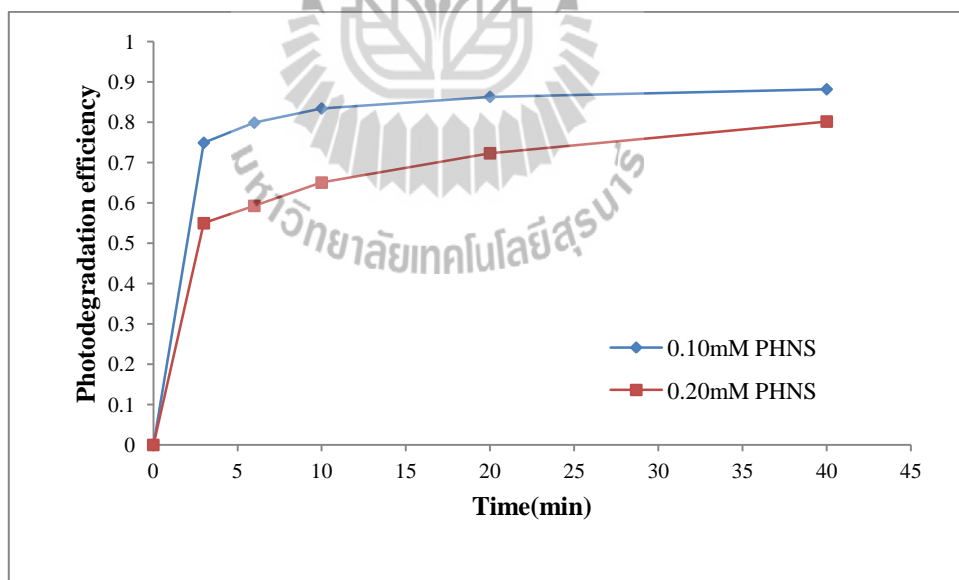


Figure 4.20 Effect of initial phenosafranin concentrations on their degradations with TiO_2 /zeolite Y prepared by sol gel method. Experiment conditions: 37.33wt% Ti/NaY-SG 0.050 g, 50 ml of 0.10 mM and 0.20 mM PHNS at pH 7.

4.3.2 Effect of pH of the Solution

The photodegradation efficiency of phenosafranin (PHNS) depending on the pH of the solution with TiO_2 /zeolite NaY prepared by ion exchange, impregnation and sol-gel method were displayed in Figures 4.21, 4.22, and 4.23, respectively. With higher pH of the solution the photodegradation was increased. It is consistent with the photodegradation efficiency of methylene blue (see section 4.2.2.3).

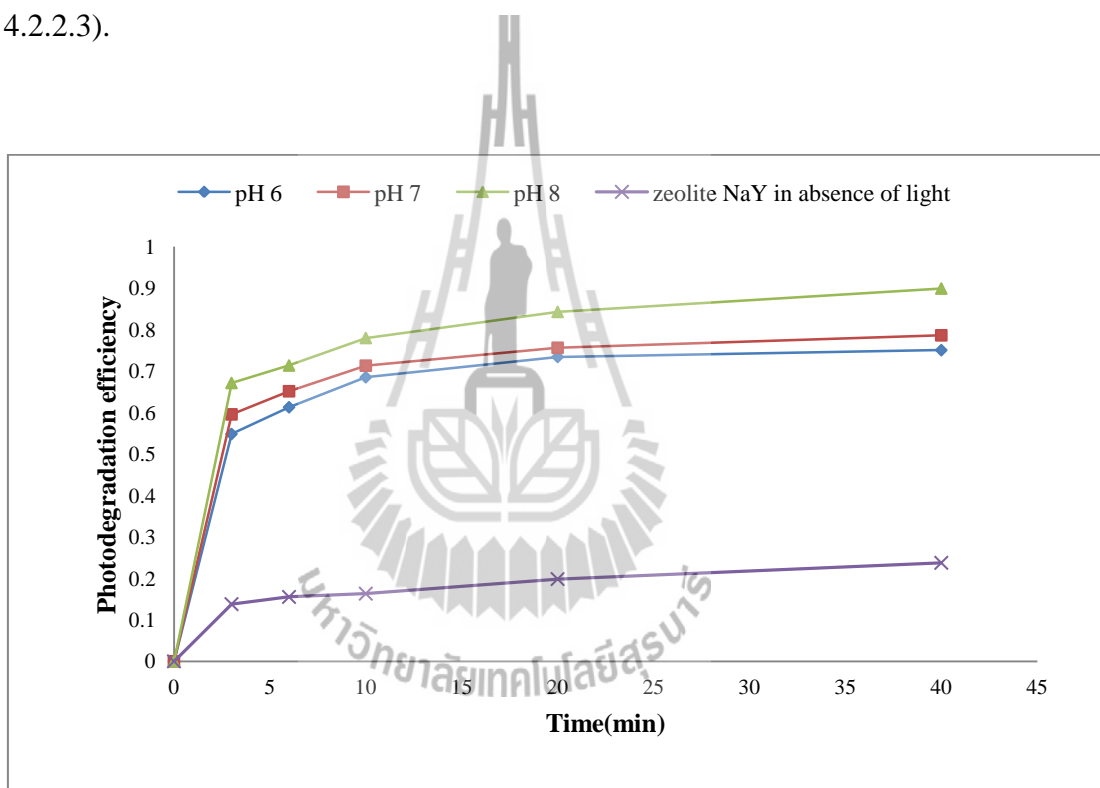


Figure 4.21 Effect of pH of the solution on the photodegradation of phenosafranin with TiO_2 /zeolite Y prepared by ion exchange method. Experiment conditions: 0.050 g of prepared TiO_2 /zeolite Y, 50 ml of 0.10 mM of PHNS.

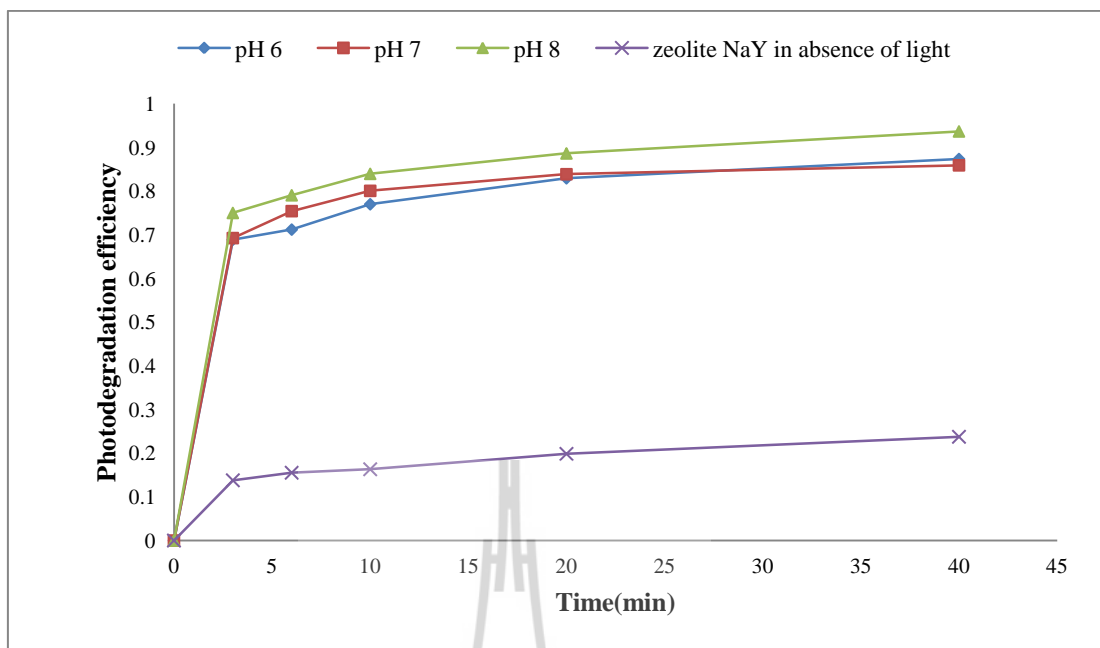


Figure 4.22 Effect of pH of the solution on the photodegradation of phenosafranin with TiO_2 /zeolite Y prepared by impregnation method. Experiment conditions: 0.050 g of prepared TiO_2 /zeolite Y, 50 ml of 0.10 mM of PHNS.

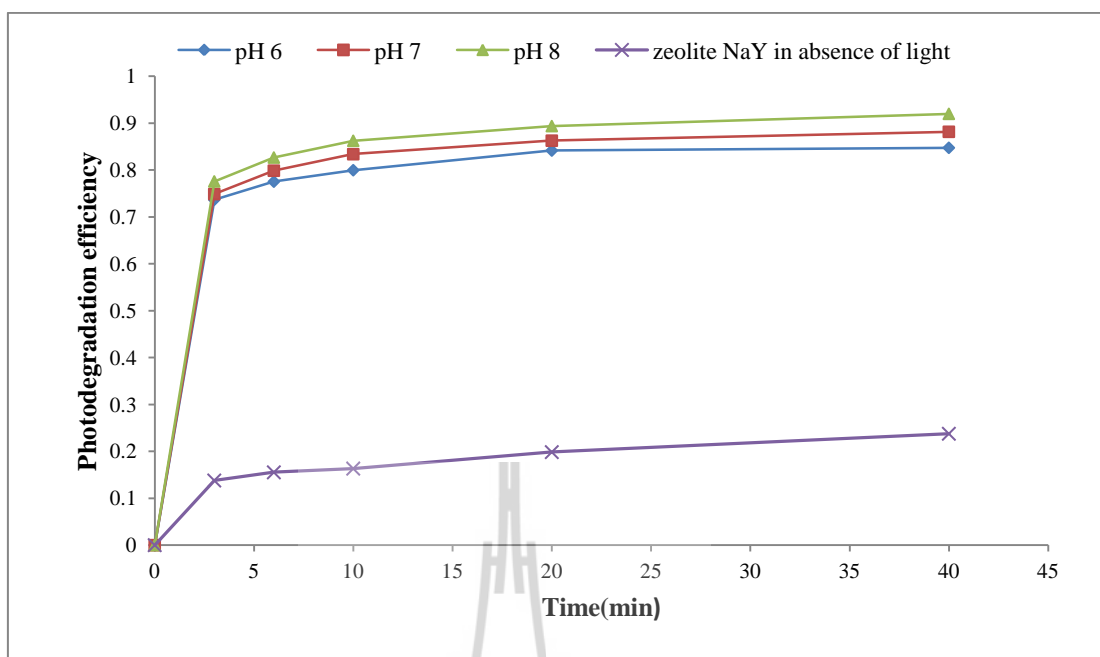


Figure 4.23 Effect of pH of the solution on the photodegradation of phenosafranin with TiO_2 /zeolite Y prepared by sol gel. Experiment conditions: 0.050 g of prepared TiO_2 /zeolite Y, 50 ml of 0.10 mM of PHNS.

4.3.3 Comparison of the Photocatalyst Activity of Catalyst Prepared by 3 Methods

Figures 4.24 and 4.25 show the efficiency of the optimum catalyst prepared from 3 methods in photodegradation of phenosafranin. The result showed the same trend of the photodegradation of methylene blue.

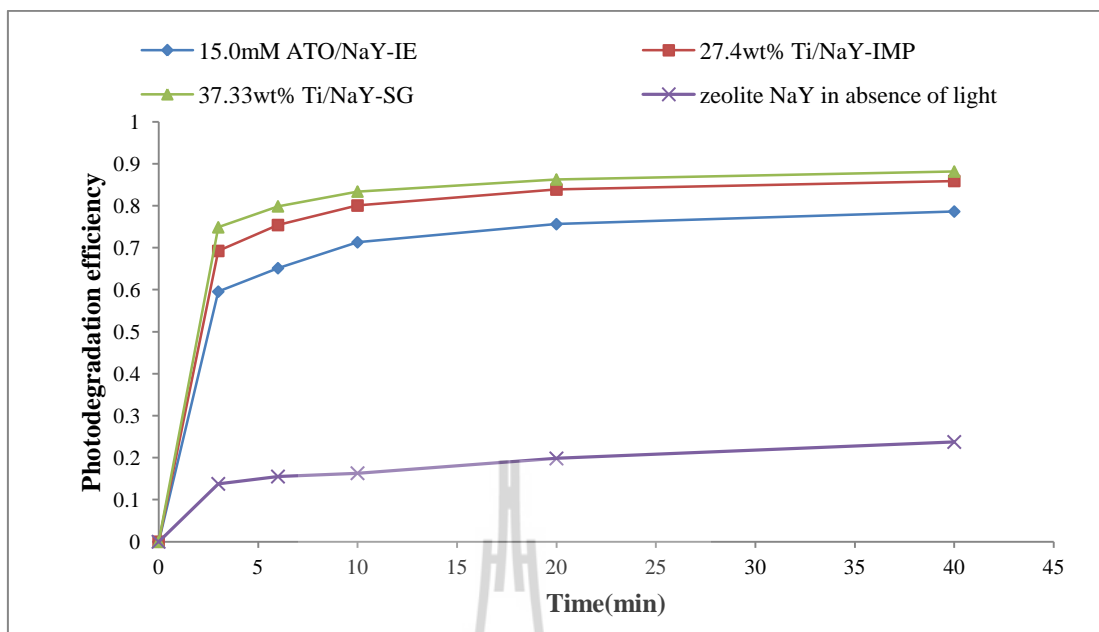


Figure 4.24 The comparison of the photodegradation efficiency of phenosafranin with photocatalysts prepared by impregnation, ion exchange and sol gel method. Experiment conditions: 0.050 g of prepared TiO_2 /zeolite Y, 50 ml of 0.10 mM of PHNS at pH 8.

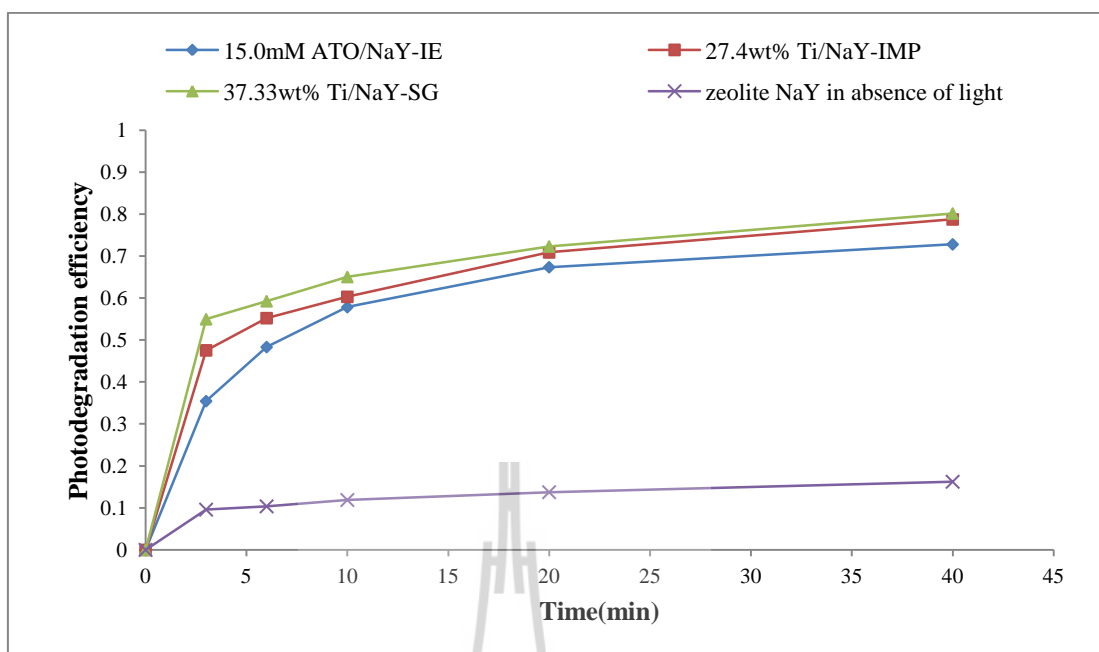


Figure 4.25 The comparison of the photodegradation efficiency of phenosafranin with photocatalysts prepared by impregnation, ion exchange and sol gel method. Experiment conditions: 0.050 g of prepared TiO_2 /zeolite Y, 50 ml of 0.20 mM of PHNS at pH 8.

CHAPTER V

CONCLUSIONS

In the study, there are two parts, the first part is the preparation of TiO_2 supported on zeolite Y using ion exchange, impregnation and sol-gel method and the characterization of the prepared samples. The second part is the study of photodegradation of methylene blue and phenosafranin using the prepared samples as photocatalyst.

The preparation TiO_2 loaded on zeolite Y was prepared by ion exchange, impregnation and sol-gel method using ammonium titanyloxalate $((\text{NH}_4)_2\text{TiO}(\text{C}_2\text{O}_4)_2)$, titanium ethoxide $(\text{Ti}(\text{OC}_2\text{H}_5)_4)$ and titanium tetraisopropoxide $(\text{Ti}[\text{OCH}(\text{CH}_3)_2]_4)$, respectively, as a precursor in the method. Many techniques were used to characterize the prepared TiO_2 /zeolite Y. The XRD results showed that under the study condition of preparation anatase phase was observed on the zeolite prepared by impregnation and sol-gel method only. FT-IR spectrum of the sample treated with 15.0 mM ATO/NaY-IE showed a new absorption band at about 910 cm^{-1} attributed to the stretching vibration of Ti-O-Si and Ti-O-Al, and the characteristic peak of zeolite Y (at 527 cm^{-1}) was not observed in the sample of 37.33wt% Ti/NaY-SG indicating that the zeolite structure was quite completely destructive. From surface area analysis all the samples of TiO_2 /zeolite Y have lower surface area than zeolite Y due to an occupancy of TiO_2 on zeolite surface area, including the destruction of zeolite structure. The sample of 27.4wt% Ti/NaY-IMP exhibited the lowest surface area that

consistent with the result of XRD and showing that the zeolite framework was mainly destroyed. TEM morphologies of 27.4wt% Ti/NaY-IMP, 18.67wt% Ti/NaY-SG, and 37.33wt% Ti/NaY-SG showed that dark spots seem to spread all over the particles. It forms small crystallites aggregated on the external surfaces of the zeolite.

The second part of the study was concerned with the use of prepared TiO_2 /zeolite NaY samples as a photocatalyst for photodegradation of methylene blue and phenosafranin. The optimal prepared TiO_2 /zeolite NaY sample from each method was studied for photodegradation of dyes. The optimum of photocatalytic activity of TiO_2 /zeolite NaY prepared by ion exchange, impregnation and sol-gel method was observed with the condition of 15.0 mM ATO/NaY-IE, 27.4wt% Ti/NaY-IMP, and 37.33wt% Ti/NaY-SG, respectively.

The effect of initial concentration of methylene blue on the photodegradation efficiency was studied. It was found that the efficiency was decreased with an increase in initial concentration of methylene blue. It could be explained that when initial concentration was increased, more dye molecules were absorbed on the surface of the catalyst. Subsequently, OH radicals were less generated at the catalyst surface because the active sites were occupied by dye cation.

The effect of pH of the solution on the photodegradation efficiency of methylenen blue was also studied. It was found that the efficiency was increased with an increase in pH of the solution. It might be that alkaline solution, attractive forces between the cationic dye and the photocatalyst surface would favour adsorption and so photodegradation efficiency will be favoured by high pH, but at low pH the photocatalyst's surface will be positively charged and repulsive forces between the

photocatalyst surface and the cationic dye will lead to a decrease in both dye adsorption and photodegradation efficiency.

Comparison between the photocatalytic activity of catalysts prepared from three methods for photodegradation showed that the highest efficiency to degradation methylene blue was observed with the catalyst prepared by sol-gel method. Because it possessed highest external surface area due to an enormous amount of fine TiO_2 particles spreading over all external surface, which was confirmed by TEM. Although the sample prepared by impregnation containing higher amount of Ti (based on ICP analysis) than that of the prepared sample from sol-gel. It may result from greater aggregation of TiO_2 particles due to high amount of Ti, that decreases its photocatalytic activity. Consequently, this sample had lower external surface and lower photocatalytic activity compared to the sample prepared by sol-gel method.

In the study of photodegradation of phenosafranin, the optimal photocatalyst from each preparation method (15.0 mM ATO/NaY-IE, 24.7wt% Ti/NaY-IMP, and 37.33wt% Ti/NaY-SG) was employed for the study of photodegradation of phenosafranin. All the results showed the same trend as study in the photodegradation of methylene blue. When the photodegradation efficiency was compared between methylene blue and phenosafranin, it was found that methylene blue was more degraded than phenosafranin. It may be the molecule of methylene blue smaller than that of phenosafranin.

REFERENCES

- Anandan, S. and Yoon, M. (2003). Photocatalytic activities of the nano-sized TiO_2 -supported Y-zeolites. **Journal of Photochemistry and Photobiology C: Photochemistry Reviews**. 4: 5-18.
- Bhatia, S. (1990). **Zeolite Catalysis: Principles and Applications**, CRC Press, Inc., Boca Raton, Florida.
- Breck, D. W. (1974). **Zeolite Molecular Sieves**. New York: Wiley.
- Chen, H., Matsumoto, A., Nishimiya, N. and Tsutsumi, K. (1999). Preparation and characterization of TiO_2 incorporated Y-zeolite. **Colloids and Surfaces A: Physicochemical and Engineering Aspects**. 157: 295-305.
- Corrent, S., Cosa G., Scaiano, J. C., Galletero, M. S., Alvaro, M. and Garcia, H. (2001). Intrazeolite photochemistry. 26. photophysical properties of nanosized TiO_2 clusters included in zeolites Y, β , and Mordenite. **Chemicals and Materials**. 13: 715-722.
- Ding, X-Z. and Liu, X-H. (1997). Synthesis and microstructure control of nanocrystalline titania powders via a sol-gel process. **Materials Science and Engineering A**. 224: 210-215.
- Do, D. D. (1998). **Adsorption Analysis: Equilibria and Kinetics**. London: Imperial College.

- Easwaramoorthi, S. and Natarajan, P. (2005). Photophysical properties of phenosafranine (PHNS) adsorbed on the TiO₂-incorporated zeolite-Y. **Microporous and Mesoporous Materials**. 86: 185-190.
- Faisal, M., Tariq, M. A. and Muneer, M. (2007). Photocatalysed degradation of two selected dyes in UV-irradiated aqueous suspensions of titania. **Dyes and Pigments**. 72: 233-239.
- Flanigen, E. M., Khatami, H. and Seymenski, H. A. In: Flanigen EM, Sands LB. (1971). *Advances in Chemistry Series 101*. American Chemical Society. 201-228.
- Ginter, D. M., Bell, A. T. and Radke, C. J. (2005). **Synthesis zeolite**. [online]. Available: <http://www.iza-online.org/synthesis/default.htm>.
- Guetta, N. and Amar, H. A. (2005). Photocatalytic oxidation of methyl orange in presence of titanium dioxide in aqueous suspension. Part I: Parametric study. **Desalination**. 185: 427-437.
- Herreros, B. (2001). **The X-Ray Diffraction Zeolite Database**. [online]. Available : <http://suzy.unl.edu/bruno/zeodat.html>.
- Herrmann, J. M. (1999). Heterogeneous photocatalysis: fundamentals and applications to the removal of various types of aqueous pollutants. **Catalysis Today**. 53: 115-129.
- Hsien, Y. H., Chang, C. F., Chen, Y. H. and Cheng, S. (2001). Photodegradation of aromatic pollutants in water over TiO₂ supported on molecular sieves. **Applied Catalysis B: Environmental**. 31: 241-249.

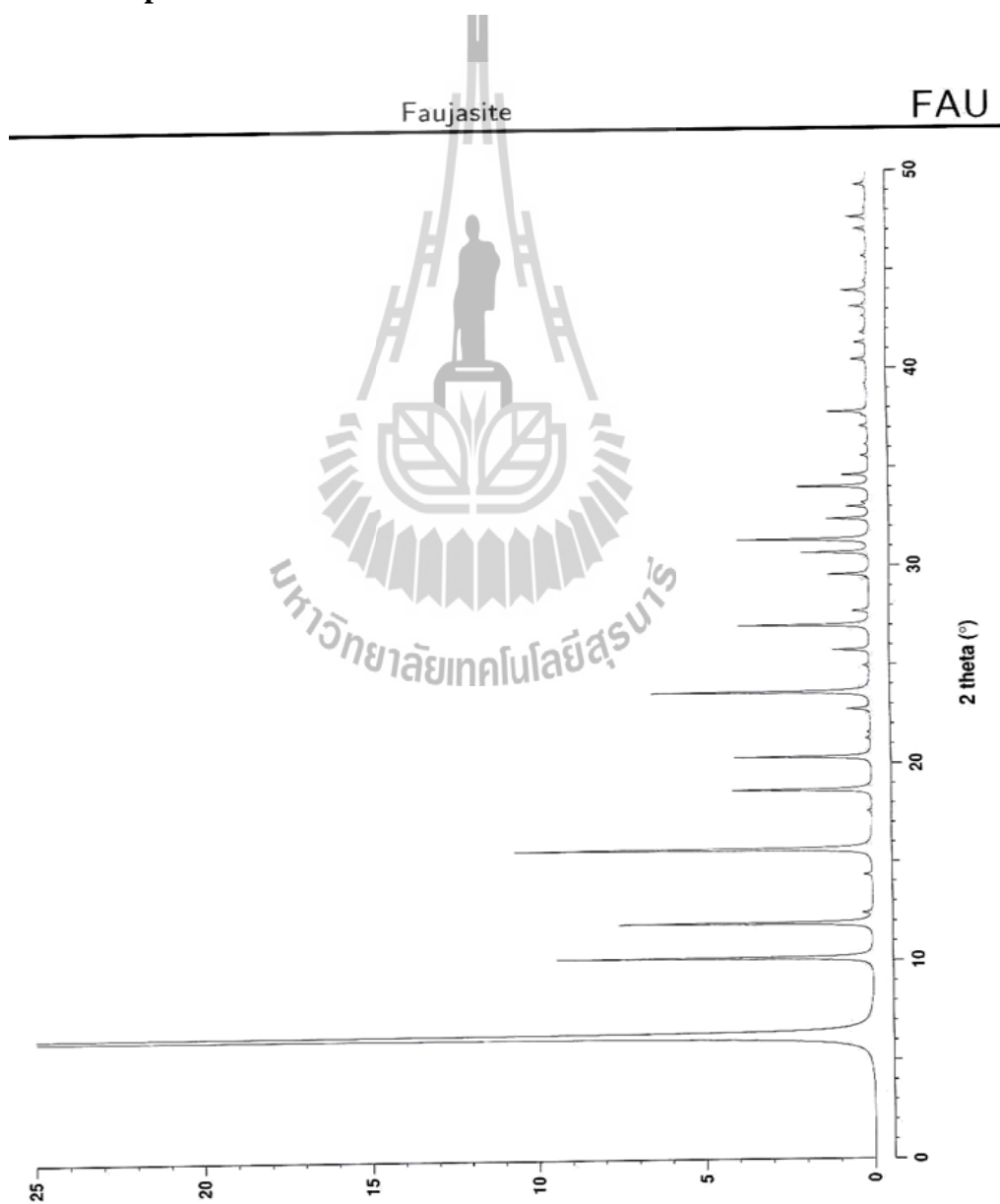
- Kabir, M. F., Vaisman, E., Langford, C. H. and Kantzas, A. (2006). Effects of hydrogen peroxide in a fluidized bed photocatalytic reactor for wastewater purification. **Chemical Engineering Journal**. 118: 207-212.
- Liu, A. R., Wang, S. M., Zhao, Y. R. and Zheng, Z. (2006). Low-temperature preparation of nanocrystalline TiO_2 photocatalyst with a very large specific surface area. **Materials Chemistry and Physics**. 99: 131-134.
- Liu, X., Iu, K. and Thomas, J. K. (1992). Encapsulation of TiO_2 in zeolite Y. **Chemical Physics Letters**. 195(2, 3): 163-168.
- Litter, M. I. (1999). Review Heterogeneous photocatalysis Transition metal ions in photocatalytic systems. **Applied Catalysis B: Environmental**. 23: 89-114.
- Meier, W. M. (2001). **The Atlas of Zeolite Structure Types** [online]. Available: <http://www-iza-sc.csb.yale.edu/IZA-SC/Atlas/AtlasHome.html>.
- Pozzo, L. Roberto, Baltanfis, A. Miguel and Cassano, E. Alberto. (1997). Supported titanium oxide as photocatalyst in water decontamination: State of the art. **Catalysis Today**. 39: 219-231.
- Saqib, M., Tariq, M. A., Haque, M. M. and Muneer, M. (2008). Photocatalytic degradation of disperse blue 1 using $\text{UV/TiO}_2/\text{H}_2\text{O}_2$ process. **Journal of Environmental Management**. 88: 300-306.
- Sen, S., Mahanty, S., Roy, S., Heintz, O., Bourgeois, S. and Chaumont, D. (2005). Investigation on sol-gel synthesized Ag-doped TiO_2 cermet thin films. **Thin Solid Films**. 474: 245-249.
- Sharma, M., Phanikrishna, V., Lalitha, K., Durgakumari, V. and Subrahmanyam, M. (2008). Solar photocatalytic mineralization of isoproturon over TiO_2/HY composite systems. **Solar Energy Materials & Solar Cells**. 92: 332-342.

- Wang, C. C., Lee, C. K., Lyu, M. D. and Juang, L. C. (2008). Photocatalytic degradation of C.I. Basic Violet 10 using TiO_2 catalysts supported by Y zeolite: An investigation of the effects of operational parameters. **Dyes and Pigments**. 76: 817-824.
- Xu, Y. and Langford, C. H. (1995). Enhanced Photoactivity of a Titanium (IV) Oxide Supported on ZSMS and Zeolite A at Low Coverage. **Journal of Physical Chemistry**. 99: 11501-11507.
- Xu, Y. and Langford, C. H. (1997). Photoactivity of Titanium Dioxide Supported on MCM41, Zeolite X, and Zeolite Y. **Journal of Physical Chemistry B**. 101: 3115-3121.
- Yahiro, H., Miyamoto, T., Watanabe, N. and Yamaura, H. (2007). Photocatalytic partial oxidation of α -methylstyrene over TiO_2 supported on zeolites. **Catalysis Today**. 120: 158-162.

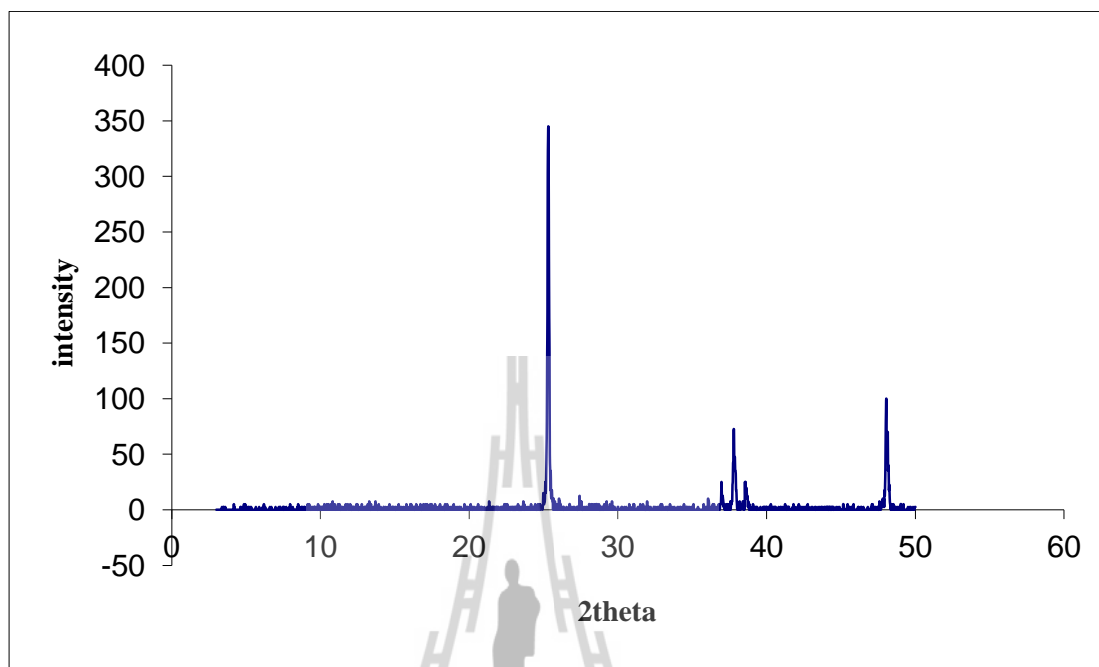
APPENDIX

Standard XRD patterns

1. XRD pattern of zeolite Y

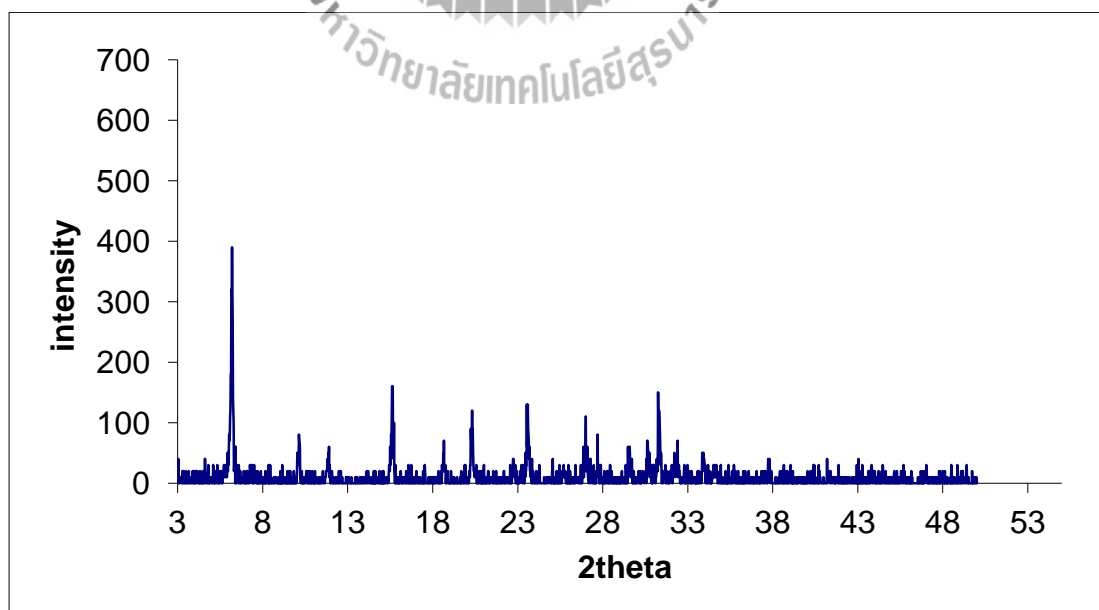


2. XRD pattern of TiO_2

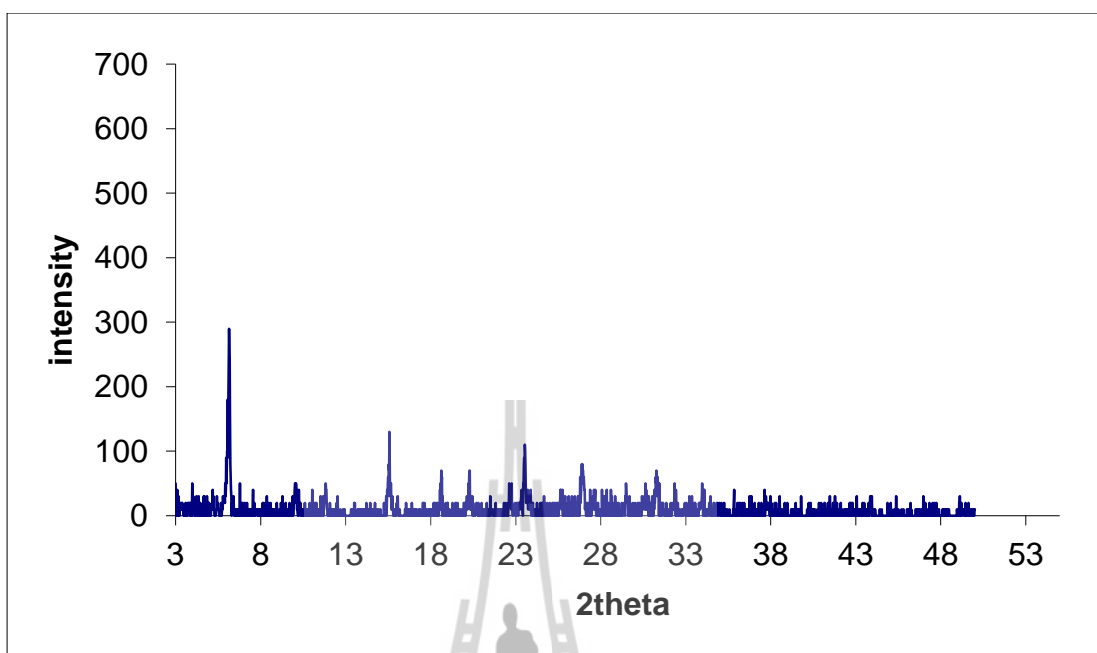


3. XRD pattern of TiO_2 supported on zeolite Y by ion exchange

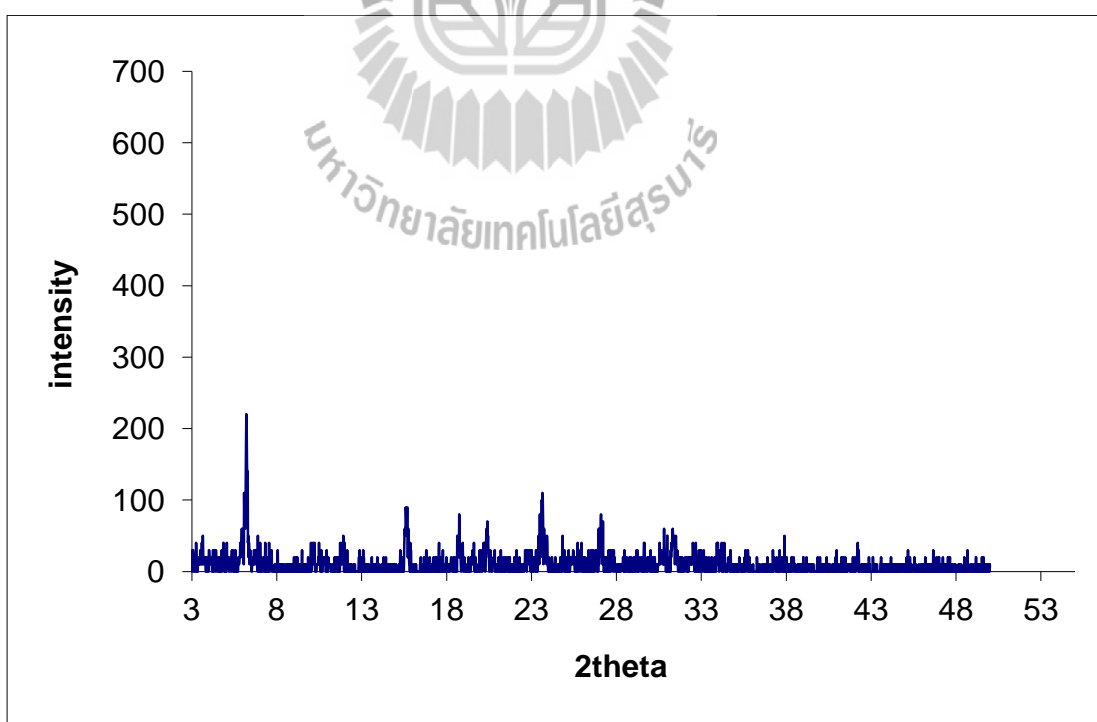
3.1 5.0 mM ATO/NaY-IE



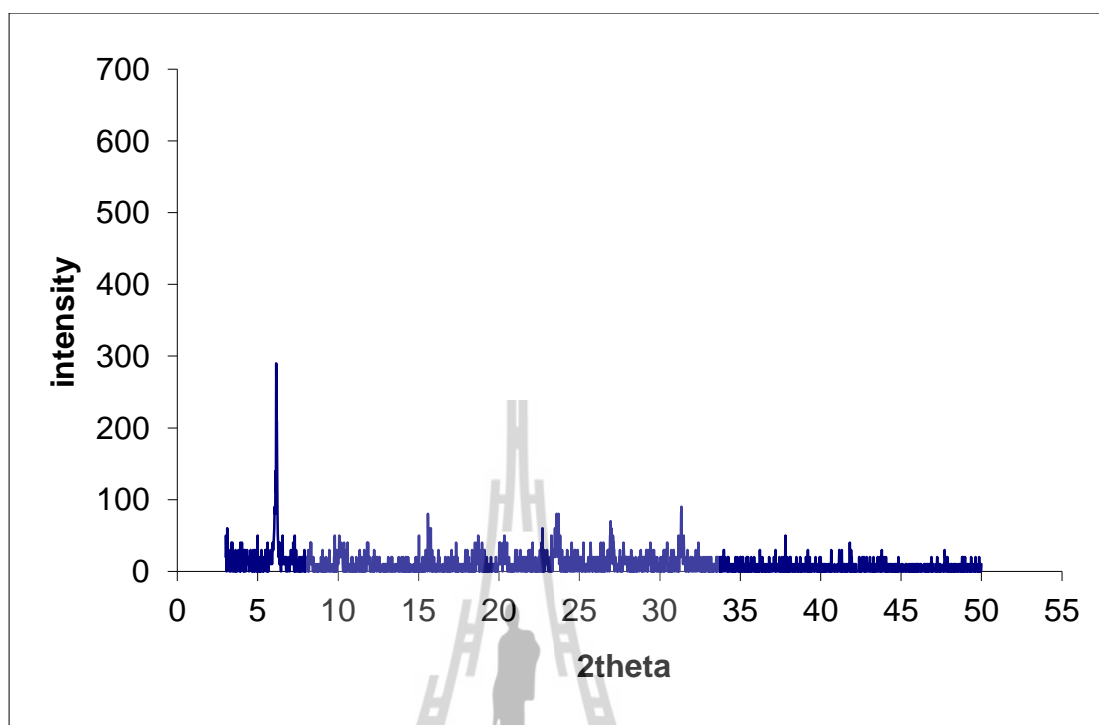
3.2 10.0 mM ATO/NaY-IE



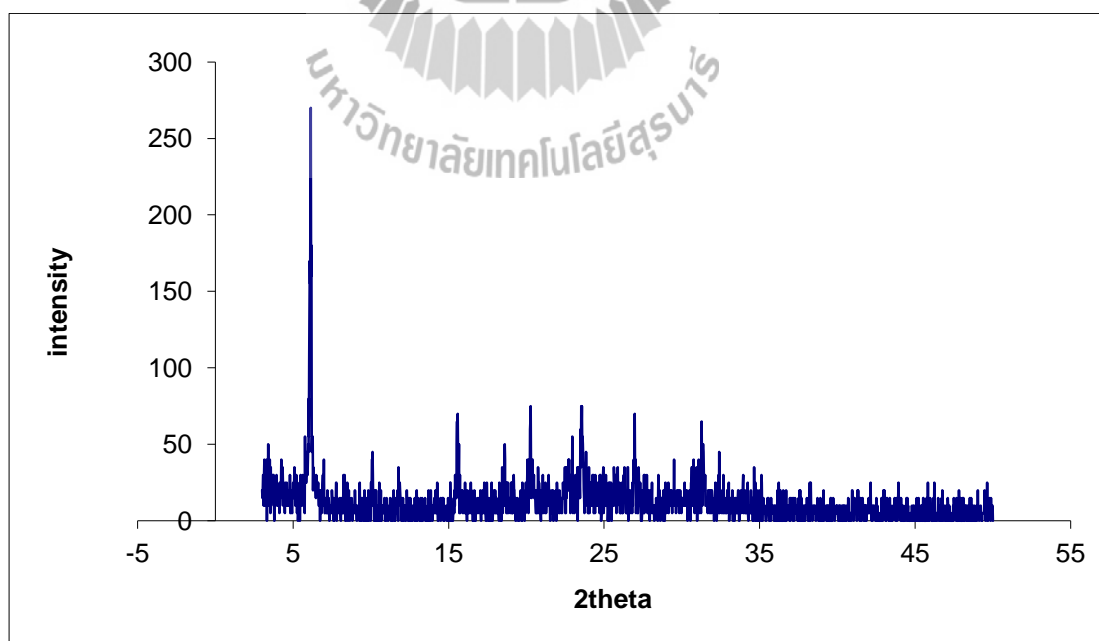
3.3 15.0 mM ATO/NaY-IE



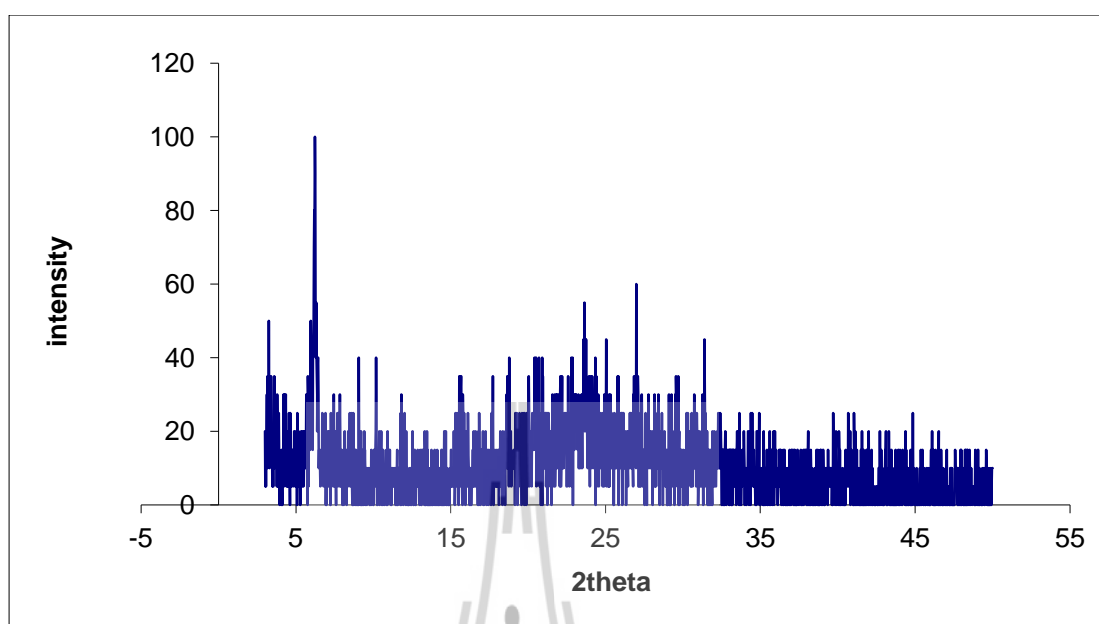
3.4 20.0 mM ATO/NaY-IE



3.5 30.0 mM ATO/NaY-IE

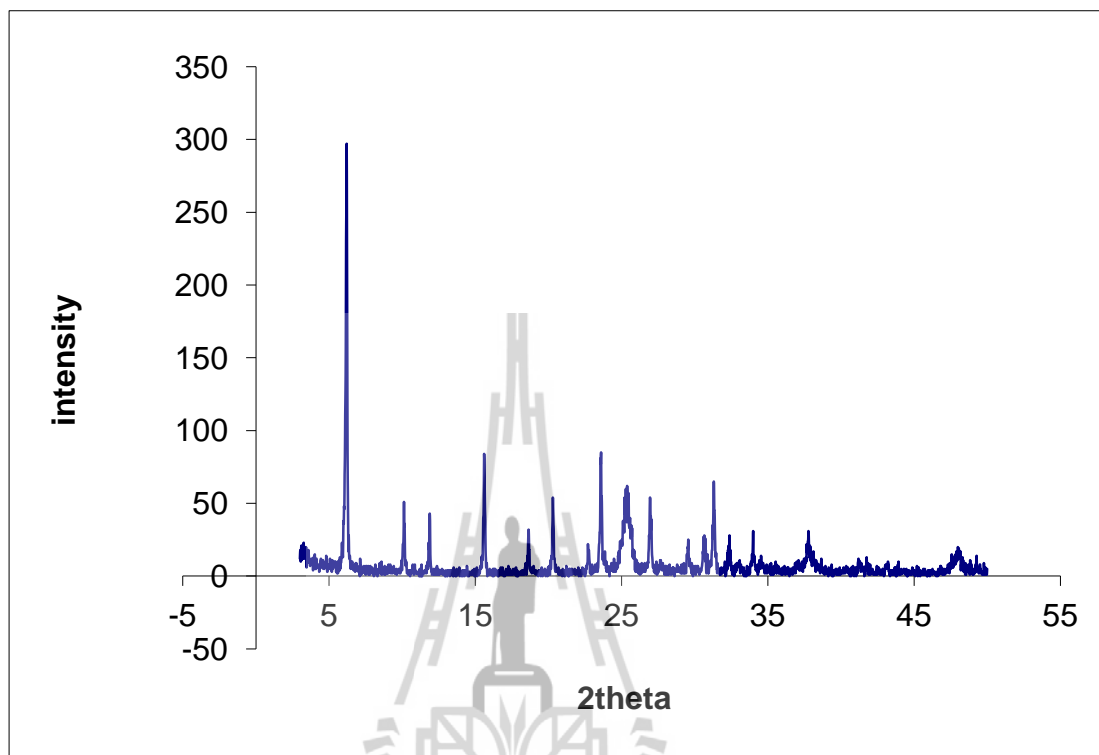


3.6 40.0 mM ATO/NaY-IE

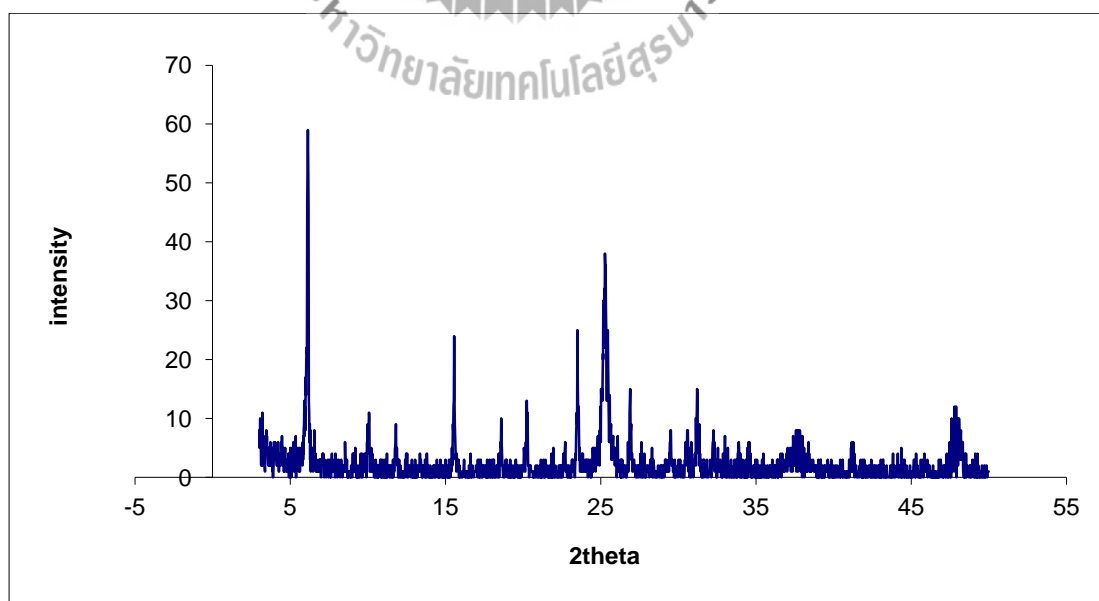


4. XRD pattern of TiO_2 supported on zeolite Y by impregnation method

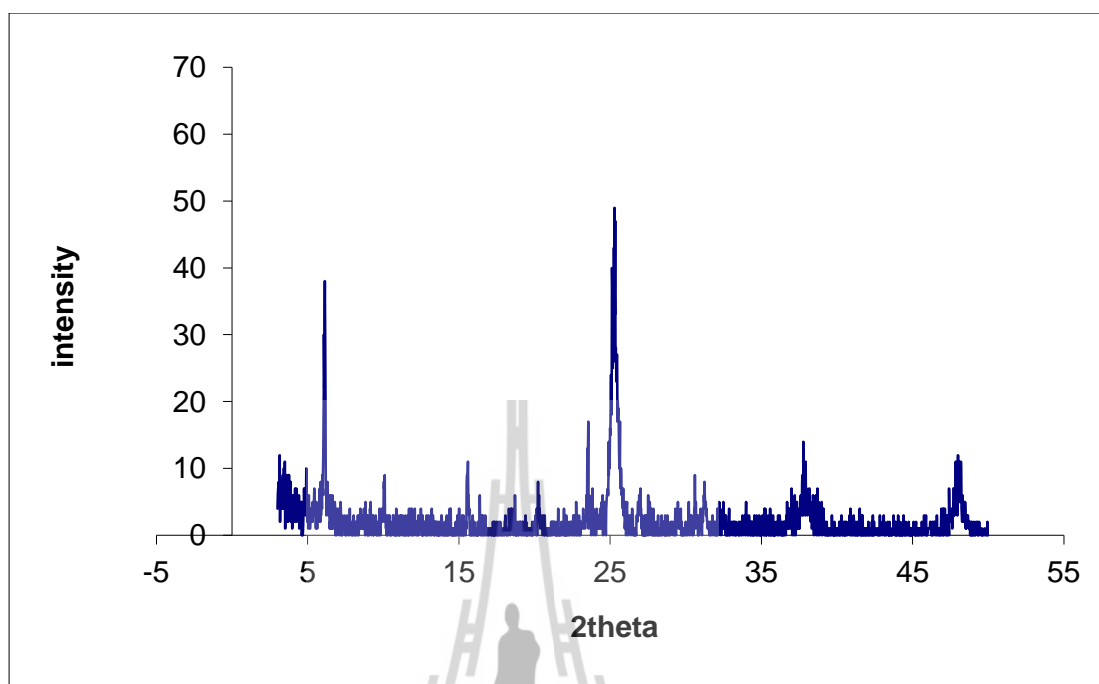
4.1 4.6 wt% Ti/NaY-IMP



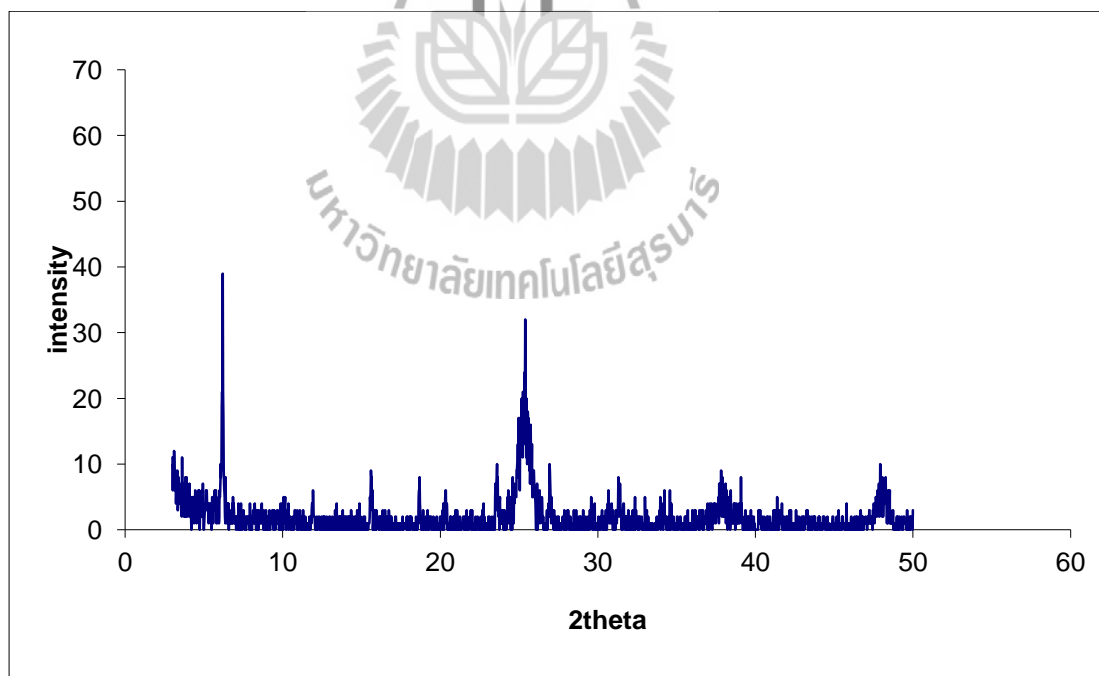
4.2 9.2 wt% Ti/NaY-IMP



4.3 18.2 wt% Ti/NaY-IMP

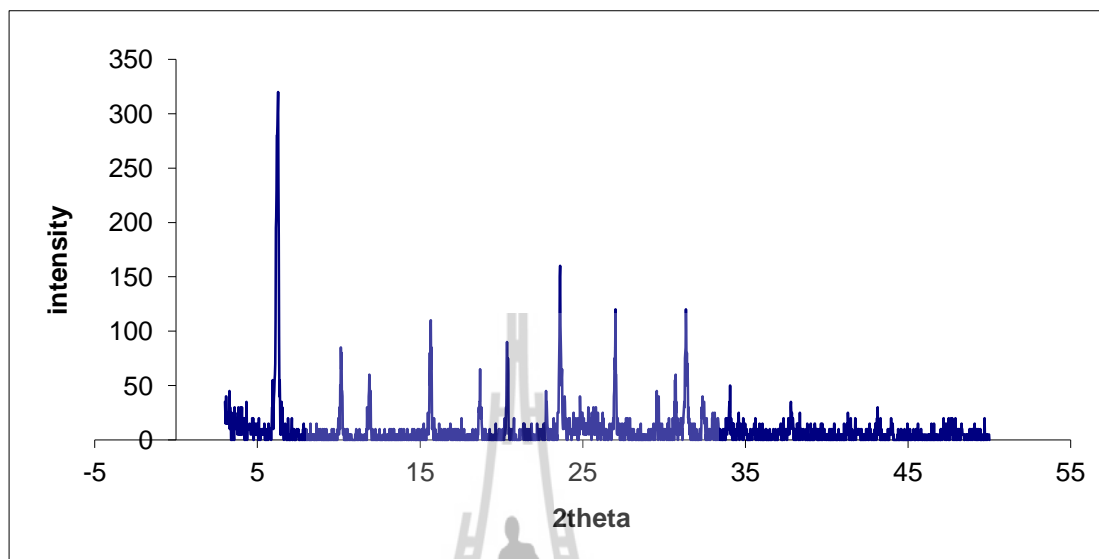


4.4 27.4 wt% Ti/NaY-IMP

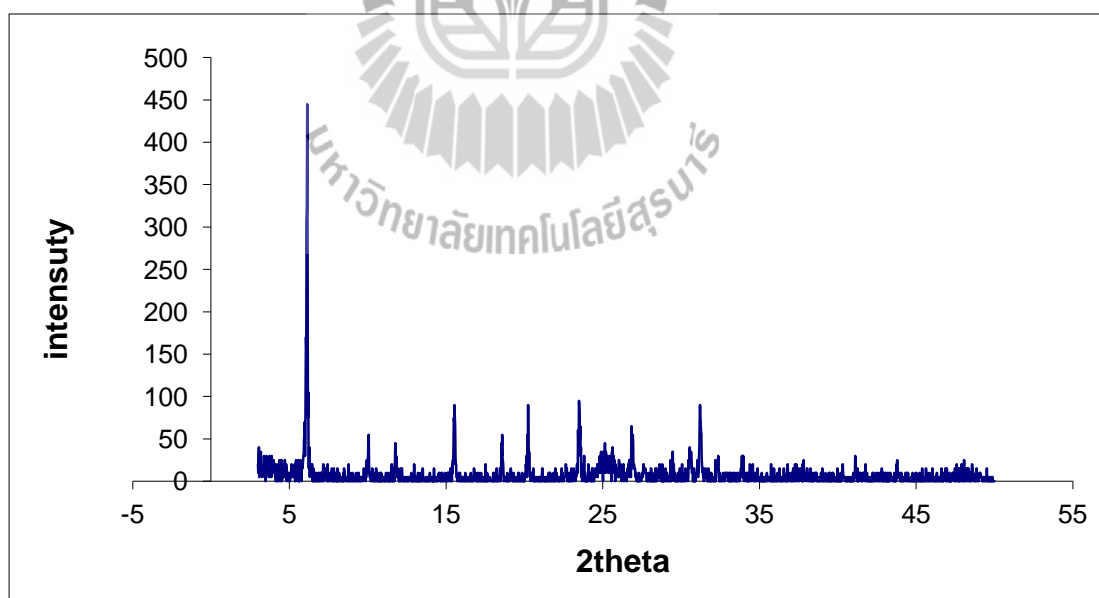


5. XRD pattern of TiO_2 supported on zeolite Y by sol gel method

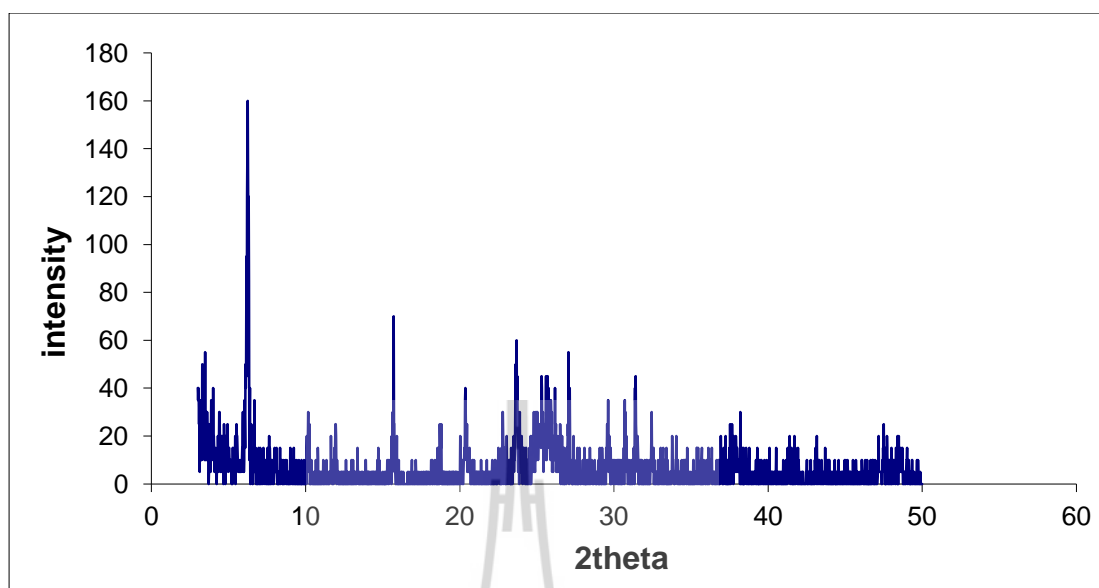
5.1 9.33 wt% Ti/NaY-SG



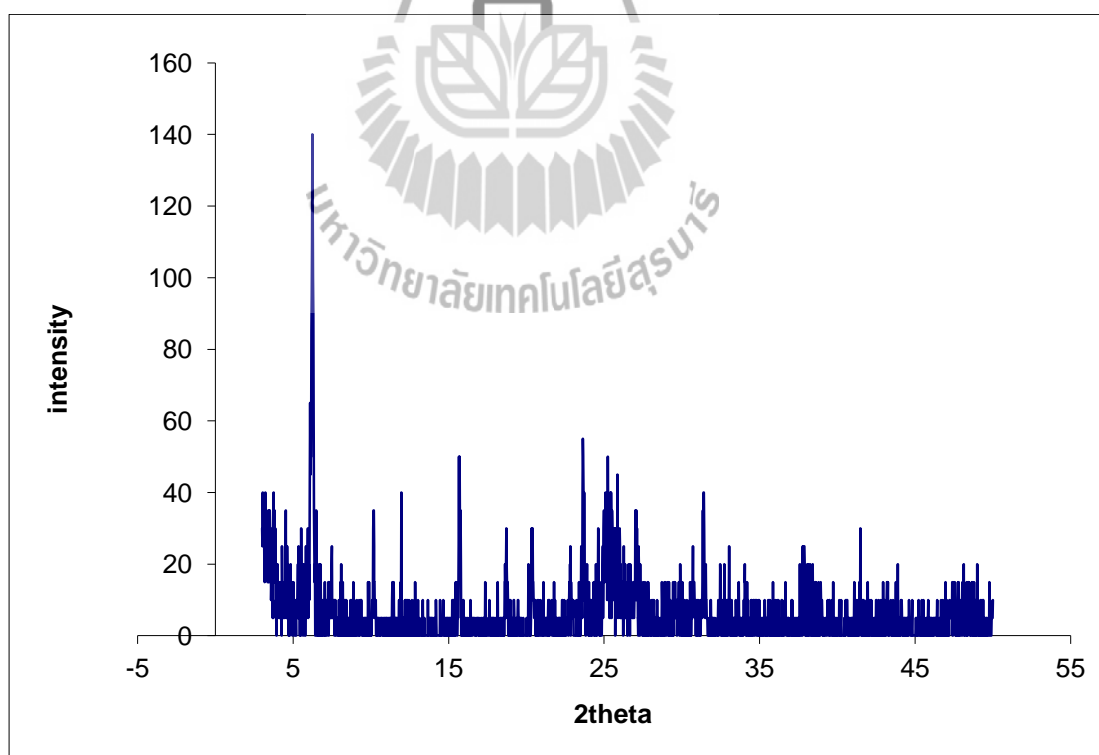
5.2 18.67 wt% Ti/NaY-SG



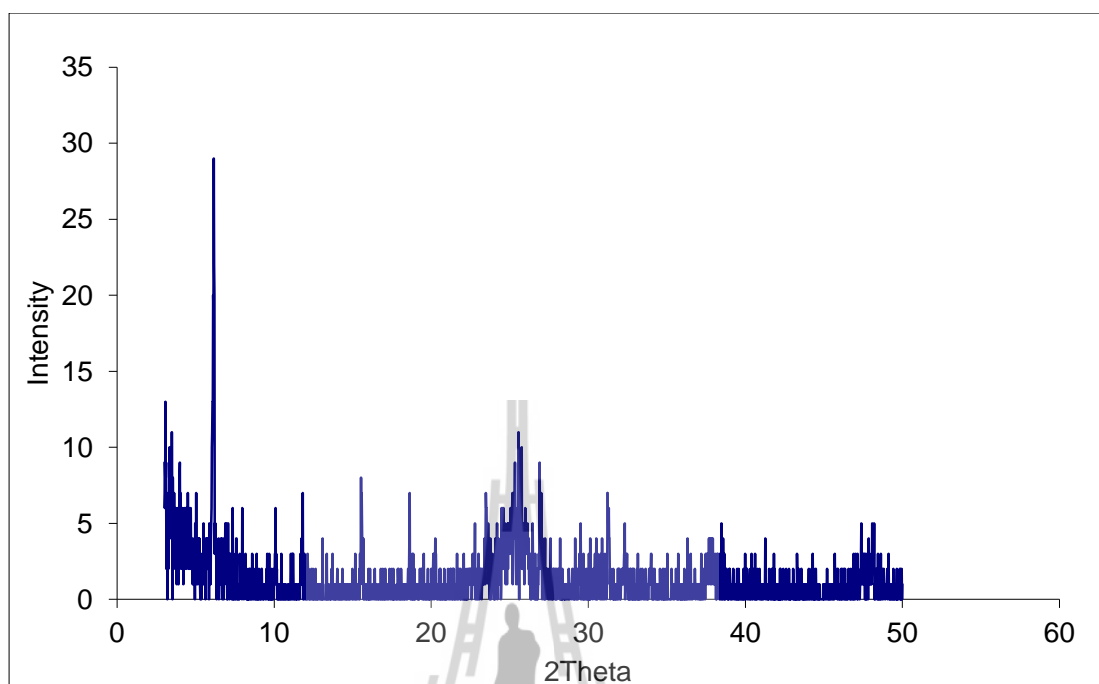
5.3 28.0 wt% Ti/NaY-SG



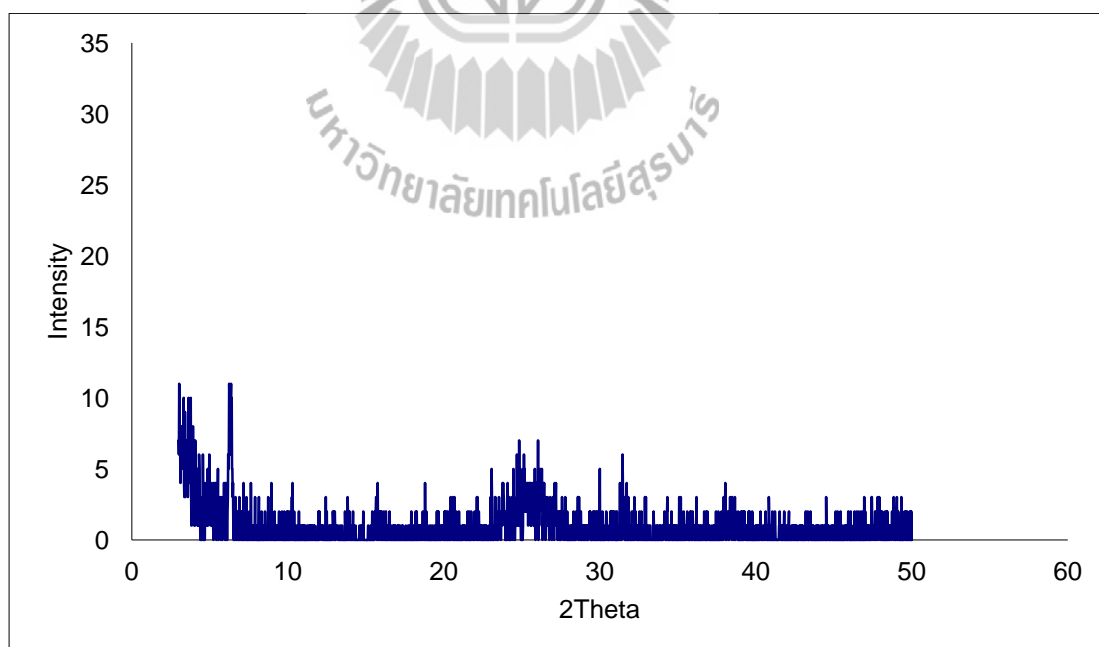
5.4 37.33 wt% Ti/NaY-SG



5.5 46.67 wt% Ti/NaY-SG



5.6 55.56 wt% Ti/NaY-IMP



CURRICULUM VITAE

NAME: Miss Kultida Pittayaporn **DATE OF BIRTH:** March 21, 1982

PLACE OF BIRTH: Nakhon Ratchasima **CITIZENSHIP:** Thailand

EDUCATION:

2000-2004 B.Sc. (General Science)

Kasetsart University, Kamphaeng Saen Campus, Thailand

PRESENTATION:

1. "PREPARATION OF TiO_2 SUPPORTED ON ZEOLITE Y AS CATALYST IN PHOTODEGRADATION OF METHYLENE BLUE", 35th Congress on Science and Technology of Thailand.
2. "PREPARATION OF TiO_2 SUPPORTED ON ZEOLITE Y AS CATALYST IN PHOTODEGRADATION OF METHYLENE BLUE", Pure and Applied Chemistry Conference 2010, Ubonratchathani University, Thailand.
3. "EFFECT OF DIFFERENT PREPARATION OF TiO_2 LOADED ON ZEOLITE Y AS PHOTOCATALYST ON METHYLENE BLUE DEGRADATION", The 3th Science Research Conference, Naresuan University, Thailand.